UNIVERSIDAD NACIONAL AUTÓNOMA DE MÉXICO

INSTITUTO DE ASTRONOMÍA

PARÁMETRO DE MOMENTO ANGULAR ADIMENSIONAL λ: CARACTERIZACIÓN DE GALAXIAS Y ESTRUCTURA A GRAN ESCALA DEL UNIVERSO

T E S I S

QUE PARA OBTENER EL GRADO ACADÉMICO DE

DOCTOR EN CIENCIAS (ASTRONOMÍA)

PRESENTA:

BERNARDO CERVANTES SODI

DIRECTOR DE TESIS

DR. XAVIER HERNÁNDEZ DORING

instituto de astronomía

unam

Ciudad Universitaria, México D. F.   2009

Resumen

En este trabajo presentamos un estudio del momento angular total de las galaxias, usando el parámetro de momento adimensional λ, definido por Peebles en 1969 como $\lambda = L \mid E \mid^{1/2} /GM^{5/2}$, donde L, E y M son respectivamente el momento angular, la energía y la masa totales del sistema, y G la constante de gravitación de Newton. Este parámetro proporciona una medida del grado de soporte rotacional del sistema. Junto con la masa, el parámetro de espín λ, es identificado en varios estudios teóricos como el principal parámetro físico responsable de la morfología de las galaxias.

Desde el punto de vista teórico, la dispersión observada en muchas características físicas de las galaxias, puede ser explicada como un efecto de la dispersión de momento angular total, una vez que la masa total de la galaxia está determinada, en conjunto con una dispersión en el tiempo de formación y la historia de agregación de masa. Como ejemplo de lo anterior, podemos citar el cociente bulbo-disco en galaxias espirales, el espesor del disco, la densidad superficial, variaciones sistemáticas en la pendiente de la curva de rotación, el tamaño del radio de escala, la abundancia química y gradientes de color, sólo por mencionar algunos. Dada la variación monotónica de todos estos parámetros con el esquema de clasificación morfológico de Hubble (1926, 1936), es razonable proponer el parámetro de momento angular λ como el principal parámetro físico detrás de la secuencia de Hubble. Para apoyar esta propuesta necesitamos algún método que nos permita calcular λ de cualquier galaxia observada. Dado que el parámetro λ está definido en términos de momento angular, masa y energía, ninguno de los cuales es un observable directamente medible, el primer paso consiste en obtener una estimación confiable de este parámetro con base a la información más básica accesible en catálogos de galaxias observadas.

Con base en un modelo muy simple, con el cual modelamos galaxias de disco con solo dos componentes: un disco para la componente bariónica con un perfil superficial de masa exponencial y un halo de materia oscura con un perfil de densidad isotermo, y haciendo algunas hipótesis generales, presentamos una expresión simple, para la cual sólo se requiere medir el radio de escala y la velocidad de rotación para obtener un estimado del parámetro de espín λ.

Para comprobar la precisión de nuestra aproximación, usamos una serie de simulaciones, provenientes de diferentes grupos de investigación, en las cuales el espín actúa como parámetro de entrada y su valor puede ser calculado con gran

precisión. Las seis diferentes simulaciones con las que probamos nuestra estimación incluyen diferentes y muy variadas formas de modelar la estructura y evolución de las galaxias simuladas. Como resultado obtuvimos que nuestra estimación simple de λ concuerda bastante bien con aquella proveniente de las simulaciones, siempre con un error menor al $30\,\%$ del valor real, lo cual motiva su uso en sistemas reales.

Con base en el mismo modelo, realizamos un análisis sobre las tendencias que esperamos obtener entre este parámetro y otras caracterísiticas físicas de las galaxias, tales como el cociente bulbo-disco, el espesor del disco, el color de la galaxia definido como $B - R$, la eficiencia de formación estelar, la metalicidad y la fracción de gas. Con el fin de comprobar estas predicciones, empleamos varios catálogos de galaxias que contienen la información requerida para calcular el espín de cada galaxia, y valores reportados de otros parámetros físicos, para obtener distribuciones de estos parámetros como función del momento angular, haciendo a la par, una comparación con las tendencias que muestran estos mismos parámetros con el tipo morfológico de Hubble.

Una de las tendencias más claras visible en la secuencia de Hubble es la transición a colores más azules al ir de tipos tempranos a tipos tardíos, misma que se reproduce al incrementarse el valor de λ, tendencia que aparece en la muestra de galaxias empleada. Otra característica que muestra un cambio sistemático a lo largo de la secuencia de Hubble es el espesor del disco, entendido como el cociente entre la altura de escala y el radio de escala h/R_d, el cual tiende a disminuir al ir de tipos tempranos a tardíos. Este comportamiento vuelve a repetirse al emplear el espín en vez del tipo de Hubble. En cuanto a parámetros estructurales, el cociente bulbo-disco, que es uno de los parámetros a evaluar para determinar el tipo de Hubble, presenta también una clara tendencia a disminuir a medida que crece el valor de λ.

Aún cuando las correlaciones entre metalicidad promedio y magnitud o tipo de Hubble son evidentes, nosotros obtuvimos correlaciones igualmente fuertes con el espín, en el sentido que galaxias con valores pequeños de λ presentan abundancias más altas, mientras que galaxias con λ grande son pobres en metales. También el contenido de gas en las galaxias correlaciona con λ, en donde sistemas con valores altos de λ presentan mayores fracciones de masa de gas que galaxias con valores pequeños de λ, destacando el importante papel que juega este parámetro en la estructura de las galaxias de disco y la propuesta de su uso como una medida del tipo morfológico.

Al observar todas estas tendencias claras tanto con el tipo morfológico como con λ, podemos hacer una asociación directa de galaxias tempranas con sistemas con valores pequeños de λ mientras que típicamente las galaxias tardías presentaran valores elevados de λ. Dividiendo las galaxias empleadas para el estudio por tipo morfológico, obtuvimos que los valores promedio de λ aumentaban al ir de tipos morfológicos tempranos a tardíos, aún cuando se presenta un traslape

considerable en valores de λ entre las poblaciones de diferente tipo morfológico.

Una vez habiendo probado la exactitud de nuestra estimación de λ con simulaciones y comprobado nuestras predicciones sobre relaciones de parámetros estructurales de galaxias observadas con valores inferidos de λ, enfocamos nuestro estudio a distribuciones estadísticamente confiables de este parámetro para poblaciones numerosas de galaxias, lo cual constituye la segunda parte de esta tesis. Con este fin hicimos uso de las muestras extensas de galaxias provenientes del Sloan Digital Sky Survey (SDSS).

Para obtener una distribución empírica de λ proveniente de una muestra de galaxias, limitada por volumen, extendimos nuestro estudio a galaxias elípticas, aplicando el mismo modelo de 2 componentes; en este caso para el material bariónico empleamos un perfil de densidad tipo Hernquist, y para la materia oscura, el mismo perfil isotermo. Empleamos un criterio de segregación de galaxias en un plano color vs. gradiente de color para separar galaxias tempranas y tardías y así calcular λ con la fórmula correspondiente a galaxias de disco o elípticas, según sea el caso. Como resultado obtuvimos la primera distribución empírica de λ derivada de una muestra observacional de galaxias. La distribución resultó estar bien descrita por una función log-normal caracterizada por el máximo de la distribución centrado en $\lambda_0 = 0.046$ y el logaritmo en su dispersión de $\sigma_\lambda = 0.535$. La forma funcional de la distribución concuerda con resultados obtenidos a partir de simulaciones cosmológicas, así como los valores obtenidos para λ_0 y σ_λ.

Dada la extrema semejanza en la distribución de λ obtenida empíricamente a partir de galaxias observadas y aquellas distribuciones provenientes de simulaciones cosmológicas, nos enfocamos a estudiar, con base a nuestras estimaciones de λ para galaxias de disco y elípticas observadas, otras propiedades estadísticas que son recurrentes en estudios teóricos empleando únicamente simulaciones numéricas. Para este tipo de estudios, empleamos una simulación cosmológica tipo ΛCDM de n-cuerpos, en la cual tenemos identificado tanto halos supermasivos como subhalos correspondientes a galaxias de tamaño regular. De esta manera podemos hacer una comparación directa entre los resultados de la simulación y los resultados obtenidos para halos inferidos de galaxias observadas.

Lo primero que investigamos fue si existía alguna dependencia del valor de λ con la densidad del medio ambiente en donde se encuentran las galaxias. Para la densidad teníamos una medida continua que consiste en una suma normalizada del volumen que ocupan las 20 galaxias vecinas más cercanas a la galaxia blanco; definición que se aplica tanto a los halos de la simulación como a las galaxias observadas. En cuanto a los resultados obtenidos con los halos provenientes de la simulación, el resultado es consistente con otros resultados previamente reportados, no existe una dependencia visible del valor de λ con la densidad de su medio circundante. Esta misma carencia de dependencia la encontramos al analizar la muestra de galaxias del SDSS, hasta este momento, todo en concordancia con los

resultados de las simulaciones de n-cuerpos.

Dado que una de las propiedades más importantes de cualquier galaxia es su masa, investigamos también si existía alguna dependencia entre λ y la masa total del sistema. Nuestros resultados anteriores mostraban una clara relación entre tipo morfológico y espín, incrementándose éste al ir de tipos tempranos a tardíos. Dado que las galaxias tempranas tienden a ser más masivas, es lógico pensar que éstas tenderán a presentar bajos valores de espín. Esta tendencia es en ocasiones observada en simulaciones cosmológicas, pero cuando se presenta resulta ser un efecto muy sutil. Al analizar nuestra simulación cosmológica no logramos distinguir ninguna tendencia clara entre la masa del halo y su λ pero al fijarnos en nuestra muestra de galaxias observadas, la tendencia apareció claramente; las galaxias de baja masa tienen, en promedio, altos valores de λ al igual que una gran dispersión, en cambio galaxias masivas tienden a tener bajos valores de λ con muy poca dispersión, resultado que es escasas veces reproducido por simulaciones cosmológicas, pero recientemente confirmado con otra muestra de galaxias, cinco veces mayor a la nuestra, por otro grupo de investigación (Berta el al. 2008) que sigue nuestra idea empleando un método parecido al nuestro en la determinación de λ al cual le han hecho modificaciones en la determinación de la masa, haciéndolo más preciso.

Nuestro trabajo provee a la comunidad una herramienta nueva para una primera estimación del espín galáctico de galaxias observadas, empleando únicamente la información más esencial asequible en muestras grandes de galaxias, como es el caso de SDSS. Este parámetro resulta ser de gran utilidad como un parámetro físico, objetivo y cuantitativo en la clasificación de galaxias. Finalmente puede ser utilizado para comparar directamente galaxias simuladas con galaxias reales.

La estructura de la tesis es la siguiente. En el primer capítulo presento un resumen conciso sobre la formación galáctica y la estructura general de galaxias de disco. En ese mismo capítulo presento la definición de λ y una teoría estándar sobre la adquisición de momento angular galáctico. Los siguientes dos capítulos, 2 y 3, constituyen la primera parte de la tesis en la que presento todos los resultados concernientes a las relaciones que encontramos entre el espín galáctico y propiedades internas de galaxias. Comienzo el capítulo 2 (Hernández & Cervantes Sodi 2006) con la deducción de la expresión que proponemos para calcular λ para cualquier galaxia de disco y después presento nuestras predicciones y comprobación de estas predicciones, de las relaciones que guarda λ con otros parámetros físicos de las galaxias espirales, entre ellas; el cociente bulbo-disco, el espesor del disco y el color de la galaxia, así como una propuesta de asociación entre λ y el tipo morfológico de la galaxia. En el capítulo 3 (Cervantes-Sodi & Hernández 2009) continúo la discusión de las relaciones entre λ y propiedades internas de las galaxias, en este caso la abundancia metálica y la fracción de gas presente en

ellas.

La segunda parte de la tesis consiste en estudios de grandes muestras de galaxias provenientes del SDSS. En el capítulo 4 (Hernández, Park, Cervantes-Sodi & Choi 2007) obtenemos la primera distribución estadística de λ para una muestra de galaxias (más de 10 000). Dado que en nuestra muestra contamos también con galaxias elípticas, en este mismo capítulo presentamos una expresión similar a la obtenida en el capítulo 2, pero en este caso para calcular λ de cualquier galaxia elíptica. En este mismo capítulo presento una discusión comparando nuestros resultados con resultados provenientes de simulaciones cosmológicas. El capítulo 5 (Cervantes-Sodi, Hernández, Park & Kim 2008) muestra un estudio comparado de la dependencia entre del espín y la masa y la densidad del medio ambiente de las galaxias, mostrando lo que se obtiene analizando una muestra de halos provenientes de una simulación cosmológica y los resultados con halos inferidos de galaxias observadas.

En el capítulo 6 presento una discusión general sobre los resultados de este trabajo y mis conclusiones finales y en en el capítulo 7 los proyectos a desarrollar en el futuro.

Índice general

Agradecimientos

Le agradezco a mi tutor, el doctor Xavier Hernández Doring por proponerme desarrollar este interesante proyecto desde el principio de la maestría y guiarme y apoyarme durante todo mi posgrado, tanto en las clases de la maestría como durante los exámenes generales y el desarrollo del doctorado. Gracias por la paciencia y los consejos, creo que aprendí mucho y además me la pase muy bien. Claro que también aprovecho para agradecer a mis excelentes profesores, los aprecio y los admiro, han sido un ejemplo a seguir, gracias. Le agradezco a mis sinodales que revisaron este trabajo y que con sus comentarios me ayudaron a enriquecerlo.

A mi santa madre que me ha apoyado siempre, te estoy eternamente agradecido, ¡te quiero! A Pipe y María, soy muy afortunado por tenerlos como hermanos. A mi papá, Adriana, Adris, Bruno, Imo y Sofía, por su cariño.

A mis amigos de siempre y mi familia, gracias por su apoyo y por tan agradables momentos. A mis nuevos amigos, son lo más preciado que me llevo de mi estancia en el IA.

A mi familia y amigos.
A todos mis seres queridos,
ustedes le dan sentido a mi vida.

Capítulo 1

Introducción.

En este capítulo presento un breve resumen sobre formación y estructura galáctica, así como el mecanismo que se cree es responsable de la adquisición de momento angular en el proceso de formación galáctica.

1.1. Formación galáctica

Observaciones del Universo, tales como las realizadas por el COBE (COsmic Background Explorer) y el WMAP (The Wilkinson Microwave Anisotropy Probe), o grandes muestreos de galaxias como el SDSS (Sloan Digital Sky Survey), sugieren que a gran escala es homogéneo e isotrópico, con muy pequeñas fluctuaciones fraccionales $(\delta\rho/\rho)_R$ en la densidad de masa (y energía), dentro de una esfera de radio R colocada de manera aleatoria, que decrecen con R en forma de una ley de potencias. Es decir, que podemos modelar al Universo como compuesto por un fondo suave con una densidad promedio, sobre el cual se encuentran superpuestas fluctuaciones en densidad de magnitud importante a escalas pequeñas, pero que decrecen al aumentar la escala.

Por otro lado, la dinámica de nuestro Universo se encuentra determinada por el factor de escala $a(t)$. En 1934 Milne y McCrea mostraron como las relaciones dinámicas que a continuación detallamos pueden ser obtenidas usando dinámica Newtoniana no relativista, dado que la escala de homogeneidad del Universo excede el radio de Schwarzschild para la cantidad de masa involucrada. Las observaciones indican que el campo de velocidad sigue la relación $\mathbf{v} = (\dot{a}/a)\mathbf{r}$ con $\dot{a} > 0$. Imaginemos ahora, tal como propone Padmanabhan (2002), una partícula de masa unitaria localizada en $\mathbf{r}$ con respecto a algún sistema de coordenadas; si igualamos la suma de su energía cinética $v^2/2$ y energía potencial $-GM(r)/r$ debida a la atracción de las partículas de materia dentro de la esfera de radio r, a una constante, el factor de escala debe satisfacer la condición

$$\frac{1}{2}\dot{a}^2 - \frac{4\pi G\rho(t)}{3}a^2 = constante,\qquad(1.1)$$

en donde ρ es la densidad media del Universo; con lo que resulta,

$$\frac{\dot{a}^2}{a^2} + \frac{k}{a^2} = \frac{8\pi G}{3}\rho(t),\qquad(1.2)$$

en donde k es una constante. Aún cuando esta deducción para la ecuación de campo de Einstein está sobre simplificada, resulta ser exacta para un universo sin constante cosmológica, que resultaría de resolver las ecuaciones relativistas para una distribución homogénea e isotrópica de materia con ρ interpretada como la densidad de energía.

La solución más simple de la ecuación 2 se obtiene para un Universo plano con $k = 0$, en el cual la densidad de materia del Universo cambia con la expansión del mismo como a^{-3}. De esta manera se obtiene $a(t) = (t/t_0)^{2/3}$ con $t_0^2 = (6\pi G\rho_0)$, y $a(t)$ normalizado a $a = 1$ al tiempo presente $t = t_0$. Para un Universo completamente homogéneo, dicha solución no produciría la estructura visible al día de hoy, pero si el Universo contaba con la más ligera inhomogeneidad en el pasado, la inestabilidad gravitatoria podría amplificar la perturbación de densidad. Para ver el efecto que produce una perturbación de este tipo, diferenciamos una vez con respecto a t la ecuación 2

$$\ddot{a} = -\frac{4\pi G\rho_0}{3a^2} = -\left(\frac{2}{9t_0^2}\right)\frac{1}{a^2}, \tag{1.3}$$

en donde $\rho = (\rho_0 a_0^3/a^3)$. Al perturbar $a(t)$ ligeramente como $a(t) + \delta a(t)$, de manera que la perturbación fraccional en la densidad sea $\delta \equiv (\delta\rho/\rho) = -3(\delta a/a)$, se encuentra que δa satisface la ecuación

$$\frac{d^2}{dt^2}\delta a = \left(\frac{4}{9t_0^2}\right)\frac{\delta a}{a^3} = \frac{4\delta a}{9t^2}, \tag{1.4}$$

con la solución $\delta a \propto t^{4/3} \propto a^2$, de manera que la perturbación en la densidad crece como $\delta \propto a$. Las perturbaciones crecen de manera proporcional al factor de escala del Universo, hasta que han crecido lo suficiente como para que su autogravedad comience a dominar de manera tal que su materia pueda colapsar para formar un sistema gravitacionalmente ligado.

La materia obscura comenzará a formar estructuras gravitacionalmente ligadas que funcionarán como pozos de potencial para la materia bariónica, que al enfriarse por radiación, se asentará en la parte central de los halos de materia obscura para formar las galaxias.

El enfriamiento del plasma caliente de bariones, con una temperatura $k_B T \simeq (GMm_p/R)$, ocurre principalmente por radiación bremsstrahlung, con una pérdida de energía proporcional a $n^2 T^{1/2}$, donde n es la densidad numérica de partículas y T es la temperatura. El tiempo de enfriamiento típico por este mecanismo está dado por

$$t_{enf} \simeq \frac{nk_B T}{(dE/dtdv)} = \left(\frac{\hbar}{m_e c^2}\right)\left(\frac{1}{n\lambda_e^3}\right)\left(\frac{k_B T}{m_e c^2}\right)^{1/2}\frac{1}{\alpha^3}, \tag{1.5}$$

con k_B la constante de Boltzman, m_e la masa del electrón, c la velocidad de la luz, α la constante de estructura fina, $\hbar$ la constante de Planck dividida entre 2π, mientras que la escala de tiempo para el colapso gravitatorio es

$$t_{grav} \simeq \left(\frac{GM}{R^3}\right)^{-1/2}. \tag{1.6}$$

Para lograr que el plasma se enfríe requerimos que $t_{enf} < t_{grav}$, que junto con la condición $k_B T \simeq (GMm_p/R)$, restringe que el radio sea $R < R_g$, donde

$$R_g \simeq \alpha^3 \alpha_G^{-1} \lambda_e (m_p/m_e)^{1/2} \simeq 74\text{kpc}, \tag{1.7}$$

donde $\alpha_G \equiv (GM_p^2/\hbar c) \approx 6X10^{-39}$ es la constante de estructura fina gravitacional, que se traduce en una condición para masa $M > M_g$ de la forma

$$M_g \simeq \alpha_G^{-2}(\alpha m_p/m_e)^{1/2} m_p \simeq 3 \times 10^{44}\text{g}. \tag{1.8}$$

Esto nos dice que estructuras con una masa aproximada de $1 \times 10^{14} M_\odot$ y un radio de alrededor de 70 kpc, puede enfriarse lo suficientemente rápido como para fragmentarse y formar estructuras gravitacionalmente ligadas, que después de enfriarse y contraerse, presentan tamaños y masas que corresponden a galaxias o cúmulos de galaxias.

1.2. Momento angular.

Además de la masa de las galaxias, otra característica física importante es su momento angular. Frecuentemente, el momento angular de las galaxias se caracteriza por el parámetro de espín λ, definido como:

$$\lambda \equiv \frac{L|E|^{1/2}}{GM^{5/2}}, \tag{1.9}$$

donde L, E y M son respectivamente el momento angular, la energía y la masa totales del sistema. Este parámetro nos proporciona una medida del soporte rotacional del sistema, siendo el cociente entre el valor de la velocidad angular real del sistema y el valor que requeriría para que todo su soporte se debiera a la rotación del mismo. Si cuantificamos el soporte rotacional como $g_{rot} \sim v_c^2/r$ y la cohesión gravitacional como $g_G \sim GM/r^2$:

$$\frac{g_{rot}}{g_G} \sim \left(\frac{v_c^2}{r}\right)\left(\frac{r_2}{GM}\right) = M^2 r^2 v_c^2 \left(\frac{GM^2}{r}\right)\left(\frac{1}{G^2 M^5}\right) \sim \frac{L^2 E}{G^2 M^5} = \lambda^2, \tag{1.10}$$

en donde $L \sim Mrv_c$ y $E \sim GM^2/r$. En escenarios de formación galáctica donde las estructuras crecen de manera jerárquica por atracción gravitacional, el modelo

comúnmente aceptado para la adquisición de momento angular es aquél en el que las protogalaxias ganan momento angular mediante torcas de marea debidas a protogalaxias vecinas, teoría propuesta y desarrollada por Hoyle (1949), Peebles (1969, 1971) y Doroshkevich (1970).

En la época previa a la que las protogalaxias se separan de la expansión general de Universo, es poco probable que tengan una forma esférica, lo que provoca que los tirones gravitacionales de las protogalaxias vecinas no se equilibren e impriman torcas a la protogalaxia que termina con una ganancia neta de momento angular. Si los valores típicos para la masa, el radio y el contraste de densidad, en esta época son M, R y δ, la aceleración producida por las fuerzas de marea es $\delta GM/aR$, suponiendo que la separación entre las concentraciones de masa es del mismo orden de magnitud que el tamaño de las protogalaxias. Si además consideramos que las masas involucradas son del orden de $M/2$ y el brazo de palanca va como $R/2$, la torca neta es del orden de

$$T \sim \frac{\delta GM}{a^2 R^2} \times \frac{M}{2} \times \frac{aR}{2} = \frac{\delta GM^2}{4aR}. \tag{1.11}$$

Para un Universo plano, $\delta \sim a$, lo que implica que la torca de marea es constante y que el momento angular crece linealmente con el tiempo, hasta el momento del desacoplamiento con la expansión del Universo, donde los brazos de palanca decrecen considerablemente por contracción gravitacional y la separación entre agregaciones de masa es bastante mayor a los tamaños típicos de las protogalaxias, con lo que este mecanismo deja de ser eficiente.

La adquisición y evolución del espín de una protogalaxia, debido a torcas de marea, es descrito con simplicidad usando la aproximación de Zeldovich (White 1993, Padmanabhan 1995). El punto de partida para esta aproximación es el resultado proveniente de la teoría lineal para el crecimiento de pequeñas perturbaciones, expresada como una relación entre las coordenadas Eulerianas y Lagrangianas de las partículas. Para un universo sin perturbaciones y una densidad uniforme, la posición de cualquier partícula $\mathbf{r}(t)$, se relaciona con su posición inicial $\mathbf{q}$ mediante

$$\mathbf{r}(t) = a(t)\,\mathbf{q}. \tag{1.12}$$

Este resultado es alterado por la presencia de perturbaciones de densidad que crecen con el tiempo. En un régimen lineal, la única modificación que se requiere es la adición de una función separable, que sea función de t y $\mathbf{q}$, de la forma $f(t)\,\mathbf{p}(\mathbf{q}) = a(t)\,b(t)\,\mathbf{p}(\mathbf{q})$. Con la inclusión de esta perturbación, la ecuación 1.12 resulta

$$\mathbf{r}(t) \equiv a(t)\,\mathbf{x}(t) = a(t)\,[\mathbf{q} + b(t)\,\mathbf{p}(\mathbf{q})] \tag{1.13}$$

donde $\mathbf{x}(t)$ es la coordenada comovil Euleriana. Esta ecuación proporciona la posición comovil ($\mathbf{x}$) y la posición propia ($\mathbf{r}$) de una partícula dada al tiempo t, suponiendo que en algún momento en el pasado tuvo la posición comovil $\mathbf{q}$. Para evitar un desarrollo no lineal, generalmente se aplica la ecuación de Zeldovich (ec. 1.13) a un campo de densidad suavizado a escalas galácticas.

El momento angular de la masa que eventualmente formará una galaxia se obtiene a partir de

$$\mathbf{L}(t) = \int_V \left[\mathbf{r}(\mathbf{q},t) - \overline{\mathbf{r}}(\,t)\right] \times \left[\mathbf{V}(\mathbf{q},t) - \overline{\mathbf{V}}\right] \rho(\mathbf{r},t)d^3\mathbf{r}, \qquad (1.14)$$

donde $\mathbf{r}$ y $\mathbf{V}$ describen la posición propia y la velocidad peculiar del elemento de masa respectivamente. La integral es sobre toda la región que eventualmente formaría la galaxia, $\overline{\mathbf{r}}$ es el centro de la masa y $\overline{\mathbf{V}}$ es la velocidad peculiar del centro de masa del sistema al tiempo t. Si la densidad inicial sin perturbar es $\overline{\rho}$, la conservación de masa implica que la densidad perturbada sea

$$\rho(\mathbf{r},t)d^3\mathbf{r} = \overline{\rho}d^3\mathbf{q}. \qquad (1.15)$$

A partir de esta ecuación de conservación, podemos convertir la integral de la ecuación 1.14 a una sobre el volumen Lagrangiano, V_L, que inicialmente contenga la masa de la galaxia. Sustituyendo la solución de Zeldovich (ec. 1.13) por $\mathbf{r}$ en la ecuación para el momento angular, obtenemos

$$\mathbf{L}(t) = a^2 \int_{V_L} \left[\left([\mathbf{q} - \overline{\mathbf{q}}] + b(t)\left[\mathbf{p}(\mathbf{q}) - \mathbf{p}(\overline{\mathbf{q}})\right]\right) \times \dot{b}(\mathbf{p}(\mathbf{q}) - \mathbf{p}(\overline{\mathbf{q}})) \right] \overline{\rho}d^3\mathbf{q}. \qquad (1.16)$$

El producto vectorial entre b y $\dot{b}$ se cancela dado que son paralelos entre sí. Dado que $\mathbf{p}(\mathbf{q}) = \nabla\Phi_0(\mathbf{q})$ donde Φ_0 es el potencial gravitacional, obtenemos

$$\mathbf{L}(t) = \overline{\rho}a^2\dot{b}\int_{V_L} (\mathbf{q} - \overline{\mathbf{q}}) \times \left[\nabla\Phi_0(\mathbf{q}) - \nabla\Phi_0(\overline{\mathbf{q}})\right] d^3\mathbf{q}. \qquad (1.17)$$

De esta manera, el momento angular adquirido por la protogalaxia es de primer orden en la perturbación. Su desarrollo temporal está determinado por el comportamiento de $a^2\dot{b}$, dado que la integral y $\overline{\rho}$ son constantes en el tiempo. Para un universo plano con $b(t) \propto a(t) \propto t^{2/3}$, obtenemos que $a^2\dot{b} \propto t$, con lo que comprobamos la dependencia lineal del momento angular con el tiempo.

Podemos obtener más información si suponemos que Φ_0 dentro de V_L puede ser aproximado por los tres primeros términos de su expansión de Taylor sobre $\overline{\mathbf{q}}$

$$\Phi_0(\mathbf{q}) = \Phi_0(\overline{\mathbf{q}}) + (q_i - \overline{q}_i)\left(\frac{\partial\Phi_0}{\partial q_i}\right)_{\overline{\mathbf{q}}} + \frac{1}{2}(q_i - \overline{q}_i)\left(\frac{\partial^2\Phi_0}{\partial q_i\partial q_j}\right)_{\overline{\mathbf{q}}}(q_j - \overline{q}_j). \qquad (1.18)$$

Sustituyendo esta expansión en la ecuación 1.17, obtenemos que

$$L_i(t) = a^2 \dot{b} \epsilon_{ijk} I_{jl} T_{lk},$$ (1.19)

donde

$$I_{il} = \int_{V_L} (q_j - \overline{q}_j)(q_l - \overline{q}_l) \overline{\rho} d^3 \mathbf{q}$$ (1.20)

es el tensor del momento de inercia de la masa contenida en V_L, y

$$T_{lk} = \frac{\partial^2 \Phi_0}{\partial q_l \partial q_k}$$ (1.21)

es proporcional al campo de marea gravitacional en $\overline{\mathbf{q}}$.

El producto tensorial en la ecuación 1.19 proporciona la torca ejercida sobre un cuerpo extendido inmerso en un campo de marea; $\mathbf{L}$ tiende a cero, sólo y sólo si los tensores T_{ij} e I_{ij} tienen los mismos ejes principales. Dado que el tensor de inercia depende sólo de la forma de la protogalaxia, mientras que T_{ij} depende de la distribución de protogalaxias vecinas, el caso $\mathbf{L} = 0$ es poco probable. La ecuación 1.19 muestra que el momento angular de una galaxia puede provenir del acoplamiento entre el primer orden del campo de marea y el orden cero del momento cuadrupolar de la distribución irregular de masa.

Aún cuando el formalismo anterior provee un método por el cual se puede explicar la adquisición de momento angular mediante torcas de marea, no nos proporciona una descripción detallada del origen preciso y la evolución del momento angular, principalmente por dos razones. En primer lugar, es difícil decidir como especificar V_L, de manera de que abarque toda la masa que finalizará formando parte de la galaxia. En segundo lugar, uno debe tomar en cuenta la evolución de $\mathbf{L}$ durante procesos completamente no lineales en la evolución del sistema. Por ello, en la actualidad, la mejor forma de estudiar la adquisición y evolución detalladas del momento angular, es por medio de simulaciones de n-cuerpos.

Tanto desarrollos analíticos (Peebles 1969, Heavens & Peacock 1988), como simulaciones de N-cuerpos (Barnes & Efstathiou 1987), han permitido estimar el valor típico de λ del orden de 0.04, valor que es bastante menor al esperado para un disco soportado por rotación. Esto puede ser entendido de la manera siguiente. Consideremos una galaxia compuesta por un halo de materia obscura y material bariónico antes de que este colapse mediante enfriamiento y se establezca en el centro de la configuración. Se espera que dicho sistema tenga un valor de espín $\lambda = L \mid E \mid^{1/2} /GM^{5/2}$, en donde todos los parámetros se refieren al conjunto de materia obscura y bariónica. Después del colapso, el gas se asienta en el lugar donde alcanza equilibrio rotacional de acuerdo a su momento angular inicial, formando un disco con $\lambda_d = L_d \mid E_d \mid^{1/2} /GM_d^{5/2}$. Dado que en la configuración inicial, la materia obscura y el material bariónico se encontraban bien

mezclados, el momento angular específico que adquirieron por torcas de marea es el mismo, con lo que $L/M = L_d/M_d$. La energía asociada a la materia obscura será del orden $\sim GM^2/R_h$, mientras que la asociada a la materia bariónica será $\sim GM_d^2/r_d$. Tomando en cuenta estas suposiciones, el cociente entre el espín inicial de la configuración y el espín asociado al disco en equilibrio de una galaxia espiral es

$$\frac{\lambda_d}{\lambda} \propto \left(\frac{R_h}{r_d}\right)^{1/2} \left(\frac{M}{M_d}\right)^{1/2} , \tag{1.22}$$

lo cual nos da valores razonables para las observaciones, tomando en cuenta predicciones de los estudios teóricos para la estimación del espín total.

Diversos estudios (Barnes & Efstathiou 1987, Cole & Lacey 1996, Vitvitska et al. 2002, Bett et al. 2007, Gottlöber & Yepes 2007) han establecido que la distribución del parámetro de espín se encuentra bien ajustada por una función log-normal de la forma

$$P(\lambda) = \frac{1}{\lambda \sigma_\lambda \sqrt{2\pi}} exp\left[-\frac{ln^2(\lambda/\lambda_0)}{2\sigma_\lambda^2}\right] . \tag{1.23}$$
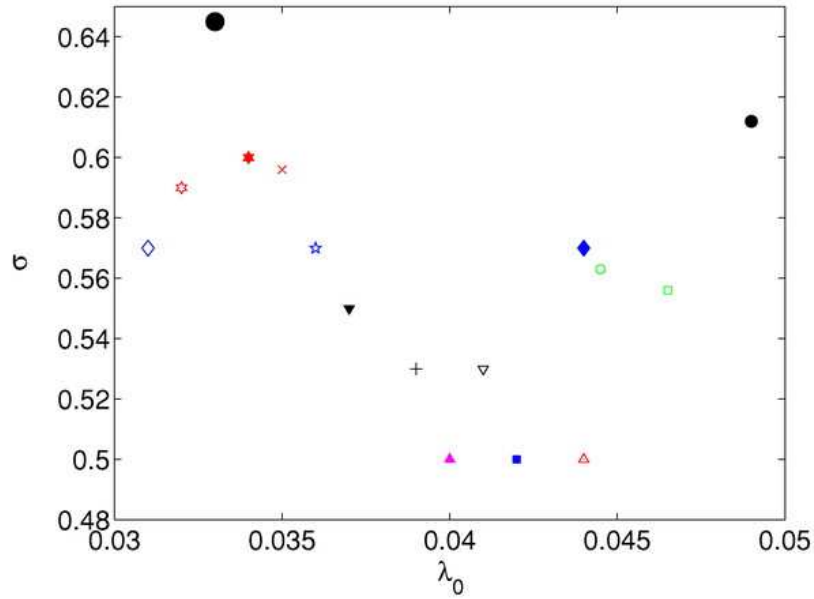

Figura 1.1: Compilación de valores para λ_0 y σ_λ provenientes de diferentes grupos de investigación usando simulaciones numéricas. Figura proveniente de Shaw et al. (2006).

Los valores típicos para el máximo en la distribución λ_0 y el logaritmo en la dispersión σ_λ se muestran en la Figura 1.1, donde se muestran valores para estos parámetros obtenidos por diferentes grupos de investigación empleando diferentes métodos, a partir de simulaciones numéricas. La primera deducción empírica para la distribución de λ a partir de datos observacionales la obtuvimos en este trabajo (Hernández, Park, Cervantes-Sodi & Choi 2007) y la presentamos en el capítulo 3.

1.3. Estructura galáctica.

El modelo que empleamos en el desarrollo del trabajo aquí presentado, es el más sencillo y general posible que nos permita hacer algunas inferencias sobre la estructura general de las galaxias, del tipo de modelo empleado en otros muchos trabajos tales como Sandage, Freeman & Stokes (1970), Brosche (1973), van der Kruit (1987), Fall & Efstathiou (1980), Firmani, Hernández & Gallagher (1996) y Mo, Mao & White (1998). El modelo describe la estructura y evolución de las galaxias de disco modelándolas mediante un halo de materia obscura con un perfil isotermo singular y un disco de materia bariónica, despreciando sus efectos gravitacionales. A continuación describo a grandes rasgos las propiedades generales de este modelo.

Para caracterizar el halo de materia obscura escogimos una esfera con un perfil de densidad isotermo singular de la forma

$$\rho(r) = \frac{V_c}{4\pi G r^2}, \tag{1.24}$$

en donde V_c es la velocidad circular que se establece a lo largo de todo el disco y cuyo valor es independiente del radio r. Esta elección responde a nuestra intención de estimar, de la forma más sencilla posible, el parámetro de espín λ, de manera que se requiera medir el menor número de parámetros y su cálculo sea fácil y rápido, ideal para el manejo de grandes muestras de galaxias, pero rescatando las características globales de las galaxias.

Este tipo de perfil presenta algunos problemas como es la divergencia central, aún cuando esta divergencia no es en la masa cuando se considera un halo truncado, como es el caso de la mayoría de los perfiles que se ajustan a los halos de materia obscura obtenidos mediante simulaciones cosmológicas de n-cuerpos (e. g. Navarro, Frenk & White 1997 abreviado como NFW, Graham, et al. 2006). Otro bemol que presenta este perfil de densidad es que es incapaz de describir características finas como son la presencia de un bulbo central, barras o brazos espirales, el aumento gradual de la velocidad circular para radios pequeños o el decaimiento de esta a radios grandes; pero dado que nuestro objetivo es una descripción global del sistema para medir λ, que es un parámetro integral, y no buscamos describir

rasgos a pequeña escala, el ajuste que obtendremos es lo suficientemente preciso para nuestro estudio. A pesar de su simplicidad, existen valiosos ejemplos de la utilidad de este modelo; por ejemplo, van der Kruit (1987) muestra como éste modelo ajusta datos observacionales y permite explicar la dispersión en el brillo superficial de las galaxias y el establecimiento de la relación Tully-Fisher, a partir de la dispersión presente en la distribución de λ. Swaters et al. (2003), empleando curvas de rotación, concluyen que el modelo isotermo ajusta mejor a la distribución de masa que el perfil NFW y más recientemente, Guimarães & Sodré (2009) alcanzan la misma conclusión, empleando en su estudio lentes gravitatorias.

Al definir el radio del halo como r_{200}, radio al cual la densidad media es $200\rho_{crit}$, siendo ρ_{crit} la densidad crítica a un corrimiento al rojo z dado, se pueden calcular tanto el radio como la masa del halo en función de z como:

$$r_{200} = \frac{V_c}{10H(z)} \tag{1.25}$$

y

$$M = \frac{V_c^2 r_{200}}{G} = \frac{V_c^3}{10GH(z)} \tag{1.26}$$

donde el parámetro de Hubble está dado por

$$H(z) = H_0 \left[\Omega_{\Lambda,0} + (1 - \Omega_{\Lambda,0} - \Omega_0)(1+z)^2 + \Omega_0(1+z)^3 \right]^{1/2}, \tag{1.27}$$

en donde H_0 es la constante de Hubble, Ω_0 la densidad total de materia y $\Omega_{\Lambda,0}$ la densidad de energía obscura.

Si consideramos que la materia bariónica que forma el disco de la galaxia es una fracción constante de la masa del halo m_d, la masa del disco es directamente

$$M_d = \frac{m_d V_c^3}{10GH(z)}. \tag{1.28}$$

Consideramos que el disco es delgado con un perfil superficial exponencial de la forma,

$$\Sigma(R) = \Sigma_0 \exp(-R/R_d), \tag{1.29}$$

en donde Σ_0 es la densidad superficial central y R_d el radio de escala del disco, que se relaciona con la masa total del disco mediante

$$M_d = 2\pi\Sigma_0 R_d^2. \tag{1.30}$$

La ecuación 1.28 establece una relación entre la velocidad de rotación del disco y la masa del mismo, dependiente del corrimiento al rojo. El establecimiento de

esta dependencia puede ser la causa de la relación Tully-Fisher (1977) que establece una dependencia entre la luminosidad y la velocidad de rotación del disco $L_B \sim V_c^\alpha$ con $\alpha \sim 3.5$, una vez establecido el cociente masa-luminosidad. Recientemente se han establecido relaciones Tully-Fisher que relacionan directamente la masa del material bariónico total o del contenido bariónico del disco con la velocidad de rotación del mismo (e.g. Gurovich 2004, Pizagno et al. 2007). Para el caso de galaxias elípticas, la relación correspondiente es la de Faber-Jackson (1976), que también establece una relación entre la dinámica del sistema y su luminosidad, en este caso la dispersión de velocidades y la luminosidad, de la forma Ł $\sim \sigma^x$ con $x \sim 4$.

Despreciando la autogravedad del disco, la curva de rotación está determinada por el perfil de densidad del halo descrito por la ecuación 1.24, el cual establece una velocidad de rotación constante de valor V_c, con lo que su momento angular resulta

$$J_d = 2\pi \int V_c \, \Sigma(R) R^2 dR = 4\pi \Sigma_0 V_c R_d^3 = 2M_d R_d V_c. \tag{1.31}$$

J_d es una fracción, $j_d = J_d/J$, del momento angular total del halo J, el cual se relaciona con el espín galáctico mediante la ecuación 1.9.

La energía total del halo la podemos obtener suponiendo que todas las partículas tienen órbitas circulares y aplicando el teorema del virial, con lo que obtenemos

$$E = -\frac{GM^2}{2r_{200}} = -\frac{MV_c^2}{2}. \tag{1.32}$$

Las expresiones para la energía total, el momento angular y el espín nos permiten calcular tanto el radio de escala como la densidad superficial central como

$$R_d = \frac{1}{10\sqrt{2}}\lambda V_c \left(\frac{j_d}{m_d}\right) H(z)^{-1}, \Sigma_0 = \frac{10}{\pi G} m_d \lambda^{-2} V_c \left(\frac{j_d}{m_d}\right)^{-2} H(z). \tag{1.33}$$

Para simplificar aún más este modelo de estructura galáctica, frecuentemente se supone que $j_d/m_d = 1$, lo que implica que el momento angular específico del halo y del disco son iguales, simplificación frecuentemente empleada en modelos semi-analíticos de formación y evolución galáctica, tales como Cole & Lacey (1996), Mo, Mao y White (1998), Somerville R. S., Primack J. R. y Faber S. M. (2001) y Avila-Reese et al. (2005) entre otros, que de no suponer esta hipótesis obtienen discos con radios de escala un factor de 10 más pequeños que los que se observan.

Esta hipótesis puede ser justificada suponiendo que tanto el gas como la materia obscura se encontraban bien mezclados antes de que el gas disipara su energía y, por lo tanto, experimentaron las mismas torcas de marea que les imprimieron su momento angular. En este tema existen muchos estudios sobre que tan realista es la aproximación, como es afectada esta relación por la fricción dinámica entre
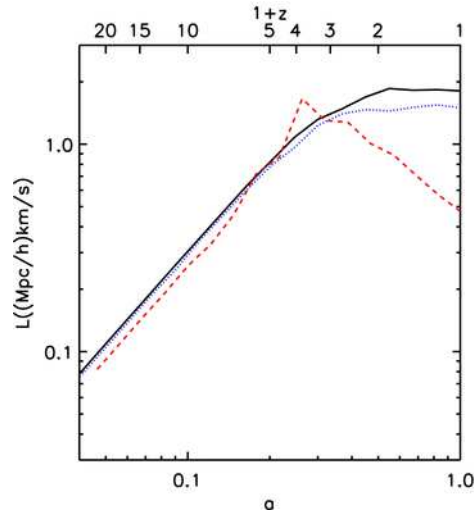
Figura 1.2: Momento angular específico de la componente de materia oscura (línea continua), y la componente bariónica del sistema dominado por el bulbo (línea roja discontinua), y el sistema dominado por el disco (línea azul punteada), en los modelos de Zavala, Okamoto & Frenk (2008)

la materia oscura y los bariones, la redistribución del momento angular por barras y brazos espirales y el papel de la retroalimentación de energía y momento angular por fenómenos de formación estelar, pero hasta la fecha no hay un consenso general. A continuación menciono algunos de estos trabajos para ejemplificar la controversia, hasta el momento, no resuelta.

Heller, Shlosman y Athanassoula (2007) estudiaron la formación de galaxias en halos de materia oscura evolucionados a partir de condiciones iniciales cosmológicas, en donde los bariones incluían la participación del gas en la formación estelar. Sus modelos presentaban configuraciones finales triaxiales, con prominentes barras y bulbos galácticos. Estudiando la respuesta del momento angular a este tipo de perturbaciones, encontraron que la materia oscura pierde entre $1\% - 3\%$ de su momento angular específico a lo largo del tiempo de Hubble, mientras que la pérdida que presenta la materia bariónica es algo mayor, entre $15\% - 25\%$, con lo que estrictamente no se cumple la condición $j_d/m_d = 1$, pero la desviación tampoco es muy grande.

Zavala, Okamoto y Frenk (2008) estudiaron la evolución del momento angular en simulaciones cosmológicas de formación galáctica, usando simulaciones de n-cuerpos con hidrodinámica acoplada y dos diferentes formas de calcular la formación estelar, una enfocada a reproducir la relación de Kennicutt y otra en la que la formación estelar es producida por gas caliente recientemente chocado. El

comportamiento del momento angular total de la materia oscura y los bariones se muestra en la figura 1.2, en donde se observa la evolución del momento angular como función del factor de escala del sistema normalizado al día presente y de su corrimiento al rojo z. Para el caso del modelo cuya formación estelar esta restringida a seguir la ley de Kennicutt (línea roja discontinua), el valor del momento angular de los bariones, al día presente, es sustancialmente menor al momento angular de la materia oscura (línea continua), pero este sistema es incapaz de formar un sistema dominado por un disco, en cambio el modelo que sigue la dinámica del gas para trazar la formación estelar, forma un sistema dominado por un disco y cuyo momento angular (línea azul punteada) sigue el comportamiento del momento angular de la materia oscura a lo largo de la evolución del sistema, resultado que favorece los modelos de formación galáctica de Fall y Efstathiou (1980) y Mo et al. (1998).

Van den Bosch et al. (2002), habían llegado a la misma conclusión que Zavala, Okamoto y Frenk (2008), sobre la estrecha relación que guardan el momento angular específico de la componente de materia oscura y la componente bariónica (figura 1.3, panel izquierdo), pero en trabajos subsecuentes (Dutton & van den Bosch 2008), empleando métodos diferentes, concluyen que para sistemas masivos, el momento angular específico de los bariones tiende a ser menor que el de la componente de materia oscura debido a que el enfriamiento deja de ser eficiente, diferencia que aumenta al incrementarse la masa de los sistemas (figura 1.3, panel derecho).
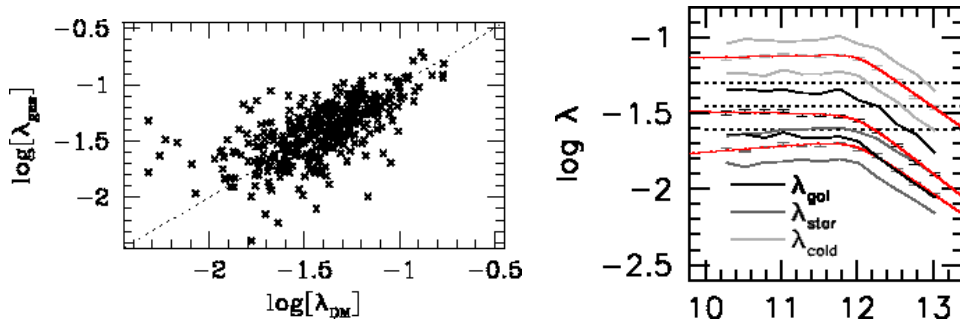
Figura 1.3: *Panel izquierdo:* Relación entre el espín de la componente de materia oscura y la componente bariónica, de las simulaciones de van den Bosch et al. (2002), siendo la línea punteada la relación uno a uno. *Panel derecho:* Valor del espín para la componente bariónica total (λ_{gal}), la componente estelar (λ_{star}), la componente de gas frío (λ_{cold}) y la componente de materia oscura (líneas punteadas), como función del logaritmo de la masa virial del sistema ($\mathrm{Log}[M_{vir}]$), en las simulaciones de Dutton y van den Bosch (2008). En este caso es visible como decrece el valor del espín de las componentes bariónicas, respecto al espín de la componente de materia oscura, para sistemas con masas viriales $M_{vir} \geq 10^{12} M_{\odot}$

Capítulo 2

Propiedades galácticas y espín.

En esta primera parte de la tesis, que comprende este capítulo y el siguiente, me enfocaré a estudiar las dependencias entre el parámetro de espín λ y otras propiedades físicas de las galaxias, a fin de mostrar la fuerte influencia que juega este parámetro en la determinación de la estructura de las galaxias y de esta manera introducir su uso como un parámetro de clasificación galáctica, que cumple con las características de ser un parámetro físico, cuantitativo, objetivo y mensurable.

En este capítulo en particular, presento el modelo empleado para deducir una fórmula que nos permita calcular λ a partir de propiedades observables de galaxias de disco, para lo cual se emplea un modelo que sólo considera un halo de materia obscura con un perfil de densidad isotermo y un disco con densidad superficial de masa exponencial para la materia bariónica. Una vez obtenida nuestra fórmula, planteamos las relaciones que deberían seguir algunas propiedades físicas de este tipo de galaxias con el espín, entre ellas; el tiempo característico de formación estelar en el disco, el espesor del mismo y el cociente bulbo-disco de la galaxia. Haciendo uso de una muestra de galaxias, mostramos cómo las relaciones que esperábamos obtener mediante argumentos teóricos se encuentran presentes en las observaciones. Para ello comparamos el comportamiento de las propiedades físicas como función de λ así como en función del tipo morfológico, para motivar el uso de λ como un parámetro para la caracterización de galaxias que puede ser directamente asociado con un parámetro físico en los estudios teóricos, tanto analíticos como numéricos.

Trabajo publicado en:

- Hernández X., Cervantes-Sodi B., 2006, MNRAS, 368, 351.

A dimensional study of disc galaxies

X. Hernandez[*] and B. Cervantes-Sodi

Instituto de Astronomía, Universidad Nacional Autónoma de México, A.P. 70-264, 04510 México, D.F.

ABSTRACT

We present a highly simplified model of the dynamical structure of a disc galaxy where only two parameters fully determine the solution, mass and angular momentum. We show through simple physical scalings that once the mass has been fixed, the angular momentum parameter λ is expected to regulate such critical galactic disc properties as colour, thickness of the disc and bulge-to-disc ratio. It is, hence, expected to be the determinant physical ingredient resulting in a given Hubble type. A simple analytic estimate of λ for an observed system is provided. An explicit comparison of the distribution of several galactic parameters against both Hubble type and λ is performed using observed galaxies. Both such distributions exhibit highly similar characteristics for all galactic properties studied, suggesting λ as a physically motivated classification parameter for disc galaxies.

Key words: galaxies: fundamental parameters – galaxies: general – galaxies: structure.

1 INTRODUCTION

The first thing an astronomer wants to know about a galaxy is its morphological type, typically expressed through the Hubble classification scheme, introduced about 80 years ago (Hubble 1926, 1936). Some modifications have been introduced to the details of the plan over the years (e.g. de Vaucouleurs 1959; Sandage 1961; Kormendy 1979), although the basics have remained relatively unchanged. The continued usage of the Hubble classification owes its success to the fact that on hearing the Hubble entry of a galaxy, one immediately forms an image of the type of galaxy that is being talked about. A wide variety of physical features of galaxies show good monotonic correlations with Hubble type, despite the presence of significant overlap and dispersion. To mention only a few, total magnitudes decrease towards later types (e.g. Ellis et al. 2005) and colours become bluer while gas fractions diminish from early to late types (e.g. Roberts & Haynes 1994). The bulge magnitudes and bulge-to-disc ratios (B/D ratios) decrease (e.g. Pahre et al. 2004) and discs become thinner (e.g. de Grijs 1998; Kregel, van der Kruit & de Grijs 2002) in going to later types, while the relevance and structure of spiral arms also show marked trends, with decreasing pitch angles, prominence and coherence when one reaches the earlier Hubble types (e.g. Ma 2002; Grosbol, Patsis & Pomoei 2004). Even the functional shape of galactic bulges correlates with types (e.g. Graham 2001).

However, galactic type classification schemes also suffer from several shortcomings. First, the several diagnostics which enter into the assignment of the type, appearance of the spiral pattern, B/D ratios, colour, etc. do so in a fundamentally subjective manner (e.g. Adams & Woolley 1994). One has to take the images to an

expert who will somehow integrate various aspects of the galaxy in question to arrive at the type parameter. That different authors generally agree, together with the correlations between type and various galactic parameters is indicative of a solid physical substrate to galaxy-classification schemes, the particular nature of which, however, has remained elusive. Secondly, type parameters are essentially qualitative (e.g. Lotz, Primack & Madau 2004), which make it difficult to relate type to definitive quantitative aspects of a galactic system, and bring into question the validity of any statistical mathematical analysis performed on galactic populations based on type.

Finally, as has been recognized by many authors, the type given to a galaxy is highly dependent on the information one has regarding the system. This stems from the inputs that determine the galactic type, the relevance of the bulge, typically redder than the disc, means that when observing at longer rest-frame bands, galaxies shift to earlier types, an effect compounded with the high wavelength sensitivity of the bright H II regions which define the structure and morphology of the spiral arms (e.g. Kuchinski et al. 2000; Grosbol, Patsis & Pomoei 2004). This last series of effects is of particular concern when attempting to compare galactic morphologies and types at low and high redshifts, for example, Labbe et al. (2003) have shown that when observing the *Hubble Deep Field* galaxies in more usual rest-frame bands, many of the reported highly disturbed merger morphologies sometimes go away, to reveal essentially standard discs. Similarly, projection effects become important, as the structure of the arm pattern completely disappears in edge-on discs, eliminating one of the diagnostics relevant to the assignment of type.

In summary, certain discomfort sometimes appears regarding the use of morphological type as the principal tool for galaxy classification, in connection to it being somewhat subjective, intrinsically qualitative, and relative to projection and observation wavelength effects.

[*] E-mail: xavier@astroscu.unam.mx

352   *X. Hernandez and B. Cervantes-Sodi*

Several attempts at improving on these problems have appeared over the years, for example, extensive work has been done in constructing an objective spectral classification scheme for galaxies. These works have concentrated sometimes on the shape of the continuum (e.g. Connolly et al. 1995), others on the relevance of spectral emission and absorption features, as in Zaritsky, Zabludoff & Willick (1995). These approaches essentially quantify properties of the underlying stellar populations, mainly yielding an objective description of the relative importance of old and young components. The good correlations observed between spectral classifications and Hubble type, indicate that, indeed, the status of a galaxy's stellar population varies monotonically along the Hubble sequence, although it might be a consequence of a more fundamental dynamical/structural physics determining type, and not the defining causal determinant of type itself. A difficulty in applying schemes of the above type massively will of course remain, in connection to the very telescope-time intensive nature of spectroscopy, which increases with the level of detail required, for example, in going from average shapes of the continuum to the details of spectral lines.

A recent related development is the work of Park & Choi (2005) who have showed that the colour–colour gradient plane is split into regions corresponding to distinct galactic types. This construction is particularly useful for large samples of galaxies, indeed, it was developed and tested using the Sloan Digital Sky Survey. Again, the physical origin of this separation by types appears to be a characterization of the average age and locality of the star formation history of a galaxy, which in turn would have to be traced back to some more fundamental dynamical/formation physics behind type.

A different approach has been the use of neural networks which are trained to reproduce the subjective process through which experts integrate features of a galaxy's image to determine its type. This has the advantage of furnishing a software which can automatically assign galactic types, without the direct intervention of a person (e.g. Adams & Woolley 1994; Naim, Ratnatunga & Griffiths 1997). However, one is left with a black box, the workings of which are difficult to decipher or translate into the physical parameters of a galaxy.

A further line of approach was introduced by Abraham et al. (1994, 1996), who introduced the concentration index C of a galaxy's image as a ratio of two radii, fixed as enclosing two given percentages of the total light of the system, at any given wavelength. This approximately corresponds to a B/D ratio, and was shown to correlate well with typical Hubble types. The scheme was extended by Schade et al. (1995) to include an objective measure of the asymmetry of the projected image, through the A index, essentially the quotient of the residual of the image's light after a $180°$ rotation of it has been subtracted, to the total light. The above approach is particularly sensitive to the effects of mergers and interacting systems, but not very relevant in telling apart the different classes of generally highly $180°$-rotationally symmetric isolated galaxies along the Hubble sequence. The last component of this image-classification scheme is the S clumpiness index introduced by Takamiya (1999) and Conselice (2003), a similar dimensionless index quantifying the degree of small-scale structure in an image, similar to the ratio of small-scale to large-scale power in a polynomial decomposition of the image (e.g. Kelly & McKay 2004). This approach essentially tackles the careful, objective, statistical description of an image through the introduction of the dimensionless parameters expected to be the most representative of the problem. Other variants have appeared, for example, Lotz et al. (2004) defined two different statistical descriptions of the distribution of light on the sky, and show that this allows an adequate automatic assignment of a galaxy's classical Hubble type.

The above methods, however, remain somewhat sensitive to projection and wavelength effects, but more seriously, do not include any explicit information of the dynamics of the problem. Certainly, the ability to deduce a galaxy's Hubble type from its concentration, asymmetry, clumpiness index (*CAS*) or other careful objective, dimensionless characterization of its image, suggests that these factors vary monotonically along the Hubble sequence. Again, it is not evident how the structural physics of the problem result in a given point in the *CAS* space.

Monotonic trends with the Hubble type suggest that after having fixed the mass, there might exist one other parameter whose variation gives rise to the Hubble sequence. Many approaches to galaxy formation and evolution have appeared over the years, generally reaching the conclusion that it is the angular momentum of a galactic system what determines its main characteristics. Some examples of which are: Sandage, Freeman & Stokes (1970), Brosche (1973), van der Kruit (1987), Fall & Efstathiou (1980), Flores et al. (1993), Firmani, Hernandez & Gallagher (1996), Dalcanton, Spergel & Summers (1997), van den Bosch (1998), Hernandez & Gilmore (1998), Avila-Reese, Firmani & Hernandez (1998), Zhang & Wyse (2000), Ferguson & Clarke (2001), Silk (2001), Bell (2002) and Kregel, van der Kruit & Freeman (2005).

A second problem is what determines the angular momentum of a galaxy at any given time, with older modellings taking this value as a fundamental parameter fixed by initial conditions in the remote past, and more recent cold dark matter (CDM) cosmological simulations deducing this value as a consequence of the tidal fields of surrounding matter, in combination with the formation history of a halo, with merger events and gas cooling being fundamental to a determination of the sometimes fluctuating value of a galactic system's angular momentum, for example, the cosmological N-body studies of Warren et al. (1992), Cole & Lacey (1996), Lemson & Kauffmann (1999), Steinmetz & Navarro (1999) and Navarro & Steinmetz (2000) or the analytical work of Catelan & Theuns (1996). Whatever the origin or evolution of this parameter, once the mass of a galaxy has been chosen, theoretical studies have typically identified the angular momentum of the system as the principal determinant of a galaxy's type. We will therefore focus our attention on this parameter.

Many different models of the structure and evolution of a disc galaxy exist, with varying degrees of detail and including diverse physical aspects of the problem, for example, asides from the above references, including a more explicit cosmological formation scenario, Frenk et al. (1985, 1988), White & Frenk (1991), Mo, Mao & White (1998), Somerville & Primack (1999), Maller, Dekel & Somerville (2002) and Klypin, Zhao & Somerville (2002), to mention only but a representative few. Here, we present the simplest possible physical treatment of the problem, not in an attempt to reproduce or understand the details of a disc galaxy, but rather to obtain a first-order approximation which might capture the monotonic trends nicely followed by the Hubble sequence. We present a highly simplistic physical modelling of a disc galaxy which allows to estimate its angular momentum parameter λ (Peebles 1969) from readily obtainable structural characteristics.

The layout of our paper is as follows. Section 2 presents the physics of the dimensional analysis of disc galaxies, leading to an observational estimate of the λ parameter for any real galaxy. This parameter is then calculated for a large sample of galaxies in Section 3, where we also explore the trends followed by different observed galactic properties with λ, and compare with the equivalent trends seen for the Hubble classification. In Section 4, we compare our estimated λ parameter for several simulated galaxies from various authors, and present a discussion of our results and conclusions.

2 THEORETICAL FRAMEWORK

As discussed in Introduction, the good monotonic trends followed by a variety of galactic properties along the Hubble sequence reflect not only the usefulness of it, but also suggest that to first order, a disc galaxy can be described by only two parameters: total mass, and some other physical parameter varying monotonically along the Hubble sequence. As mentioned in Introduction, extensive theoretical work leads to the angular momentum as a natural choice for this parameter.

Having chosen the angular momentum as our second parameter, we now construct a simple physical model for a galaxy which allows to estimate this parameter directly from observed galactic properties.

In the interest of capturing the most essential physics of the problem, the model we will develop will be the simplest one could possibly propose, little more than a dimensional analysis of the problem.

2.1 Estimating λ from observations

We will model only two galactic components, the first one a disc having a surface mass density $\Sigma(r)$ satisfying

$$\Sigma(r) = \Sigma_0 e^{-r/R_d}, \tag{1}$$

where r is a radial coordinate and Σ_0 and R_d are two constants which are allowed to vary from galaxy to galaxy. The total disc mass is now

$$M_d = 2\pi\Sigma_0 R_d^2. \tag{2}$$

The second component will be a fixed dark matter halo having an isothermal $\rho(r)$ density profile, and responsible for establishing a rigorously flat rotation curve V_d throughout the entire galaxy, an approximation sometimes used in simple galactic evolution models (e.g. Naab & Ostriker 2006), such that

$$\rho(r) = \frac{1}{4\pi G}\left(\frac{V_d}{r}\right)^2, \tag{3}$$

and a halo mass profile $M(r) \propto r$. Since the total mass of the disc is finite, we define the disc mass fraction as $F = M_d/M_H$. Requiring a finite total halo mass, M_H, will now imply a truncation radius for the dark halo, R_H given by the equation

$$M_H = \int_0^{R_H} \frac{V_d^2}{G}\,dr \Rightarrow \tag{4}$$

$$R_H = \frac{M_H G}{V_d^2}.$$

The disc mass fraction F is expected to be of the order of 1/10 or smaller (e.g. Flores et al. 1993; Hernandez & Gilmore 1998), hence, we will use global parameters for the entire system indistinctly from halo parameters, consistent with having ignored disc self-gravity in equation (3).

It will be convenient to refer not to the total angular momentum L, but to the dimensionless angular momentum parameter

$$\lambda = \frac{L\,|\,E\,|^{1/2}}{G M^{5/2}}, \tag{5}$$

where E is the total energy of the configuration and G is Newton's gravitational constant. λ in fact gives the ratio of the actual angular momentum of the system to it's maximum possible break-up value, $\lambda = 1$ is hence an upper limit.

We must now express λ in terms of structural galactic parameters readily accessible to observations. First, we assume that the total potential energy of the galaxy is dominated by that of the halo; and secondly, that this is a virialized gravitational structure, which allows to replace E in the above equation for $W/2$, one-half the gravitational potential energy of the halo, given by

$$W = -4\pi G \int_0^{R_H} \rho(r)M(r)r\,dr. \tag{6}$$

Use of equation (3) yields

$$W = -V_d^2 M_H, \tag{7}$$

assuming that the specific angular momenta of disc and halo are equal, $l_d = l_H$, as would be the case for an initially well-mixed protogalactic state, and generally assumed in galactic formation models (e.g. Fall & Efstathiou 1980; Mo, Mao & White 1998).

The specific angular momentum of the disc, following the assumption of a rigorously flat rotation curve and equation (1), will now be $l_d = 2V_d R_d$. We can now replace L for $M_H l_d$. Introducing this last result together with equation (7) into equation (5) yields

$$\lambda = \frac{2^{1/2}V_d^2 R_d}{G M_H}. \tag{8}$$

Finally, we can replace M_H for M_d/F, and introduce a disc Tully–Fisher relation:

$$M_d = A_{TF} V_d^{3.5} \tag{9}$$

into equation (8) to yield

$$\lambda = \left(\frac{2^{1/2}F}{A_{TF}}\right)\frac{R_d}{G V_d^{3/2}}. \tag{10}$$

The existence of a general baryonic Tully–Fisher relation between the total baryonic component and V_d of the type used here, rather than a specific Tully–Fisher relation involving total magnitude in any particular band, is supported by recent studies, in general agreement with the 3.5 exponent, we assume (e.g. Gurovich et al. 2004, or Kregel et al. 2005 who found 3.33 ± 0.37). All that remains is to choose numeric values for F and A_{TF}, to obtain an estimate of the spin parameter of an observed galaxy in terms of the structural parameters readily accessible to observations, R_d and V_d.

Taking the Milky Way as a representative example, we can use a total baryonic mass of $1 \times 10^{11}\,M_\odot$ and $M_H = 2.5 \times 10^{12}\,M_\odot$ (where the estimate of the baryonic mass includes all such components, disc, bulge, stellar halo, etc., e.g. Wilkinson & Evans 1999; Hernandez, Avila-Reese & Firmani 2001), as suitable estimates to obtain $F = 1/25$. For a rotation velocity of $V_d = 220\,\mathrm{km\,s^{-1}}$, the above numbers imply $A_{TF} = 633\,M_\odot\,(\mathrm{km\,s^{-1}})^{-3.5}$; this in turn allows to express equation (10) as

$$\lambda = 21.8\frac{R_d/\mathrm{kpc}}{\left(V_d/\mathrm{km\,s^{-1}}\right)^{3/2}}, \tag{11}$$

which is the final result of this subsection. The above equation allows a direct estimate of λ, a dimensionless numerical parameter with a clear physical interpretation for any observed galaxy, with no degree of subjectivity and little sensitivity to orientation effects. The only ambiguity which remains is the definition of the wavelength at which R_d is measured. Recently, de Grijs (1998) and Yoachim & Dalcanton (2005) have measured significant variations in R_d with wavelength. In the spirit of obtaining global mass distribution parameters, it is clear that observations in the r band or near-infrared are required for the measure of R_d, necessary in equation (11). Also, given the Tully–Fisher relation, it is clear that V_d in equation (11) can be replaced for

354   *X. Hernandez and B. Cervantes-Sodi*

total magnitude on a given band, for cases where the rotation velocity is not available. It is clear from its derivation that equation (11) is only an approximate way of inferring the λ parameter of an observed galaxy, intended as an objective and quantitative improvement on current classification schemes, and not as a detailed measurement of the angular momentum of a real galaxy. If one intended a more careful measurement of λ, a full dynamical modelling of the rotation curve and bulge and disc matter distribution would be required, of the type found in, for example, Tonini et al. (2006).

For the Galactic values used above, equation (11) yields $\lambda_{MW} = 0.0234$, in excellent agreement with recent estimates of this parameter, for example, through a detailed modelling of the Milky Way within a CDM framework; Hernandez et al. (2001) found $\lambda_{MW} = 0.02$.

2.2 Expected scalings with λ

We now study the expected scaling between λ and other observables of a disc galaxy, for example, colour, gas fraction, star formation activity, degree of flatness of the disc and B/D ratios. The main ingredient will be the Toomre parameter

$$Q(r) = \frac{\kappa(r)\sigma(r)}{\pi G \Sigma(r)}, \tag{12}$$

where $\kappa(r)$ is the epicyclic frequency at a given radius, and $\sigma(r)$ is the velocity dispersion and $\Sigma(r)$ the disc surface density of any given galactic disc component. This parameter measures the degree of internal gravitational stability of the disc, with $\kappa(r)$ accounting for the disruptive shears induced by the differential rotation, $\sigma(r)$ modelling the thermal pressure of a component, both in competition with $\Sigma(r)G$, the self-gravity of the disc. Values of $Q \leqslant 1$ are interpreted as leading to gravitational instability in a 'cold' disc. In the interest of the simplicity of the description, and bearing in mind that the angular velocity and the epicyclic frequency are within a factor of the order of unity of each other, for example, in a flat rotation curve, $\kappa(r) = \sqrt{2}\Omega(r)$, we will replace $\kappa(r)$ in equation (12) with $\Omega(r) = V_d/r$, the angular velocity of the disc.

The star formation processes in the disc have often been thought of as forming a self-regulated cycle. The gas in the regions where $Q < 1$ is gravitationally unstable; this leads to collapse and the triggering of star formation processes, which in turn result in significantly energetic processes. The above include radiative heating, the propagation of ionization fronts, shock waves and in general an efficient turbulent heating of the gas media, raising σ locally to values resulting in $Q > 1$. This restores the gravitational stability of the disc and shuts off the star formation processes. On time-scales longer than the few $\times 10$ Myr of massive stellar lifetimes, an equilibrium is expected where star formation proceeds at a rate equal to that of gas turbulent dissipation, at time-averaged values of $Q \sim 1$. Examples of the above can be found in Dopita & Ryder (1994), Koeppen, Theis & Hensler (1995) and Silk (2001).

For example, Silk (2001) used ideas of this type to derive the local volume density of star formation $\dot{\rho}_{sf}$ as

$$\dot{\rho}_{sf} = \Omega \rho_g \sigma_g, \tag{13}$$

where volume densities will be given by $\rho = \Sigma/h$, h the disc scaleheight. Employing the Toomre criterion at $Q = 1$ to rewrite the gas velocity dispersion in terms of the gas surface density, equation (13) may be written as follows:

$$\dot{\Sigma} = \pi G \Sigma_g^2. \tag{14}$$

The above represents a simple derivation of a Schmidt law; other similar options have been proposed that also lead to Schmidt laws with exponents between 1 and 2 (e.g. Firmani, Hernandez & Gallagher 1996). We now use a characteristic time for the star formation process in the disc $\tau_{sf} = \Sigma_g/\dot{\Sigma}$, that gives an idea of the time a galaxy can support a star formation rate of constant magnitude; if its value is small, the duration of star formation processes will be short, the population presently old and consequently, the galaxy will be red and have a low gas fraction. On the other hand, a galaxy with large τ_{sf} will experience a long star formation duration, and show a young population resulting in bluer colours and a high gas fraction.

From the above relation τ_{sf} becomes

$$\tau_{sf} = \frac{\pi G}{\Sigma_g} = \frac{2\pi^2 G R_d^2}{M_d}. \tag{15}$$

Note that at fixed disc mass (or fixed V_d, through the Tully–Fisher relation), from equation (11), λ will scale with R_d, which translates into a relation between τ_{sf} and λ:

$$\tau_{sf} \propto \lambda^2. \tag{16}$$

In the above, representative values of $\kappa(r)$, $\Omega(r)$, $\Sigma(r)$, $\sigma(r)$ and $\rho_g(r)$ have been assumed, for example, evaluating all variables at $r = R_d$. If one assumes a different star formation scheme from what was used above, equation (16) will change. However, for a variety of similar simple schemes, the proportionality given will be altered only in the change of the exponent, which will remain >1. Alternatively, one could start from an empirical Schmidt law of power n, a scaling $\tau_{sf} \propto \lambda^n$ will always result, which does not alter our conclusions provided $n > 1$, a general trait of Schmidt laws found in the literature (e.g. Silk 2001).

Large values of λ will correspond to long star formation periods; for this case, we expect to have galaxies with young populations and looking relatively blue. Galaxies with low λ will have short star formation periods; for them, we will hardly see young stars and they will look red and gas poor. A scatter on this trend will be introduced by variations in total mass, together with a systematic reduction in τ_{sf} in going to larger masses (cf. equation 15), in accordance with larger average galactic masses found at earlier types.

The ratio of disc scaleheight to disc scalelength, h/R_d, is another measurable characteristic of galaxies which it is easy to show, will also scale with λ. Assuming a thin disc, virial equilibrium in the vertical direction (Binney & Tremaine 1987) yields a relation between h and Σ:

$$h = \frac{\sigma_g^2}{2\pi G \Sigma}. \tag{17}$$

We use this relation for h to replace the gas velocity dispersion appearing in equation (12) for a combination of h and the surface density. The dependence on Σ is replaced by a dependence on M_d, M_H and λ to get a new expression for Toomre's stability criterion, which evaluating radial dependences at $r = R_d$ yields

$$Q^2 = e\, 2^{5/2} \left(\frac{M}{M_d} \right) \left(\frac{h}{R_d} \right) \lambda. \tag{18}$$

With $F = 1/25$, evaluating at $Q = 1$, the stability threshold suggested by the self-regulated star formation cycles, the ratio h/R_d is obtained as

$$\frac{h}{R_d} = \frac{1}{390\lambda}, \tag{19}$$

a simplified version of the result of van der Kruit (1987). For the Galactic value derived above of $\lambda_{MW} = 0.0234$, equation (19) gives

$R_d = 9h$, not in conflict with the parameters for the Milky Way. For galaxies with large values of λ, we expect thin systems, while galaxies with small values of λ, will show thick discs, as the observed trend of (h/R_d) decreasing in going from early-type discs to late-type galaxies (e.g. de Grijs 1998; Yoachim & Dalcanton 2005).

Another important observable characteristic of the morphology of a galaxy, which shows clear trends with Hubble type, is the B/D ratio. From observations, it is clear that the central regions of the disc of a galaxy are dynamically 'hot', because of the large velocity dispersion present in comparison to the tangential rotation velocity. With this in mind, we introduce a kinematic definition of the bulge (e.g. Hernandez 2000) as the region where the velocity dispersion is comparable to the circular velocity of the disc. The ratio will be given by

$$\frac{B}{D} = \frac{\int_0^a 2\pi\Re\Sigma(\Re)d\Re}{\int_a^\infty 2\pi\Re\Sigma(\Re)d\Re}, \tag{20}$$

with $\Re$ defined as $\Re = r/h$ and a a dimensionless parameter $\geqslant 1$. The bulge mass is the mass contained from the centre of the disc to a distance equal to a multiple of h; ah, and the disc mass is the remainder. The dependence of the h/R_d ratio is changed for a dependence in λ, using equation (19). The above equation leads to:

$$\frac{B}{D} = \frac{L(e^{a/L} - 1) - a}{L + a}, \tag{21}$$

where we have introduced $L = 390\lambda$. We expect to find galaxies with large bulges for the low-λ values. Of course, other processes which we have not considered, such as all manner of galactic interactions, will result in angular momentum transfer and generally the induction of matter flows towards the bottom of the potential well, that is, an increase in the B/D ratios. This leads us to expect significant spread.

Also, the analysis of this section implies an increase in the values of R_d and a decrease in Σ_0 for more flattened, high-λ discs. This could account for the observation of a negative correlation between R_d and Σ_0 found by Kregel et al. (2005). These authors also find through dynamical modelling of galaxies having 2D photometry, that the mass-to-luminosity ratios of galaxies increase for more flattened (low h/R_d ratios) discs. This last trend appears naturally, if we think of flattened discs as coming from the high-λ values, leading to large R_d and hence galactic discs that extend far out into their dark haloes, out to regions where the dominance of the dark component is increasingly obvious. Compounding the above is the fact that the volume density of discs scales with $(hR_d^2)^{-1}$, hence since h scales with λ^{-1} and R_d does so with λ^2, to this level of the analysis, the volume density of the disc will decrease linearly with λ, leading to a decrease in the gravitational potential of the disc. Variations in mass will again introduce scatter into the above trends.

As we have shown in this subsection, in general, galaxies with small values of λ would be expected to be red, have a low gas content, show little present star formation, thick discs and typically large B/D ratios, the defining traits of early spirals. On the other hand, for large values of λ, we expect blue, thin galaxies showing the small B/D ratios of late-type and low surface brightness discs. It appears reasonable to expect the observational estimates of λ of equation (11) to show all the trends of the Hubble sequence, indeed, from the point of view of galactic formation scenarios, it is λ what defines a galaxy's type (e.g. Fall & Efstathiou 1980; van der Kruit 1987; Flores et al. 1993; Dalcanton et al. 1997; Hernandez & Gilmore 1998; van den Bosch 1998).

Note that this simple model will be valid independently of the formation scenario of a disc galaxy. Whether low values of λ for early spirals are fixed in the remote past as initial conditions, or the

result of cancellation of angular momentum due to repeated mergers, equation (11) will still give a reasonable estimate of the value of λ for a disc galaxy at a given time of observation. The model presented in this section isolates the main physical ingredients responsible for the correlations between the galactic observables described. Other more complex and complete models have been presented in the past which, however, do not deviate significantly from the basic assumptions of Section 2.1, and consequently reach conclusions not drastically different from the ones of Section 2.2, if we limit the comparison to only the specific aspects of the problem being treated here. Examples of the above are the analytical schemes of van der Kruit (1987), refined later by Dalcanton et al. (1997), or the more numerical schemes of Fall & Efstathiou (1980) and Flores et al. (1993), before the arrival of fuller hydrodynamical and cosmological simulations.

3 OBSERVATIONAL DATA

To compare the relations obtained in the preceding section with the observational data of real galaxies, we used two samples of galaxies: the Atlas for Structural Studies of Spiral Galaxies (ASSSG) of the Spiral Galaxy data base of Courteau (1996, 1997) and a sample taken from de Grijs (1998) based on the Surface Photometry Catalogue of the ESO-Uppsala Galaxies (ESO-LV; Lauberts & Valentijn 1989), and the subsequent re-analysis of these data by Kregel et al. (2002), henceforth dGKK. This last work considers carefully issues related to dust contamination, projection and radial variations in disc scaleheight. The ASSSG consists of a data base of 304 late-type spiral galaxies, including structural parameters such as rotation velocities and R_d, measured in the R band. This last point is important, as we require a measure of the extent of the disc mass, and red bands are more sensitive to underlying old stellar populations and are little affected by dust.

From this sample, we used the reported disc circular velocity measured at 2.15 disc scalelengths, the corrected disc scalelength, the colour term $B - R$ and the ratio of fitted disc light to total measured light for the whole galaxy. The last component is used to estimate the B/Ds. The spectral band used for these measurements was the R band. All the galaxies which show some kind of interaction were suppressed for the analysis, together with spherical and irregular galaxies. One difficulty of using this sample, in connection with our present goals, is the lack of early-type spirals. This will make trends with Hubble type appear harder to detect, as it is often between the Sa and the latter types that the largest changes occur. However, the uniform treatment of the data, the large sample and the long observational wavelengths make the ASSSG sample worthwhile. If some trends can be seen even in the absence of Sa galaxies, as it is indeed the case, it is to be expected that their inclusion would only strengthen further our conclusions.

The dGKK sample consists of 33 edge-on galaxies from which we used the I-band exponential scaleheight and exponential scalelength and the maximum rotational velocity. Again, it is the red wavelength of observation that makes this particular sample relevant to our analysis.

As mentioned in the preceding section, we expect a correlation between the λ parameter and the Hubble type, since the analysis of Section 2 leads one to suspect that it is this what primarily determines the properties of the galaxy which are taken into account for its classification. In Fig. 1, we present the distribution of the ASSSG sample as a function of λ, estimated through equation (11). For the entire sample, the mean value is $\langle \lambda \rangle = 0.0645$. We see an approximately Gaussian shape, with a considerable extension towards the
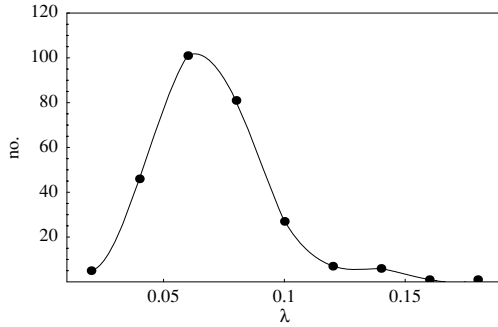
356   *X. Hernandez and B. Cervantes-Sodi*

Figure 1. Distribution of values of λ through equation (11) for the complete ASSSG sample, with dots showing the binning.

Figure 3. Hubble type as a function of the circular velocity for the galaxies in the ASSSG sample.

larger values of λ. We do not explore the details of this distribution further, as the ASSSG sample is not intended to be complete or statistically unbiased in any sense. However, use of equation (11) in one such sample should prove useful in obtaining an empirical distribution of λ parameters, to compare, for example, against predictions from cosmological models. These models yield theoretical distributions for galactic values of λ resulting from tidal interactions of the material accreting onto a protogalaxy and global surrounding dark matter tidal fields, which are sensitive to cosmological parameters such as Ω_Λ and the details of the initial fluctuation spectrum (e.g. Warren et al. 1992; Catelan & Theuns 1996; Cole & Lacey 1996; Lemson & Kauffmann 1999). The above parameters could in principle then be constrained through empirical inferences of the present-day distribution of λ inferred through equation (11) and a large unbiased sample of galaxies.

Secondly, we divide the ASSSG sample by Hubble type into three groups: Sb, Sbc and Sc. The result is shown in Fig. 2, where the continuous curve in panel (a) shows the distribution of the values of λ for the Sb sample, and the dashed curve for the Sc sample. We see that, as expected, the Sc galaxies are characterized by larger values of λ, although significant overlap occurs. Panel (b) gives the λ distribution for the Sbc subclass, by comparing to panel (a), it is interesting that this class appears as a superposition of the previous two classes, with the exception of the tail towards large values of λ seen in the Sc sample. This last point highlights the difficulty in making detailed distinctions among the subclasses in the Hubble sequence, and agrees with the conclusions of Ellis et al. (2005), who analysed and classified automatically through a variety of elaborate
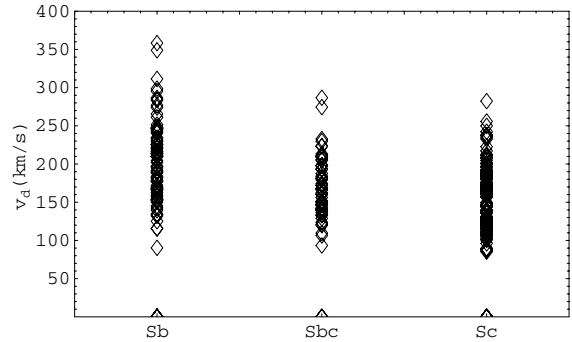
statistical analyses on many galactic parameters a large sample of galaxies, and concluded that only two definitive classes are naturally suggested by the data, late and early spirals.

In general, the bulk of a galactic population moves to larger values of λ for later types; the mean value for each group is: $\langle \lambda \rangle_{Sb} = 0.0574$, $\langle \lambda \rangle_{Sbc} = 0.0649$ and $\langle \lambda \rangle_{Sc} = 0.0689$.

Next, we analyse and compare the statistical distributions of V_d as functions of Hubble type and λ, also for the ASSSG. In Fig. 3, we present the distribution of galactic rotation velocities V_d with morphological type. Earlier types present a wide dispersion of velocities, which diminishes slightly for the later types, where lower mean values are found. For this analysis, we obtained mean values for every subsample: $\langle v \rangle_{Sb} = 205.41 \, \mathrm{km\,s^{-1}}$, $\langle v \rangle_{Sbc} = 172.42 \, \mathrm{km\,s^{-1}}$ and $\langle v \rangle_{Sc} = 155.95 \, \mathrm{km\,s^{-1}}$, a monotonic trend is clear, although very significant overlap is present. This result is well known, and reflects the similar trend of decreasing total luminosities with type (e.g. Roberts & Haynes 1994; Ellis et al. 2005).

Fig. 4 gives a plot of V_d versus λ for the galaxies appearing in Fig. 3. We see that, despite considerable dispersion and overlap, galaxies with large values of λ are restricted to the lower values of V_d, while at low values of λ, a much wider range of V_d is present. The mean V_d at each λ decreases with λ, as is seen when plotting against Hubble type in Fig. 3.

An important measurable parameter for the classification of a galaxy is its colour, giving information on the evolutionary state of the stellar population. One of the clearest trends seen along the Hubble sequence is precisely the shift to bluer colours when going
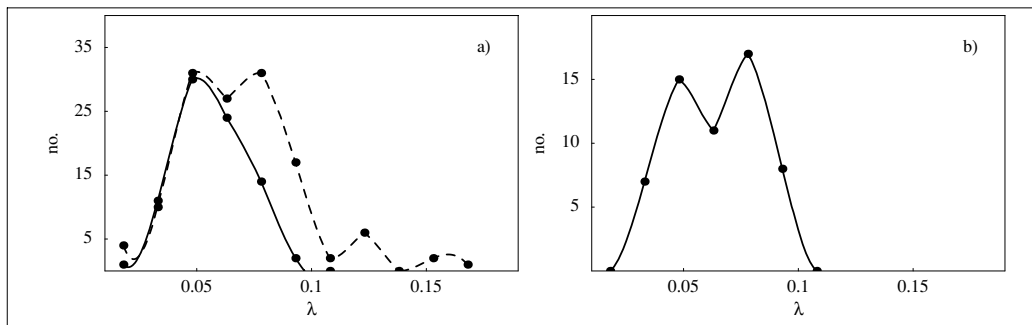

Figure 2. (a) The solid line represents the distribution of values of λ through equation (11) for Sb galaxies in the ASSSG sample, the dashed line gives the equivalent distribution for Sc galaxies. (b) Distribution of values of λ for the Sbc galaxies in that same sample. Dots showing the binning.
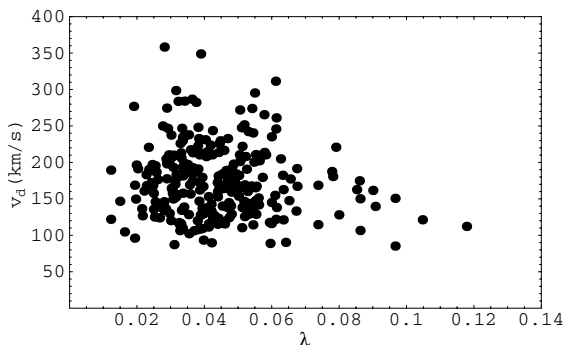
Figure 4. Values of the circular velocity plotted against λ through equation (11) for the galaxies in the ASSSG sample.
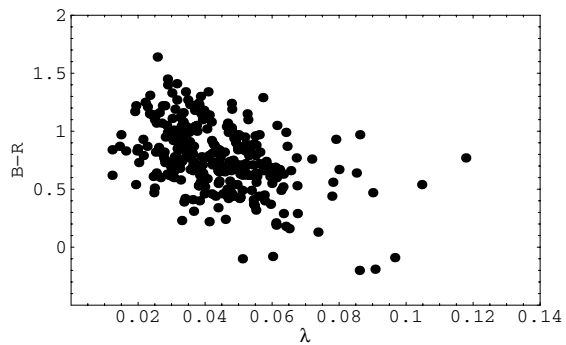

Figure 6. Values of the $B - R$ colour term plotted against λ through equation (11) for all the galaxies in the ASSSG sample.
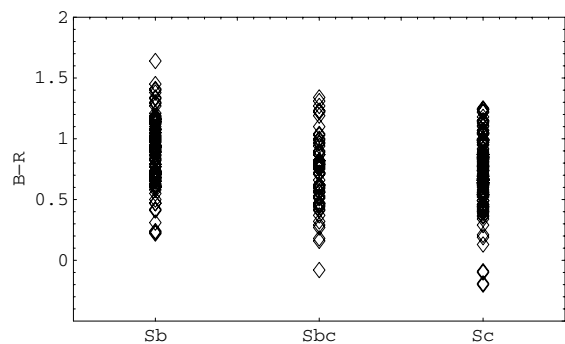

Figure 5. Relation between the Hubble type and the $B - R$ colour term, for the galaxies in the ASSSG sample.
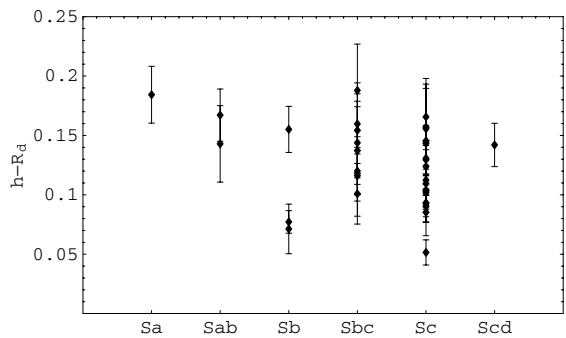

Figure 7. h/R_d ratios for galaxies according to their Hubble type, for galaxies in the dGKK sample.

towards the later types (e.g. Roberts & Haynes 1994; Park & Choi 2005). The ASSSG sample shows this expected relation clearly in Fig. 5, where we plot $B - R$ colour for the different types.

In Section 2, we proposed a relation between λ and the colour of a galaxy supported by the idea of the existence of a characteristic time-scale for the star formation process, which should increase with λ. In order to examine the validity of our statement, we present the relation of these two parameters for the ASSSG sample, in Fig. 6. It is clear that the sample follows a marked tendency, the $B - R$ term decreases with λ, which is in agreement with our predictions. The agreement of this trend with the equivalent one seen for the Hubble types reinforces the idea that the single most important galactic parameter which is varying along the Hubble sequence is precisely λ.

The analysis of the distribution of h/R_d ratios was made with the dGKK sample. It contains galaxies with more morphological types: from Sa to Scd galaxies. This spread of types allows us to see clearly if there is any kind of tendency regarding the h/R_d ratio and the Hubble types. Fig. 7 shows early galaxies presenting varied values for the h/R_d ratio, although the mean shows a clear diminishing trend in going to latter types, very similar to what was seen for V_d and colour. Late-type galaxies at the Sc end clearly show on average much thinner discs than the earlier types, as confirmed by several authors over the last few years (e.g. Yoachim & Dalcanton 2005). It is interesting to note that in the re-analysis of the de Grijs (1998) data by Kregel et al. (2002), not only do the values of R_d and h change but, perhaps surprisingly, also the Hubble types of the

galaxies are significantly shifted around, sometimes by more than one subtype. This last point highlights again the subjective nature of 'type'-classification schemes for galaxies.

The complementary plot to Fig. 7 is given in Fig. 8, where instead of presenting h/R_d versus λ, we use a logarithmic plot to better detect the presence of a relation between these two parameters of the type the dimensional analysis of Section 2 leads us to expect, cf. equation (19). The line drawn in Fig. 8 is the best-fitting straight line for the sample, having a slope of -0.4 ± 0.9, not at odds with the value of -1, predicted by the simple model. The expectations of the model are seen to be generally borne out by the data, albeit the large errors present.

The last galactic property which we analyse is the B/D ratios. For this, we return to the ASSSG sample, and attempt an estimate of this parameter from the reported total light, and the reported extrapolation for a total disc light coming from the interpolated central disc brightness and measured disc scalelength values, by assuming that the total measured light is the sum of the disc light and the light coming from the bulge. This is, of course, not ideal, as for example, truncated discs will give artificially large values of the B/D ratio. This and other effect, however, will affect all the galaxies of the sample in the same way. Therefore, the error is of the same order of magnitude for each and it allows us to look for and compare trends against both Hubble type and λ, although the actual values of the B/D ratios might be off, and the dispersion artificially broadened.

Fig. 9 gives these B/D ratios against Hubble type, the extent of values found for each class is comparable, but the means show a
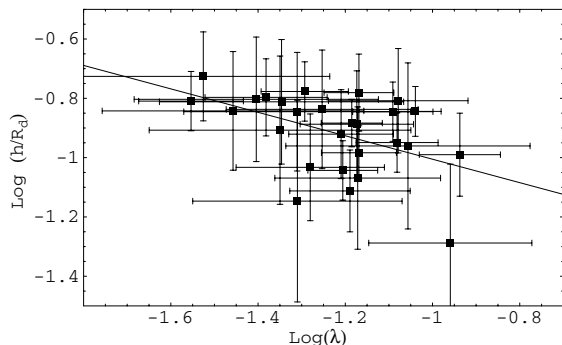
358   *X. Hernandez and B. Cervantes-Sodi*

Figure 8. Logarithmic plot of the relation between λ and h/R_d, for galaxies in the dGKK sample, the solid line shows a linear fit to the data, yielding a slope of -0.4 ± 0.9.
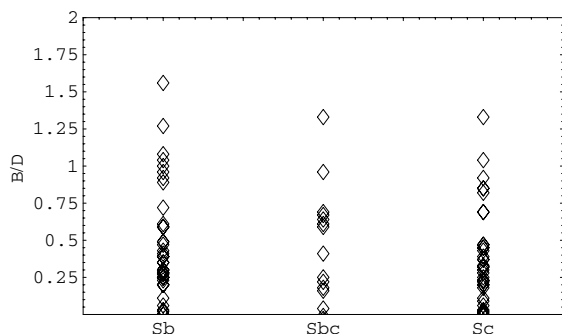

Figure 9. B/Ds for galaxies classified by their Hubble type, for the ASSSG sample.

very clear trend, with 'Sc' clustering at low values of B/D. This trend is again well known, and in fact, small bulges are one of the defining characteristics of late-type galaxies.

The final plot of this section, Fig. 10, gives the same values of the B/D of Fig. 9, but plotted this time against the value of λ derived for each galaxy in the ASSSG sample through equation (11). We again see something very similar to what the corresponding 'type' figure shows. Indeed, all the galactic properties examined show very similar trends, large dispersions which drop towards later types, with
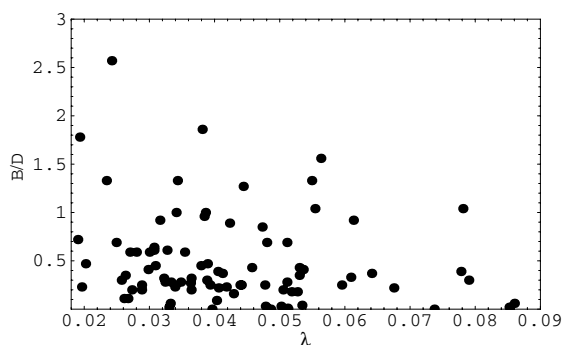

Figure 10. Plot of the B/Ds for galaxies in the ASSSG sample, as a function of their inferred values of λ from equation (11).

means that show distinctive and very similar decreasing trends with either type or λ. The close equivalence of trends against Hubble type and λ strongly supports the idea that a combination of spatial extent (through R_d) and dynamics (through V_d) given by the dimensionless λ parameter of equation (11) most closely yields the monotonically changing physical parameter of a galaxy responsible for its Hubble type. All the trends seen against λ are noisy, but not more so than the corresponding ones against Hubble type, and often better, with the advantages of λ being objective, readily obtainable through the simple relation of equation (11) and representing a dimensionless parameter having a direct physical interpretation.

4 DISCUSSION

In this final section, we discuss some aspects of the ideas proposed, and include a small comparison of equation (11) against CDM galactic computer formation codes. A physical model simplified to the extreme, as what was presented in Section 2, will only be of any use if the few ingredients which remain manage to capture the fundamental physical processes responsible for the aspects of the problem one is interested in. For example, in a strong explosion, the first phases are completely determined by the energy released and the density of the medium where the explosion takes place, these two numbers and a trivial dimensional analysis suffice to obtain the Sedov–Taylor solution, which is an accurate description of the problem. Indeed, the complex hydrodynamical computer codes, tracing the energetics and dynamics of shocks and explosions, are often tested and calibrated in their myriad numerical details against such a simplistic analytic solution.

We must now check our estimate of λ in the cases where this parameter is, in fact, known, galaxy formation simulations where λ acts as an input parameter. We use results from two groups, the Firmani, Avila-Reese & Hernandez (1998) approach, models calculated in connection with a study of star formation in disc galaxies applied to the Milky Way (Hernandez et al. 2001), and the models published by van den Bosch & Dalcanton (2000). A very brief description of such models is included below.

The first of these models includes a very wide range of physics; initial conditions are supplied by a statistical sampling of a cosmological primordial fluctuation spectrum, giving a mass-aggregation history of gas and dark matter. No Tully–Fisher type of relation is assumed a priori, indeed, this codes attempt to recover such a relation as a final result of the physics included. A fixed value of λ is assumed for the infalling material which settles into a disc in centrifugal equilibrium and differential rotation; viscous friction results in the radial flows of matter and angular momentum. The redistribution of mass affects the rotation curve in a self-consistent way, through a Poisson equation including the disc self-gravity and a dark halo which responds to mass redistributions through an adiabatic contraction. The star formation is followed in detail, with an energy-balance cycle of the type discussed in Section 2 being introduced.

A simple population synthesis code then traces the luminosities and colours of the various stellar populations at all radii and times. The details of the van den Bosch & Dalcanton (2000) models vary in numerical approaches, resolution, time-step issues and the level of approximation and inclusion of the many different physical aspects of the complicated problem. Fig. 11 shows the λ_{model} values given as input by the above authors to their detailed formation codes, with the y-axis showing λ from equation (11) applied to the final results of the code evolution which followed the model for $\sim$13 Gyr. Stars
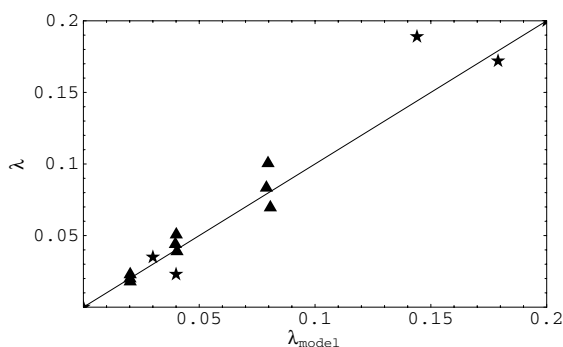
Figure 11. A comparison of the input value of λ in a series of cosmological CDM galactic evolution scenarios, λ_{model}, and λ calculated on the final result of the given simulations through equation (11). The triangles are models from Hernandez et al. (2001) and stars from van den Bosch & Dalcanton (2000).

for the van den Bosch & Dalcanton (2000) results and triangles for the Hernandez et al. (2001) models.

It is interesting that the particular features of a galactic formation scenario which we are interested in treating here, λ, final resulting R_{d} and flat rotation region V_{d}, are evidently very well modelled by the trivial physics that went into equation (11), across more than 2.5 orders of magnitude covered by the masses in the modelled galaxies. This can be understood by considering that equation (11) is the result of two fundamental hypothesis: (i) an exponentially decreasing surface density profile for the disc; and (ii) a dominant dark halo responsible for a flat rotation curve, linked to the disc through a Tully–Fisher relation. Whenever these two conditions are met, as is the case for the final state of all published modelled galaxies and real observed systems, basic physics strongly constrains results to lie not far from equation (11). For example, Kregel et al. (2005) clearly identified the good agreement between the models of Dalcanton et al. (1997) and their dynamical and photometric data, as an unavoidable corollary of the two hypotheses listed above, within an approximately constant Q parameter, irrespective of the actual galactic formation scenario.

This, of course, is not to say that equation (11) replaces a detailed galactic formation scenario, which is really the only way of treating the time-evolution of the problem, and to arrive at the physical origin of many of the well-known galactic features which were introduced as empirical facts into the development leading to equation (11). To mention only two such problems, the origin of Tully–Fisher relation can be traced through CDM galactic formation simulations (e.g. Avila-Reese et al. 1998; Steinmetz & Navarro 1999; Navarro & Steinmetz 2000), as can the causes of the observed exponential density surface brightness profiles of galaxies (e.g. Saio & Yoshii 1990; Struck-Marcell 1991; Firmani et al. 1996; Silk 2001; Zhang & Wyse 2000; Bell 2002).

To conclude, we have presented an easily applicable way of estimating the λ parameter, a theorist's favourite descriptor of a galaxy type, for any real observed disc galaxy. We have shown that four determinant galactic properties crucial in the subjective assignment of a Hubble type to an observed disc system correlate well with the introduced λ parameter, in ways very similar to what is seen when comparing against the classical Hubble type for late-type galaxies. We suggest that any other dimensionless galactic parameter for late-type discs will also show analogous trends with λ of equation (11), as would be expected from Buckinham's theorem of dimensional

analysis (Sedov 1993). The well defined and objective nature of the dimensionless λ parameter, both in simulations and in real galaxies through equation (11), should make it a useful tool in comparing the output of numerical galactic formation scenarios and real galaxy samples.

REFERENCES

Abraham R. G., Valdes F., Yee H. K. C., van den Bergh S., 1994, ApJ, 432, 75
Abraham R. G., Tanvir N. R., Santiago B. X., Ellis R. S., Glazebrook K., van den Bergh S., 1996, MNRAS, 279, L47
Adams A., Woolley A., 1994, VA, 38, 273
Avila-Reese V., Firmani C., Hernandez X., 1998, ApJ, 505, 37
Bell E. F., 2002, ApJ, 581, 1013
Binney J., Tremaine S., 1987, Galactic Dynamics. Princeton Univ. Press, Princeton, NJ
Brosche P., 1973, A&A, 23, 259
Catelan P., Theuns T., 1996, MNRAS, 282, 455
Cole S., Lacey C., 1996, MNRAS, 281, 716
Connolly A. J., Szalay A. S., Bershady M. A., Kinney A. L., Calzetti D., 1995, AJ, 110, 1071
Conselice C., 2003, ApJS, 147, 1
Courteau S., 1996, ApJS, 103, 363
Courteau S., 1997, AJ, 114, 2402
Dalcanton J. J., Spergel D. N., Summers F. J., 1997, ApJ, 482, 659
de Grijs R., 1998, MNRAS, 299, 595
de Vaucouleurs G., 1959, Hanbuch der Physik, 53, 275
Dopita M. A., Ryder S. D., 1994, ApJ, 430, 163
Ellis S. C., Driver S. P., Allen P. D., Liske J., Bland-Hawthorn J., De Propris R., 2005, MNRAS, 363, 1257
Fall S. M., Efstathiou G., 1980, MNRAS, 193, 189
Ferguson A. M. N., Clarke C. J., 2001, MNRAS, 325, 781
Frenk C. S., White S. D. M., Efstathiou G., Davis M., 1985, Nat, 317, 595
Frenk C. S., White S. D. M., Davis M., Efstathiou G., 1988, ApJ, 327, 507
Flores R., Primack J. R., Blumenthal G. R., Faber S. M., 1993, ApJ, 412, 443
Firmani C., Hernandez X., Gallagher J., 1996, A&A, 308, 403
Firmani C., Avila-Reese V., Hernandez X., 1998, ApJ, 505, 37
Graham A. W., 2001, AJ, 121, 820
Grosbol P., Patsis P. A., Pomoei E., 2004, A&A, 423, 849
Gurovich S., McGaugh S. S., Freeman K. C., Jerjen H., Staveley-Smith L., De Blok W. J. G., 2004, PASA, 21, 412
Hernandez X., Avila-Reese V., Firmani C., 2001, MNRAS, 327, 329
Hernandez X., 2000, in Franco J., Terlevich E., López-Cruz O., Aretxaga I., eds, ASP Conf. Ser. Vol. 215, Cosmic Evolution and Galaxy Formation: Structure, Interactions and Feedback. Astron. Soc. Pac., San Francisco, p. 113
Hernandez X., Gilmore G., 1998, MNRAS, 294, 595
Hubble E. P., 1926, ApJ, 64, 321
Hubble E. P., 1936, Realm of the Nebulae. Yale Univ. Press, New Haeven
Kelly B. C., McKay T. A., 2004, AJ, 127, 625
Kregel M., van der Kruit P. C., de Grijs R., 2002, MNRAS, 334, 646
Kregel M., van der Kruit P. C., Freeman K. C., 2005, MNRAS, 358, 503
Klypin A., Zhao H., Somerville R. S., 2002, ApJ, 573, 597
Koeppen J., Theis C., Hensler G., 1995, A&A, 296, 99
Kormendy J., 1979, ApJ, 227, 714

360   *X. Hernandez and B. Cervantes-Sodi*

Kuchinski L. E. et al., 2000, ApJS, 131, 441

Labbe I. et al., 2003, ApJ, 591, L95

Lauberts A., Valentijn E. A., 1989, The Surface Photometry Catalogue of the ESO-Upssala Galaxies. ESO (ESO-LV), Garching

Lemson G., Kauffmann G., 1999, MNRAS, 302, 111

Lotz J. M., Primack J., Madau P., 2004, AJ, 128, 163

Ma J., 2002, A&A, 388, 389

Maller A. H., Dekel A., Somerville R., 2002, MNRAS, 329, 423

Mo H. J., Mao S., White S. D. M., 1998, MNRAS, 295, 319

Naab T., Ostriker J. P., 2006, MNRAS, 366, 899

Naim A., Ratnatunga K. U., Griffiths R. E., 1997, ApJ, 476, 510

Navarro J. F., Steinmetz M., 2000, ApJ, 538, 477

Pahre M. A., Ashby M. L. N., Fazio G. G., Willner S. P., 2004, ApJS, 154, 235

Park C., Choi Y., 2005, ApJ, 635, 29

Peebles P. J. E., 1969, ApJ, 155, 393

Roberts M. S., Haynes M. P., 1994, ARA&A, 32, 115

Sandage A., 1961, The Hubble Atlas of Galaxies. Carnegie Institution of Washington, Washington D.C.

Sandage A., Freeman K. C., Stokes N. R., 1970, ApJ, 160, 831

Saio H., Yoshii Y., 1990, ApJ, 363, 40

Sedov L. I., 1993, Similarity and Dimensional Methods in Mechanics, 10th edn. CRC Press Boca Raton FL

Schade D., Lilly S. J., Crampton D., Hammer F., LeFevre O., Tresse L., 1995, ApJ, 451, L1

Silk J., 2001, MNRAS, 324, 313

Somerville R. S., Primack J. R., 1999, MNRAS, 310, 1087

Steinmetz M., Navarro J. F., 1999, ApJ, 513, 555

Struck-Marcell C., 1991, ApJ, 368, 348

Takamiya M., 1999, ApJS, 122, 109

Tonini C., Lapi A., Shankar F., Salucci P., 2006, ApJ, 638, L13

Toomre A., 1964, ApJ, 139, 1217

van den Bosch F. C., 1998, ApJ, 507, 601

van den Bosch F. C., Dalcanton J. J., 2000, ApJ, 534, 146

van der Kruit, P. C., 1987, A&A, 173, 59

Warren M. S., Quinn P. J., Salmon J. K., Zurek W. H., 1992, ApJ, 399, 405

Wilkinson M. I., Evans N. W., 1999, MNRAS, 310, 645

White S. D. M., Frenk C. S., 1991, ApJ, 379, 52

Yoachim P., Dalcanton J. J., 2006, AJ, 131, 226

Zaritsky D., Zabludoff A. I., Willick J. A., 1995, AJ, 110, 1602

Zhang B., Wyse R. F. G., 2000, MNRAS, 313, 310

This paper has been typeset from a TEX/LATEX file prepared by the author.

Capítulo 3

Abundancias químicas y contenido de gas.

En el capítulo anterior describí el modelo empleado para calcular λ a partir de parámetros que pueden ser deducidos a partir de observaciones; la velocidad de rotación y el radio de escala. También se presenta evidencia de la dependencia de varias propiedades físicas en el valor de λ, entre ellas el color, el espesor del disco y el cociente bulbo-disco. En este capítulo exploramos las dependencias de la abundancia química y el contenido de gas con λ, comparando los resultados con la dispersión que se encuentra al analizar la dependencia con el tipo de Hubble.

Aún cuando las correlaciones entre metalicidad promedio y magnitud o tipo de Hubble son evidentes, nosotros obtuvimos correlaciones igualmente fuertes con el espín, en el sentido de que galaxias con valores pequeños de λ presentan abundancias más altas, mientras que galaxias con λ grande son pobres en metales. También el contenido de gas en las galaxias correlaciona con λ, en donde sistemas con valores altos de λ presentan mayores fracciones de masa de gas que galaxias con valores pequeños de λ, destacando el importante papel que juega este parámetro en la estructura de las galaxias de disco y la propuesta de su uso como una medida del tipo morfológico.

Trabajo publicado en:

- Cervantes-Sodi B., Hernández X., 2009, RevMexA&A, 45, 75.

CHEMICAL ABUNDANCES AND GAS CONTENT IN DISK GALAXIES: CORRELATIONS WITH THE λ SPIN PARAMETER

B. Cervantes-Sodi[1] and X. Hernández[1,2]

RESUMEN

Usando un modelo simple y general para describir la dinámica de las galaxias de disco, estimamos el parámetro de espín λ para una muestra de galaxias observadas y presentamos un estudio que muestra cómo varias propiedades físicas se encuentran relacionadas intrínsecamente con la dinámica de los sistemas. Aún cuando las correlaciones entre metalicidad promedio y magnitud o tipo de Hubble son evidentes, nosotros obtuvimos correlaciones igualmente fuertes con el espín, en el sentido de que galaxias con valores pequeños de λ presentan abundancias mas altas, mientras que galaxias con λ grande son pobres en metales. También el contenido de gas en las galaxias se correlaciona con λ, en donde sistemas con valores altos de λ presentan mayores fracciones de masa de gas que galaxias con valores pequeños de λ, destacando el importante papel que juega este parámetro en la estructura de las galaxias de disco y la propuesta de su uso como una medida del tipo morfológico.

ABSTRACT

By using a very simple and general model to describe the dynamics of disk galaxies, we estimate the λ spin parameter for a sample of observed galaxies and present a study in which we show that several important physical properties are intrinsically related to the dynamics of the systems. Although correlations between average metallicity with magnitude or Hubble type are evident, we obtain equally strong correlations with the spin parameter, where galaxies with low λ values present higher abundances and galaxies with high λ values are poor in metals. Also, the gas content of the galaxies correlates with λ, with high λ systems showing higher gas mass fractions than low λ galaxies, highlighting the important role this parameter plays in the structure of disk galaxies and the proposal of λ as a robust and objective physical measure of galactic morphology.

Key Words: galaxies: abundances — galaxies: fundamental parameters — galaxies: general — galaxies: structure

1. INTRODUCTION

One recurrent issue in the study of galaxies is their classification, most frequently treated through the Hubble type (Hubble 1926, 1936). This classification scheme is extensively used and owes it success to the ample and broad range of physical characteristics involved in its construction, such that all show good monotonic correlations with it. Just to mention some of them, total magnitudes decrease towards later types (e.g. Ellis et al. 2005), and

colours become bluer going from early to late types (e.g. Roberts & Haynes 1994), the blue magnitudes and bulge to disk ratios decrease (e.g. Pahre et al. 2004) and disks become thinner (e.g. Kregel, van der Kruit, & de Grijs 2002) going to late types.

All these clear correlations point towards the notion that the sequence of morphologies indicates an underlying sequence of values for one or more physical parameters, which ultimately determine the type of the galaxies. The Hubble scheme of classification owes its success precisely to this fact; it orders galaxies by properties that reflect essential physics, but not without some shortcomings. The classifica-

[1]Instituto de Astronomía, Universidad Nacional Autónoma de México, Mexico.

[2]GEPI, Observatoire de Paris, Meudon, France.

76   CERVANTES-SODI & HERNÁNDEZ

tion of galaxies using this scheme is usually done by visual inspection and requires skill and experience, which not only makes it a subjective scheme, but also renders it impractical when dealing with large samples containing hundreds or thousands of galaxies, as is the case of the Sloan Digital Sky Survey (SDSS) or the 2dF Galaxy Redshift Survey. Naim et al. (1995) and Lahav et al. (1995), studied the agreement between expert morphologists classifying different samples of galaxies and both collaborations reported a non-negligible scatter between observers, making the subjective character of the Hubble scheme evident.

Another important problem with the Hubble scheme is that it is based on a qualitative analysis of observable features, which makes it difficult to relate type to definitive quantitative physical aspects of a galactic system. That the scheme is ultimately qualitative casts serious doubts on the validity of any statistical analysis performed on galactic populations based on galactic type.

The study of high-z galaxies whose light has been redshifted into other bands, shows a wavelength dependence of morphology for different Hubble types. In general, it is found (Kuchinski et al. 2000) that the dominance of young stars in the far-ultraviolet produces the patchy appearance of a morphological type later than inferred from optical images. Apart from the observational band dependence, the low signal-to-noise levels in faint images of distant galaxies, projection effects and low resolution, can strongly affect the morphological type assigned to a given galaxy (e.g. Abraham et al. 1994). This makes the Hubble scheme relative to the observation band, the redshift and the orientation available for a given galaxy, as the spiral arms vanish for edge-on disks.

From the theoretical study of galactic structure and formation, it generally emerges that the principal physical origin of galactic type morphology, lies in the choice of mass and angular momentum. Some examples of the above are: Fall & Efstathiou (1980), Firmani, Hernández, & Gallagher (1996), Dalcanton, Spergel, & Summers (1997), Mo, Mao, & White (1998), and van den Bosch (1998). Theoretically, the observed spread in many physical features of the galaxies can be understood as arising from a spread in the halo angular momentum once the mass has been fixed, coupled with a spread in the formation redshifts, this last once a particular formation model has been assumed. For example, the bulge to disk ratio (van den Bosch 1998), the thickness of the disk (Kregel, van der Kruit, & Freeman 2005), the surface density (Dalcanton et al. 1997), systematic variations in the slope of rotation curves (Flores et

al. 1993), scalelength (Hernández & Gilmore 1998; Jiménez et al. 1998), chemical abundances and color gradients (Prantzos & Boissier 2000), and gas content, abundance gradients (Churches, Nelson, & Edmunds 2001; Boissier et al. 2001) and the spread in the Tully-Fisher relation, once the slope is determined by the total galactic mass (Koda, Sofue, & Wada 2000), to mention but a few. Hence, the proposal of the angular momentum as the principal physical parameter responsible for the Hubble sequence (Silk & Wyse 1993; van den Bosch 1998; Zhang & Wyse 2000; Firmani & Ávila-Reese 2003) is not surprising. It has often been suggested that the angular momentum of a galaxy should be an adequate proxy for the Hubble sequence, or rather, that it is precisely this parameter the one for which the Hubble sequence has been serving as a proxy.

In Hernández & Cervantes-Sodi (2006, henceforth Paper I), using a sample of observed galaxies, we presented a series of correlations confirming the dependence on angular momentum of several key structural parameters such as disk to bulge ratio, thickness of the disk and rotational velocity, and in Hernández et al. (2007, Paper II), we matched Hubble type with the angular momentum parameter using a color versus color gradient criterion (Park & Choi 2005), where the segregation by angular momentum coincides with the segregation by Hubble type, as visually assigned for a large sample of spiral galaxies from the SDSS.

In the present work, we give a general review to introduce the use of the angular momentum parameter as a physical classification criterion for spiral galaxies, which we reinforce by presenting additional independent correlations recently found. In § 2 we present the underlying ideas behind proposing physical correlations between structural galactic parameters and angular momentum, and an account of previous results, in § 3 we explore possible scalings between chemical abundances, gas content and angular momentum, which we test in § 4. § 5 presents a discussion of our results and general conclusions.

2. THEORETICAL FRAMEWORK

A generally accepted picture for galaxy formation is the ΛCDM model, where overdense regions of the expanding Universe at high redshift accrete baryonic material through their gravitational potential to become galaxies. Their principal global characteristics, according to theoretical studies, are determined by their mass and angular momentum. The angular momentum is commonly characterized by the dimensionless angular momentum parameter (Peebles

1969)

$$\lambda = \frac{L \mid E \mid^{1/2}}{GM^{5/2}}, \qquad (1)$$

where E, M and L are the total energy, mass and angular momentum of the configuration, respectively. In Paper I we derived a simple estimate of λ for disk galaxies in terms of observational parameters, and showed some clear correlations between this parameter and structural parameters, such as the disk to bulge ratio, the scaleheight and the colour. Here we briefly recall the main ingredients of the simple model. The model considers only two components, a disk for the baryonic component with an exponential surface mass density $\Sigma(r)$:

$$\Sigma(r) = \Sigma_0 e^{-r/R_d}, \qquad (2)$$

where r is a radial coordinate and Σ_0 and R_d are two constants which are allowed to vary from galaxy to galaxy, and a dark matter halo having a singular isothermal density profile $\rho(r)$, responsible for establishing a rigorously flat rotation curve V_d throughout the entire galaxy:

$$\rho(r) = \frac{1}{4\pi G}\left(\frac{V_d}{r}\right)^2. \qquad (3)$$

In this model we are further assuming: (1) that the specific angular momentum of the disk and halo are equal e.g. Fall & Efstathiou (1980), Mo et al. (1998), Zavala, Okamoto, & Frenk (2008); (2) that the total energy is dominated by that of the halo which is a virialized gravitational structure; (3) that the disk mass is a constant fraction of the halo mass; $F = M_d/M_H$ (Brooks et al. 2007; Crain et al. 2007). These assumptions allow us to express λ as

$$\lambda = \frac{2^{1/2}V_d^2 R_d}{GM_H}. \qquad (4)$$

Finally, we introduce a baryonic Tully-Fisher relation: $M_d = A_{TF}V_d^{3.5}$, in consistency with Gurovich et al. (2004) and Kregel et al. (2005). We see the total mass fixing the bulk dynamical structure of the galaxy, with internal distributions being then determined by the choice of λ, e.g. Fall & Efstathiou (1980) and references thereof. Taking the Milky Way as a representative example, we evaluate F and A_{TF} to obtain

$$\lambda = 21.8 \frac{R_d/\mathrm{kpc}}{(V_d/\mathrm{km \ s^{-1}})^{3/2}}. \qquad (5)$$

The accuracy in our estimation of λ is proved in Cervantes-Sodi et al. (2008), comparing the estimation using equation (5) with the values arising from numerical simulations of six distinct groups, where the actual value of λ is known, as it is one of the parameters of the simulated galaxies, and where we can also estimate it through equation (5), as baryonic disk scale lengths and disk rotation velocities are part of the output. This shows a one-to-one correlation, with very small dispersion leading to typical errors $< 30\%$. This level of accuracy is encouraging, when comparing what is little more than an order of magnitude estimate against detailed physical modeling spanning a wide range of masses and λ values, including disk self-gravity, the presence of galactic bulges, detailed dark halo structure and often complex formation histories. The only ambiguity which remains in assigning a value of λ to an observed galaxy through equation (5), is in the choice of the restframe band in which the disk scalelength is to be measured. This is clearly to be chosen in a way which maximally reflects the underlying mass distribution, and not the recent star formation, highly sensitive to a small number of young stars. Therefore, the restframe band in which R_d is to be measured if equation (5) is to be used optimally, is a red or infrared one, see Paper I.

Having an estimate for the spin parameter, we applied it to a large sample of disk galaxies taken from the SDSS. Park & Choi (2005), showed a criterion using the colour versus colour gradient plane, to separate galaxies by galactic type, from early to late type (see Figure 1, left panel). We see the ellipticals appearing in a very compact region, with red colours and minimal colour gradients. In Figure 1 right panel, are plotted the 7,753 galaxies from the SDSS sample of Paper II, in the same color versus colour gradient plane, where the shading gives the average values of λ within each shaded square, calculated through equation (5). We can see that high λ disk galaxies are located in the lower left area of the plane, occupied by later types in Figure 1 left panel, whilst low λ disk galaxies populate the right upper zone, precisely where earlier types are evident in Figure 1 left panel. Comparing with the spread of galactic types, the match of late spirals with high λ values and early spirals with low λ values is validated.

With equation (5) in Paper I we showed several correlations between λ and physical features of disk galaxies such as: the disk to bulge ratio, one of the main morphological parameters that sets the classification of galaxies in the revised Hubble diagram (van den Bosch 1998), which decreases when λ increases, while the thickness of the disk diminishes and the colour becomes bluer. A clear trend for mean λ val-

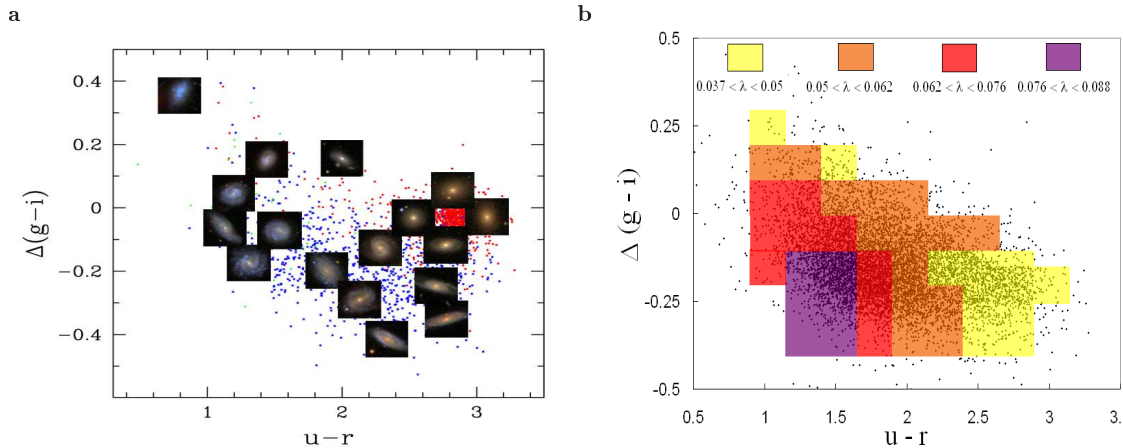78   CERVANTES-SODI & HERNÁNDEZ

a

b

Fig. 1. (*a*) Sample of galaxies from Park & Choi (2005) in a color, color-gradient plane, with photos of galaxies representative of the morphological type found in each region. (*b*) Spiral galaxies from Paper II on a color, color-gradient plane; the shading shows the average λ value in each shaded region, calculated using equation (5).

ues increasing in going towards later Hubble types, as visually assigned, was also established. In the following section we present the underlying ideas behind expecting additional correlations involving gas fractions and chemical abundances, with the aim of reinforcing the use of λ as an objective and quantitative classification tool.

3. EXPECTED CORRELATIONS BETWEEN λ AND CHEMICAL ABUNDANCES AND GAS CONTENT

The gas mass and chemical composition in disk galaxies span wide ranges, early-type galaxies presenting systematically lower gas mass fractions and higher metallicity abundances (Vila-Costas & Edmunds 1992; Oey & Kennicutt 1993; Roberts & Haynes 1994; Zaritsky, Kennicutt, & Huchra 1994, hereafter ZKH). As pointed out by Kennicutt et al. (1993), it is tempting to associate the higher abundances with the early morphological types, but differences in other parameters such as galaxy luminosity or rotational velocity may also be important. Over the last twenty years there have been several studies exploring the connection between metallicity and other physical parameters of galaxies; luminosity, rotational velocity and mass, among others.

The correlation between metallicity and luminosity, in the sense that the higher the luminosity of the system, the higher the metal abundance, is now well established e.g. Garnett & Shields (1987), Hunter & Hoffman (1999), Pilyugin (2001), and Melbourne & Salzer (2002). Thinking of the luminosity as a tracer for the mass of the galaxy, and given the Tully-Fisher

relation, we find equally a metallicity rotation velocity relation. Compared with the luminosity metallicity relation, the above shows no qualitative difference (Garnett 1998), only a slightly better correlation, presumably due to differences among mass to light ratios. The mechanism that might be responsible for the origin of such correlations is, at present, open to debate, but the most common hypothesis is the loss of heavy elements through galactic winds (e.g. Franx & Illingworth 1990; Kauffmann 1996; Pilyugin, Vílchez, & Contini 2004, hereafter PVC) in low mass galaxies, while higher mass galaxies present deeper gravitational potentials and lower heavy elements losses. The correlation with Hubble type, however, is more difficult to explain given the fact that this last is not a physical parameter as such.

If besides the mass, there is another physical parameter which determines abundances in galaxies, it should correlate with the Hubble type. It is reasonable to think that the angular momentum parameter could play an important role. In order to see how a causal relation between λ and both the characteristic abundances and gas content of galaxies might arise, one can start from the star formation rate (SFR), assuming a generic Schmidt law in terms of SFR surface density and gas surface density:

$$\Sigma_{SFR} \propto \Sigma^n \,. \tag{6}$$

We define the star formation efficiency ϵ evaluated at R_d as:

$$\epsilon = \frac{\Sigma_{SFR}(R_d)}{\Sigma(R_d)} \propto \Sigma_0^{n-1} \,, \tag{7}$$

and using equation (2), we can write Σ_0 in terms of the mass of the disk and the scalelength, from where the dependence in R_d can be replaced by a dependence in λ at fixed mass, resulting in

$$\epsilon \propto \lambda^{2(1-n)}. \tag{8}$$

Both empirically (Kennicutt 1998; Wong & Blitz 2002) and theoretically (Tutukov 2006) inferred values for n fall in the range 1–2, being 1.4 a standard value; in this case, we have $\epsilon \propto \lambda^{-0.8}$, in agreement with previous results from theoretical studies (Boissier et al. 2001). For any value of n in the cited range (excluding one of the extremes), the exponent in equation (8) is negative, so systems with large λ values will show typically low star formation efficiencies, while galaxies with small λ may present a very efficient star formation process. In other words, extended galaxies, with large scalelengths for their total mass, present lower star formation efficiencies than more compact ones, those with small scalelength at a given mass. The scaling corresponding to equation (8), for ϵ as a function of mass at fixed λ yields $\epsilon \propto M^{(n-1)/7}$. For standard values of n, we see the expected positive correlation of ϵ vs. mass, opposite to what happens vs. λ, leading to an increasingly later type appearance as one goes to larger masses, at fixed λ.

Studying the chemical and spectrophotometric evolution of galactic disks, using semi-analytic models of galactic evolution, Boissier & Prantzos (2000) reached similar conclusions. In their models, the shortest characteristic time-scales correspond to the more massive and compact disks with smaller λ values, favoring rapid early star formation and the existence of relatively old stellar populations today.

From equation (8), the most efficient galaxies at forming stars and therefore metals, are the compact ones, with low λ values, being also the most efficient at turning their gas into stars. If we assume that all galaxies start forming stars at the same time and that the amount of gas in each of them is proportional to their gravitational potential, extended galaxies with high λ should appear today to be systems with large amounts of gas and poor in metals, while compact galaxies, with low λ and very efficient at forming stars at the onset, will now be systems poor in gas with large metal abundances. Prantzos & Boissier (2000) reported this same result arising from their semi-analytic models, where the most compact disks with low λ values presented the higher abundances, being this type of galaxies the most efficient at forming stars and metals, consuming their gas and showing low gas mass fractions. The above applies only to large and medium disk galaxies; the clear mass metallicity relation in spheroidal systems, from dSphs to elliptical galaxies, systems where the angular momentum plays only a very minor role, most probably arises from the differential efficiencies of galactic winds. We see how the two parameter nature of galactic systems reduces to a one parameter space when one goes from the spirals to the ellipticals, where the angular momentum becomes close to negligible and ceases to determine the internal structure of the galaxy to any substantial level.

4. OBSERVATIONAL DATA COMPARISONS

The observational data used to check our expected correlations were compiled by PVC. The compilation comprises more than 1000 published spectra of HII regions in 54 spiral galaxies. The oxygen and nitrogen abundances were obtained using the P-method described in Pilyugin (2003).

For the present work, we used the exponential scalelengths measured by Garnett (2002), ZKH, and Elmegreen & Elmegreen (1984), for 36 of the 54 galaxies in the PVC sample, preferentially using reported values in red bands in order to account for the mass distribution of the galaxy. Using the rotation velocity reported in PVC we calculate λ for each galaxy in the sample using equation (5). As described in the previous section, we expect galaxies with low λ values to present very efficient early star formation processes, capable of enriching their interstellar media with metals, and hence presenting today higher oxygen abundances than the more extended galaxies with higher λ, where we would expect lower oxygen abundances. To check this, we employed the characteristic oxygen of the galaxies, defined as the oxygen abundance in the disk at $r = 0.4R_{25}$, following ZKH. In Figure 2 we show the characteristic oxygen of the sample as a function of λ (top panel) and type (bottom panel), the straight line being the best linear fit to the data, described by the equation:

$$12 + \log(O/H) = -3.401(\pm 0.037)\lambda + 8.667(\pm 1.03), \tag{9}$$

which gives also the $1 - \sigma$ uncertainties in the parameters of the fit, given our 30% uncertainties in the estimates of individual λs. The figure shows a clear correlation between the characteristic oxygen and λ, with a correlation coefficient of -0.493. Despite the large error bars and high dispersion, large empty regions to the upper right and lower left are evident. The above correlation coefficient is comparable to that obtained against rotation velocity of
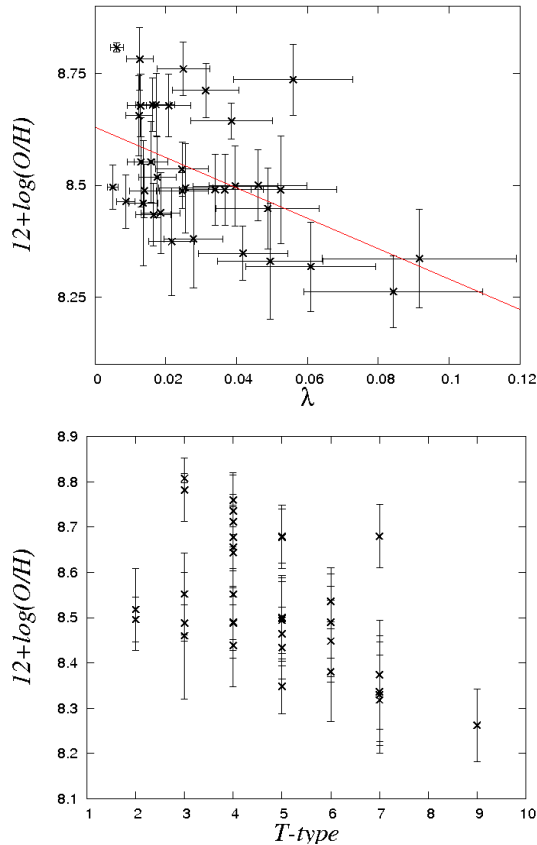
80   CERVANTES-SODI & HERNÁNDEZ

Fig. 2. Characteristic oxygen abundance as a function of λ (top panel) and type (bottom panel) for the 36 galaxies in the PVC sample for which disk scale lengths in red bands are available. The solid line is the best linear fit to the data.

0.608, or against luminosity of 0.469, for the correlations against characteristic oxygen. The average value of the dispersion in characteristic oxygen for the sample used in Figure 2 is of 0.136 dex. Although the spread seen in this figure could be intrinsic, it is also consistent with the internal errors in the estimates of λ; in this sense, the metallicity λ relation could in fact be much tighter than what the figure shows. The good correlation against rotation velocity mentioned above, given the Tully-Fisher relation, highlights again the equally important role of mass in galactic structure and evolution, as often recognised.

The trend with λ is clearer than the trend with type, the upper panel of Figure 2 gives a metallicity vs. λ relation, having the advantage of the entirely

objective nature of its calculation and of it being quantitative, hence useful for meaningful statistics or to establish mathematical relations with other physical parameters such as equation (9). It must be taken into account that the assigned type of each galaxy is entirely subjective and not free of errors due to lack of information; in this sense we could assign error bars to the data plotted in Figure 2, spanning up to three types around the reported value.

From Figure 2, it is clear that the correlation of the metallicity of the galaxies with λ is as strong as that of metallicity against both the rotational velocity and the luminosity or, given the Tully-Fisher relation, the mass of the system. From the data we see that the studied properties of the galaxies are largely determined by fixing the mass and λ, but until now, we are not sure if the dependence with λ is only a reflection of the mass metallicity relation. In order to separate the respective dependencies, we can plot the residuals of the relation of the metallicity with one of the variables and test if they correlate with the other variable. To trace the mass of the galaxies we chose the absolute magnitude, because to calculate λ using equation (5) we employed V_d; in this form the measurement will be completely independent. In Figure 3 are plotted the residuals: (a) to the $O/H - \lambda$ relationship, plotted against M_B and (b) to the $O/H - M_B$ relationship, plotted against λ. We can see a correlation in both cases which indicates a systematic variation due to both variables, the mass and λ, as we expected. We hence see that the metallicity is a function of both mass and λ. As often found in theoretical studies of galactic formation and evolution, we see observable properties of galaxies appearing as two parameter families of solutions, determined by the choice of mass and λ.

A similar test was done by ZKH using the Hubble type and the velocity as a measure of the mass, and they found no clear trends, perhaps because the Hubble type is not an objective, quantitative physical parameter, while λ satisfies these conditions.

Results from several surveys of galactic abundances show clearly that most disk galaxies present negative abundance gradients similar to what is observed in our own galaxy (Henry & Worthey 1999). While characteristic abundances increase with galactic mass, no correlation has been found between metallicity gradients, normalized to the respective galaxy's isophotal radius, and mass. If instead of using the gradient normalized to the isophotal radius, the gradient is measured in dex kpc^{-1}, a correlation appears, such that more luminous galaxies have flatter slopes (Garnett 1998). With this in mind, we
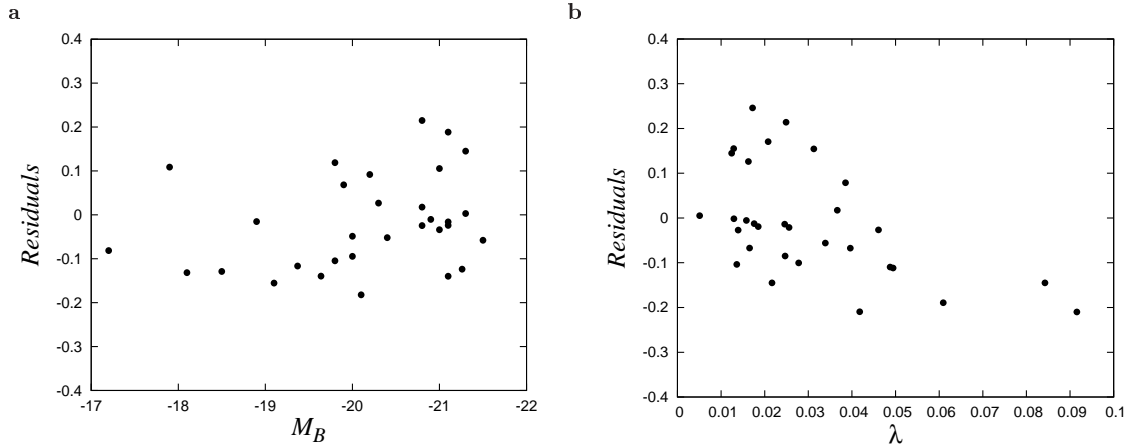
a

b

Fig. 3. The residuals to correlations. (*a*) Residuals to the $O/H - \lambda$ relationship, plotted against M_B. (*b*) Residuals to the $O/H - M_B$ relationship, plotted against λ.

search for a dependence of the abundance gradients with λ. The abundance gradients of the galaxies in the PVC sample are given in dex/R_{25} and we find no clear trend with λ, as predicted in theoretical studies (see below), but trends between λ and abundance gradients in dex kpc^{-1} have been predicted. Theoretical studies by Churches et al. (2001) show that both the gaseous and stellar abundance gradients in dex kpc^{-1} are functions of λ in the sense that increasing λ generally produces shallower gradients, and Prantzos & Boissier (2000) predicted that this effect should be more marked in low-mass disks.

To study this relation we employed a sample of 38 galaxies from ZKH, where the oxygen abundance gradients are given in dex kpc^{-1}. Using the reported disk scale length and the rotation velocity for each galaxy we obtain λ, again using equation (5). A plot of the abundance gradient as a function of λ is presented in Figure 4, where the sample has being split into 3 slices, through a luminosity ranking, each one containing one third of the total sample. The top panel presents the galaxies with the higher luminosities showing almost a constant value and very low dispersion, the middle panel again shows low dispersion and in general low gradients, but as we move to the smaller galaxies (bottom panel), the dispersion increases, showing deeper gradients for galaxies with low λ, confirming the theoretical predictions of Churches et al. (2001) and Prantzos & Boissier (2000), where in low-mass galaxies the increase of λ produces shallower gradients. Again, the two parameter nature of galaxies becomes apparent in the two fold dependence of abundance gradients against
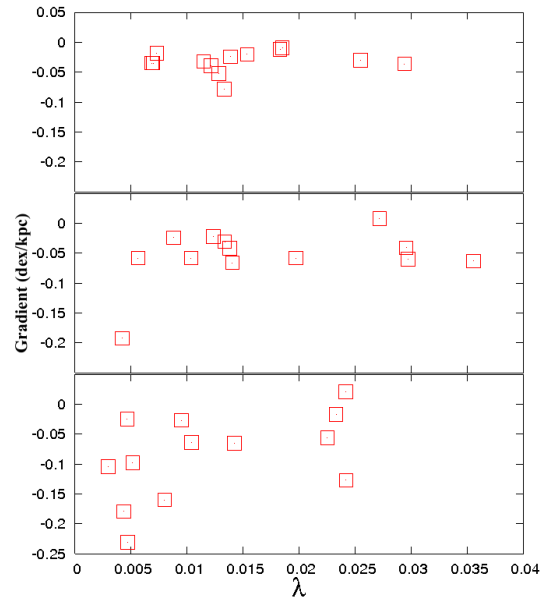
Fig. 4. Abundance gradients for the 38 galaxies from the ZKH sample, as a function of λ. From top to bottom, subsets of the sample splited by decreasing luminosity.

both mass and λ, the role played by the mass being predominant in this case.

An extreme case would be that of the Low Surface Brightness galaxies, having very extended disks and large λ values (Hernández & Gilmore 1998) which then should exhibit small abundance gradients or none at all (Jiménez et al. 1998). Observations of

de Blok & van der Hulst (1998), shows exactly this behavior, explained as a result of a constant evolution rate over the entire disk.

The high star formation efficiency of low spin galaxies should be reflected in the gas content of such systems. To measure this effect, we employed the gas fraction μ defined as:

$$\mu = \frac{M_{HI} + M_{H2}}{M_{HI} + M_{H2} + kL_B}, \qquad (10)$$

where M_{HI} is the mass in atomic hydrogen, M_{H2} is the mass in molecular hydrogen, L_B is the blue luminosity, and k is the mass to luminosity ratio, here fixed to a value of $k = 1.5$, following the work of Garnett (2002). The value of μ reported in PVC, is plotted as a function of λ, estimated through equation (5), and type, in a logarithmic scale, and presented in Figure 5, where the solid line is a fit to the data corresponding to a relation between μ and λ of the form:

$$\log(\mu) = 0.384(\pm 0.159)\log(\lambda) + 0.082(\pm 0.097), \qquad (11)$$

with a correlation coefficient of 0.562. Again, equation (11) gives also the $1 - \sigma$ confidence intervals on the fitted parameters, given our uncertainties in λ. The average value of the dispersion shown by the data in Figure 5 is 0.167 dex. The clear trend in the expected sense given our hypothesis is as clear as that obtained with the rotational velocity, which presents a correlation coefficient of -0.605, slightly better than what is observed against the luminosity, with a correlation coefficient of -0.477. In comparison with type, the trend is similar, but in this case the allocation of λ is completely objective and quantitative, which allow us to calculate empirical correlations as equation (11), that would be senseless to try using type, given its qualitative nature.

Thinking of λ as the main physical determinant of galactic type, the large gas fractions and low metallicities found for both late type spirals and high λ systems in the sample we treat are consistent with the expectations of § 3. High λ disks have long star formation timescales, and hence appear today as low metallicity, high gas fraction systems. Hence, one would also expect these galaxies to show high present star formation rates, as low λ systems would have exhausted their gas fuel in the remote past. We note that Berta et al. (2008) recently adopted a slightly modified and higher accuracy version of equation (5) to determine λ for a large sample (52,000) of SDSS galaxies, and strongly confirm the relation between this physical parameter and galactic type. In the
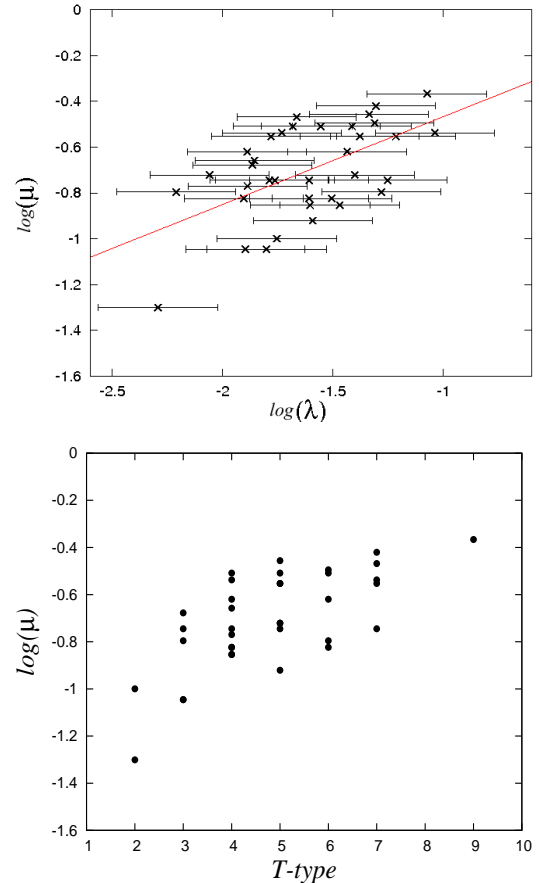

Fig. 5. Logarithmic plot of the gas fraction of the 36 galaxies from the PVC sample, as a function of λ (top panel) and type (bottom panel). The solid line is the best fit to the data.

particular case of the recent star formation, which they accurately trace through detailed spectral synthesis modeling, they find a positive correlation with λ, which is what would be expected from the preceding argument. The work of Berta et al. (2008) offers independent support for both the high gas mass fractions and the low metallicities of high λ galaxies we found, after the critical dependence on total mass has been considered. Further, in that work the authors strongly support the identification of λ and mass as the parameters determining the Hubble sequence.

5. CONCLUSIONS

We use a simple dynamical model for spiral galaxies to infer the value of λ for a sample of observed

disk galaxies, for which detailed chemical and gas mass studies exist.

We confirm general results from theoretical studies of chemical galactic evolution: systems with low λ spin parameter present typically higher metallicities and lower gas mass fractions than systems with large λ. In low mass disk galaxies, the abundance gradients in dex kpc^{-1} are more pronounced for low λ systems. Asides from the trends found, we present numerical relations between the variables involved which could be used to calibrate numerical studies of galactic formation.

The trends here discussed together with correlations between λ and other physical observable parameters such as the disk thickness, the bulge to disk ratio, colour and colour gradients, as stressed by several authors (van der Kruit 1987; Dalcanton et al. 1997; van den Bosch 1998; Hernández & Cervantes-Sodi 2006; Hernández et al. 2007), reinforce the idea of the use of this physical parameter as an objective and quantitative tool for galaxy classification.

It appears clear that once the total mass of a galaxy has been fixed, and the integral properties hence determined (e.g. through the Tully-Fisher relation), it is λ what then establishes the internal structure, disk scale lengths, star formation efficiencies and other derived quantities.

REFERENCES

Abraham, R. G., Valdés, F., Yee, H. K. C., & van den Bergh, S. 1994, ApJ, 432, 75

Berta, Z., Jiménez, R., Heavens, A. F., & Panter, B. 2008, MNRAS, 391, 197

Boissier, S., Boselli, A., Prantzos, N., & Gavazzi, G. 2001, MNRAS, 321, 733

Boissier, S., & Prantzos, N. 2000, MNRAS, 312, 398

Brooks, A. M., et al. 2007, ApJ, 655, L17

Cervantes-Sodi, B., Hernández, X., Park, C., & Kim, J. 2008, MNRAS, 388, 863

Churches, D. K., Nelson, A. H., & Edmunds, M. G. 2001, MNRAS, 327, 610

Crain, R. A., Eke, V. R., Frenk, C. S., Jenkins, A., McCarthy, I. G., Navarro, J. F., & Pearce, F. 2007, MNRAS, 377, 41

Dalcanton, J. J., Spergel, D. N., & Summers, F. J. 1997, ApJ, 482, 659

de Blok, W. J. G., & van der Hulst, J. M. 1998, A&A, 335, 421

Ellis, S. C., Driver, S. P., Allen, P. D., Liske, J., Bland-Hawthorn, J., & De Propris, R. 2005, MNRAS, 363, 1257

Elmegreen, D. M., & Elmegreen, B. G. 1984, ApJS, 54, 127

Fall, S. M., & Efstathiou, G. 1980, MNRAS, 193, 189

Firmani, C., & Ávila-Reese, V. 2003, RevMexAA (SC), 17, 107

Firmani, C., Hernández, X., & Gallagher, J. 1996, A&A, 308, 403

Flores, R., Primack, J. R., Blumenthal, G. R., & Faber, S. M. 1993, ApJ, 412, 443

Franx, M., & Illingworth, G. 1990, ApJ, 359, L41

Garnett, D. R. 1998, RevMexAA (SC), 7, 58

_____. 2002, ApJ, 581, 1019

Garnett, D. R., & Shields, G. A. 1987, ApJ, 317, 82

Gurovich, S., McGaugh, S. S., Freeman, K. C., Jerjen, H., Staveley-Smith, L., & De Blok, W. J. G. 2004, Publ. Astron. Soc. Australia, 21, 412

Henry, R. B. C., & Worthey, G. 1999, PASP, 111, 919

Hernández, X., & Cervantes-Sodi, B. 2006, MNRAS, 368, 351 (Paper I)

Hernández, X., & Gilmore, G. 1998, MNRAS, 294, 595

Hernández, X., Park, C., Cervantes-Sodi, B., & Choi, Y. 2007, MNRAS, 375, 163 (Paper II)

Hubble, E. P. 1926, ApJ, 64, 321

_____. 1936, Realm of the Nebulae (New Heaven: Yale Univ. Press)

Hunter, D. A., & Hoffman, L. 1999, AJ, 117, 2789

Jiménez, R., Padoan, P., Matteucci, F., & Heavens, A. F. 1998, MNRAS, 299, 123

Kauffmann, G. 1996, MNRAS, 281, 475

Kennicutt, R. C. 1998, ApJ, 498, 541

Kennicutt, R. C., Oey, M. S., Zaritsky, D., & Huchra, J. P. 1993, RevMexAA, 27, 21

Koda, J., Sofue, Y., & Wada, K. 2000, ApJ, 532, 214

Kregel, M., van der Kruit, P. C., & de Grijs, R. 2002, MNRAS, 334, 646

Kregel, M., van der Kruit, P. C., & Freeman, K. C. 2005, MNRAS, 358, 503

Kuchinski, L. E., et al. 2000, ApJS, 131, 441

Lahav, O., et al. 1995, Science, 267, 859

Melbourne, J., & Salzer, J. J. 2002, AJ, 123, 2302

Mo, H. J., Mao, S., & White, S. D. M. 1998, MNRAS, 295, 319

Naim, A., et al. 1995, MNRAS, 274, 1107

Oey, M. S., & Kennicutt, R. C. 1993, ApJ, 411, 137

Pahre, M. A., Ashby, M. L. N., Fazio, G. G., & Willner, S. P. 2004, ApJS, 154, 235

Park, C., & Choi, Y. 2005, ApJ, 635, L29

Peebles, P. J. E. 1969, ApJ, 155, 393

Pilyugin, L. S. 2001, A&A, 374, 412

_____. 2003, A&A, 399, 1003

Pilyugin, L. S., Vílchez, J. M., & Contini, T. 2004, A&A, 425, 849 (PVC)

84   CERVANTES-SODI & HERNÁNDEZ

Prantzos, N., & Boissier S. 2000, MNRAS, 313, 338

Roberts, M. S., & Haynes, M. P. 1994, ARA&A, 32, 115

Silk, J., & Wyse, F. G. 1993, Phys. Rep., 231, 293

Tutukov, A. V. 2006, ARep, 50, 526

van den Bosch, F. C. 1998, ApJ, 507, 601

van der Kruit, P. C. 1987, A&A, 173, 59

Vila-Costas, M. B., & Edmunds, M. G. 1992, MNRAS, 259, 121

Wong, T., & Blitz, L. 2002, ApJ, 569, 157

Zaritsky, D., Kennicutt, R. C., & Huchra, J. P. 1994, ApJ, 420, 87 (ZKH)

Zavala, J., Okamoto, T., & Frenk, C. S. 2008, MNRAS, 387, 364

Zhang, B., & Wyse, R. F. G. 2000, MNRAS, 313, 310

B. Cervantes-Sodi: Instituto de Astronomía, Universidad Nacional Autónoma de México, Apdo. Postal 70-264, 04510 México, D. F., Mexico (bcervant@astroscu.unam.mx).

X. Hernández: Instituto de Astronomía, Universidad Nacional Autónoma de México, Apdo. Postal 70-264, 04510 México, D. F., Mexico and GEPI, CNRS UMR 8111, Observatoire de Paris, 5 Place Jules Janssen, 92195 Meudon Cedex, France (xavier@astroscu.unam.mx).

Capítulo 4

Distribuciones empíricas de λ a partir del SDSS.

Los dos capítulos anteriores se refieren a las implicaciones que tiene el parámetro de espín λ en la estructura interna de las galaxias. En esta segunda parte de la tesis que comprende este capítulo y el siguiente, nos enfocaremos a estudiar las distribuciones de λ inferidas a partir de muestras grandes de galaxias, limitadas por volumen, provenientes del SDSS.

Este capítulo en particular consiste en obtener una distribución para λ usando una muestra proveniente del SDSS, con el propósito de compararla con resultados provenientes de simulaciones cosmológicas. Con tal fin, y dado que nuestra muestra de galaxias contiene además de galaxias espirales, galaxias elípticas, dedujimos una expresión general para calcular λ a cualquier galaxia elíptica, en función de variables fácilmente medibles a partir de observaciones: la excentricidad, el eje mayor y la dispersión de velocidades.

Para discriminar entre galaxias de disco y elípticas, empleamos un criterio de segregación mediante color, gradiente de color e índice de concentración propuesto por Park & Choi (2005). Una vez identificada la morfología de cada galaxia en la muestra, calculamos λ aplicando la fórmula correspondiente para obtener distribuciones de λ, tanto para galaxias de disco como para la muestra completa. La distribución obtenida a partir de la submuestra de galaxias de disco, se ajusta con gran precisión a una función log-normal, función que se usa recurrentemente en simulaciones cosmológicas para ajustar la distribución total de λ. Antes de obtener la distribución total para λ de nuestra muestra, mostramos cómo el valor medio de λ correlaciona fuertemente con el tipo morfológico asignado por inspección visual.

Una vez calculado λ para todas las galaxias de nuestra muestra obtuvimos su distribución, que se encuentra bien descrita por una función log-normal con parámetros $\lambda_0 = 0{,}0394 \pm 0{,}005$ y $\sigma_\lambda = 0{,}509 \pm 0{,}05$.

Trabajo publicado en:

- Hernández X., Park C., Cervantes-Sodi B., Choi Y., 2007, MNRAS, 375, 163

Empirical distributions of galactic λ spin parameters from the Sloan Digital Sky Survey

X. Hernandez,[1]⋆ Changbom Park,[2] B. Cervantes-Sodi[1] and Yun-Young Choi[2]

[1]*Instituto de Astronomía, Universidad Nacional Autónoma de México A. P. 70–264, México 04510 D.F., México*
[2]*Korea Institute for Advanced Study, Dongdaemun-gu, Seoul 130-722, Korea*

ABSTRACT

Using simple dimensional arguments for both spiral and elliptical galaxies, we present formulae to derive an estimate of the halo spin parameter λ for any real galaxy, in terms of common observational parameters. This allows a rough estimate of λ, which we apply to a large volume-limited sample of galaxies taken from the Sloan Digital Sky Survey data base. The large numbers involved (11 597) allow the derivation of reliable λ distributions, as signal adds up significantly in spite of the errors in the inferences for particular galaxies. We find that if the observed distribution of λ is modelled with a lognormal function, as often done for this distribution in dark matter haloes that appear in cosmological simulations, we obtain parameters $\lambda_0 = 0.04 \pm 0.005$ and $\sigma_\lambda = 0.51 \pm 0.05$, interestingly consistent with values derived from simulations. For spirals, we find a good correlation between empirical values of λ and visually assigned Hubble types, highlighting the potential of this physical parameter as an objective classification tool.

Key words: galaxies: formation – galaxies: fundamental parameters – galaxies: statistics – galaxies: structure – cosmology: miscellaneous – cosmology: observations.

1 INTRODUCTION

Perhaps one of the most useful tools for describing the nature of observed galactic populations is the luminosity function. The relative number of galaxies of different luminosities offer a quantitative description of the result of the structure formation scenario of the Universe, nowadays available for inspection even as a function of redshift. The luminosity function, or mass function of galaxies, once a modelling of star formation histories and dust is included to yield mass-to-light ratios, is indeed one of the principal constraints against which cosmological simulations and structure formation theories in general are tested. Often star formation efficiencies and histories are calibrated through a fitting of predicted halo mass functions and observed luminosity functions, e.g. Davis et al. (1985) and references thereof.

Galaxies, however, have many more properties than just their mass, most notably, galactic classification schemes centre on sorting galaxies as ellipticals, lenticulars and spirals, subdividing the latter again into types, typically along the Hubble sequence. In spite of the many well-known virtues of this classification scheme, its somewhat subjective, qualitative and relative nature has made it difficult to use in comparison against cosmological simulations, where the 'type' of a modelled galaxy is rather difficult to assess, in terms of Hubble's classification scheme.

Inspired by varied theoretical studies which invariably identify the λ spin parameter of a host halo as the principal physical parameter in determining the morphological and visual characteristics of a spiral galaxy, which are then subjectively integrated into the qualitative assignment of 'type', in Hernandez & Cervantes-Sodi (2006) (henceforth HC06) two of us derived a simple estimate of λ for any observed spiral. There it was shown that the scalings of the derived λ against various type determining properties such as colour, disc thickness and bulge-to-disc ratio, are comparable to the corresponding scalings of these parameters against Hubble type, using a large sample of nearby spirals.

It is interesting that a generic prediction of cosmological *N*-body simulations over the past two decades has been the functional form and parameters which define the predicted distribution of λ for dark matter haloes (e.g. Bullock et al. 2001). Nevertheless, it has not been easy to test this prediction directly, as λ is not a straightforward observable feature of a real galaxy. A measurable λ distribution is relevant not only as a test of the general structure formation scheme but also as a further way of independently constraining cosmological parameters, which to a certain extent alter its details (e.g. Gardner 2001).

Having the approximate estimates of HC06, here we set out to measure empirical distributions of galactic λ spin parameters. First, given the approximate nature of these estimates, the only way of having signal adding up to something significant is through the use of very large samples. Also, if we want a meaningful comparison against cosmological models, use of a volume-limited sample is

⋆E-mail: xavier@astroscu.unam.mx

164   *X. Hernandez et al.*

crucial. These two constraints drive us inevitably to the Sloan Digital Sky Survey (SDSS). Two of us have worked extensively with this data base, and recently constructed an interesting morphology segregation scheme of galaxies in the SDSS in Park & Choi (2005), henceforth PC05. Here we use a volume-limited sample from the SDSS having galaxies with redshifts in the interval $0.025 < z < 0.055$, corresponding to distances between 75 and $162.57\,h^{-1}$ Mpc, assuming a *Wilkinson Microwave Anisotropy Probe* cosmology of $\Omega_{\mathrm{M}} = 0.27$, $\Omega_{\Lambda} = 0.73$ and $h = 0.71$, which we keep throughout.

The following section includes a review of the derivation of λ spin parameters for spirals of HS06, and gives our results for the spirals in our SDSS sample. The correspondence between λ for spirals, galactic type through visual inspection and the colour and colour gradient morphology segregation scheme of PC05 is also made in Section 2. These are well fitted by a lognormal function, and give parameters in accordance with recent cosmological simulations. In Section 3, we extend the dimensional estimate of λ for ellipticals, and construct and analyse the empirical distributions of λ for the complete sample. Our results are summarized in Section 4.

2 λ DISTRIBUTIONS FOR SPIRAL GALAXIES

We are concerned with the determination of the dimensionless angular momentum parameter of a galactic halo

$$\lambda = \frac{L \mid E \mid^{1/2}}{GM^{5/2}}, \tag{1}$$

where E, M and L are the total energy, mass and angular momentum of the configuration, respectively. None of the quantities which appear in the above definition are accessible to direct observation. In HC05, we derived a simple estimate of λ for disc galaxies in terms of observational parameters, which we summarize below.

We will model only two galactic components: the first one is a disc having a surface mass density $\Sigma(r)$ satisfying

$$\Sigma(r) = \Sigma_0 \mathrm{e}^{-r/R_\mathrm{d}}, \tag{2}$$

where r is a radial coordinate and Σ_0 and R_d are two constants which are allowed to vary from galaxy to galaxy. The total disc mass is now

$$M_\mathrm{d} = 2\pi\Sigma_0 R_\mathrm{d}^2. \tag{3}$$

The second component will be a fixed dark matter halo having an isothermal $\rho(r)$ density profile, and responsible for establishing a rigorously flat rotation curve V_d throughout the entire galaxy, an approximation sometimes used in simple galactic evolution models (e.g. Naab & Ostriker 2006). Under a flat rotation curve the disc specific angular momentum from equation (2) will be $l_\mathrm{d} = 2V_\mathrm{d}R_\mathrm{d}$, and the halo density will satisfy

$$\rho(r) = \frac{1}{4\pi G}\left(\frac{V_\mathrm{d}}{r}\right)^2, \tag{4}$$

having a halo mass profile $M(r) \propto r$. We define the disc mass fraction as $F = M_\mathrm{d}/M_\mathrm{H}$, expected to be of the order of 1/10 or smaller (e.g. Flores et al. 1993; Hernandez & Gilmore 1998); we will use global parameters for the entire system indistinctly from halo parameters, consistent with having ignored disc self-gravity in equation (4).

We must now express λ in terms of structural galactic parameters readily accessible to observations. First, we assume that the total potential energy of the galaxy is dominated by that of the halo, and that this is a virialized gravitational structure, which allows

us to replace E in equation (1) for $W/2$, one-half the gravitational potential energy of the halo, given by

$$W = -V_\mathrm{d}^2 M_\mathrm{H}. \tag{5}$$

Assuming that the specific angular momenta of disc and halo are equal, $l_\mathrm{d} = l_\mathrm{H}$ (as would be the case for an initially well-mixed protogalactic state, and generally assumed in galactic formation models; e.g. Fall & Efstathiou 1980; Mo, Mao & White 1998); we can replace L with $M_\mathrm{H}l_\mathrm{d}$. Introducing this last result together with equation (5) into equation (1) yields

$$\lambda = \frac{2^{1/2}V_\mathrm{d}^2 R_\mathrm{d}}{GM_\mathrm{H}}. \tag{6}$$

Finally, we can replace M_H with M_d/F, and introduce a disc Tully–Fisher relation

$$M_\mathrm{d} = A_{\mathrm{TF}}V_\mathrm{d}^{3.5} \tag{7}$$

into equation (6) to yield

$$\lambda = \left(\frac{2^{1/2}F}{A_{\mathrm{TF}}}\right)\frac{R_\mathrm{d}}{GV_\mathrm{d}^{3/2}}. \tag{8}$$

The existence of a general baryonic Tully–Fisher relation between the total baryonic component and V_d of the type used here, rather than a specific Tully–Fisher relation involving total magnitude in any particular band, is supported by recent studies, in general in agreement with the exponent 3.5 we assume (e.g. Gurovich et al. 2004 or Kregel, van der Kruit & Freeman 2005 who find 3.33 ± 0.37). All that remains is to choose numeric values for F and A_{TF}, to obtain an estimate of the spin parameter of an observed galaxy in terms of structural parameters readily accessible to observations, R_d and V_d.

Taking the Milky Way as a representative example, we can use a total baryonic mass of $1 \times 10^{11}\,\mathrm{M_\odot}$ and $M_\mathrm{H} = 2.5 \times 10^{12}\,\mathrm{M_\odot}$ (where the estimate of the baryonic mass includes all such components, disc, bulge, stellar halo, etc.; e.g. Wilkinson & Evans 1999; Hernandez, Avila-Reese & Firmani 2001) as suitable estimates to obtain $F = 1/25$. For a rotation velocity of $V_\mathrm{d} = 220$ km s^{-1}, the above numbers imply $A_{\mathrm{TF}} = 633\,\mathrm{M_\odot}$ (km s^{-1})$^{-3.5}$, this in turn allows us to express equation (8) as

$$\lambda = 21.8\frac{R_\mathrm{d}/\mathrm{kpc}}{(V_\mathrm{d}/\mathrm{km\,s^{-1}})^{3/2}}. \tag{9}$$

For the Galactic values used above, equation (9) yields $\lambda_{\mathrm{MW}} = 0.0234$, in excellent agreement with recent estimates of this parameter; e.g. through a detailed modelling of the Milky Way within a cold dark matter framework, Hernandez et al. (2001) find $\lambda_{\mathrm{MW}} = 0.02$.

First, we note that by construction, what we are estimating is not strictly λ, but what has been defined as λ', the equivalent λ for a singular truncated isothermal halo. The relation between λ and λ' is slightly a function of halo structure; for example, for Navaro–Frenk–White profiles with concentration of 10, one gets $\lambda' = 0.9\lambda$ (e.g. Mo et al. 1998). This slight difference is smaller than the error introduced through the dispersion in the Tully–Fisher relation used, and will not be considered further, in any case, it is more rigorously λ' and not λ that we will be talking about. Also, it is clear that equation (9) is at best a first-order approximation, and not a precise evaluation of λ for a real galaxy.

However, in HC06 it was shown that this λ parameter shows a one-to-one correlation, with small dispersion, when compared to the input λ of detailed galactic formation models from two distinct cosmological groups. Also, the scalings seen against colour, disc

thickness and bulge-to-disc ratios, for a sample of nearby spirals from Courteau (1996, 1997), de Grijs (1998) and Kregel, van der Kruit & de Grijs (2002), similar to what is seen against Hubble type, highlight the use of this parameter as a physical classification scheme. This is not surprising, as it is λ as defined by equation (1), what has been repeatedly identified in analytic and numerical studies of galactic formation as the principal determinant of galactic type (e.g. Fall & Efstathiou 1980; Flores et al. 1993; Firmani, Hernandez & Gallagher 1996; Dalcanton, Spergel & Summers 1997; Zhang & Wyse 2000; Silk 2001; Kregel et al. 2005).

For example, the ratio of disc scaleheight to disc scalelength, h/R_d, is one of the type defining characteristics of a galaxy which it is easy to show, will scale with λ. Starting from Toomre's stability criterion

$$Q(r) = \frac{\kappa(r)\sigma(r)}{\pi G \Sigma(r)}, \tag{10}$$

where $\kappa(r)$ and $\sigma(r)$ are the epicycle frequency and velocity dispersion at a given point in the disc, assuming a thin disc, virial equilibrium in the vertical direction (Binney & Tremaine 1987) yields a relation between h and Σ,

$$h = \frac{\sigma_g^2}{2\pi G \Sigma}. \tag{11}$$

We use this relation for h to replace the gas velocity dispersion appearing in equation (10) for a combination of h and the surface density. The dependence on Σ is replaced by one on M_d and R_d through the disc profile. Replacing $\kappa(r)$ with $\sqrt{2}V_d/r$, and V_d with λ, R_d and M_H through equation (6) to get a new expression for Toomre's stability criterion, which evaluating radial dependences at $r = R_d$, yields

$$Q^2 = e2^{5/2} \left(\frac{M_H}{M_d}\right) \left(\frac{h}{R_d}\right) \lambda. \tag{12}$$

With $F = 1/25$, evaluating at $Q = 1$, the stability threshold suggested by self-regulated star formation cycles (e.g. Dopita & Ryder 1994; Koeppen, Theis & Hensler 1995 and Silk 2001), the ratio h/R_d is obtained as

$$\frac{h}{R_d} = \frac{1}{390\lambda}, \tag{13}$$

a simplified version of the result of van der Kruit (1987). For the Galactic value derived above $\lambda_{MW} = 0.0234$, equation (13) gives $R_d = 9h$, not in conflict with parameters for the Milky Way. For galaxies with large values of λ, we expect thin systems, while galaxies with small values of λ will show thick discs, as the observed trend of (h/R_d) decreasing in going from early-type discs to late-type galaxies (e.g. de Grijs 1998; Yoachim & Dalcanton 2006).

Having a way of estimating λ, we now need to define the optimal sample to use. As already mentioned, requiring as large as possible a volume-limited sample makes the SDSS an ideal data base. Since most published cosmological distributions of λ report data at $z = 0$, we will start by taking a volume-limited, absolute magnitude-limited sample with $M_r - 5 \log h \leqslant -18.5$, in a low redshift range, $0.025 < z < 0.055$, allowing an optimal comparison with reported cosmological studies. This sample contains 31 685 galaxies for which exponential disc scales, absolute magnitudes, velocity dispersions, de Vacouleurs radii and eccentricities have been determined (Choi, Park & Vogeley 2006). It is important to note that the above structural parameters were determined in red and infrared bands, in the spirit of obtaining global mass distribution parameters, it is clear that this is what is required for the measure of R_d necessary in equation (9).

The first step is to identify the spiral galaxies in our sample. This is done using the colour, colour-gradient and concentration criteria developed in PC05, where extensive testing and corroboration of the morphological segregation criteria were preformed against large training sets of visually classified galaxies. This procedure yields 21 184 spirals and 10 501 ellipticals.

Since we have no rotation curves for the spiral galaxies, as required by equation (9), we must infer this through the absolute magnitudes of the observed systems, and use of an appropriate Tully–Fisher relation. Hence, internal absorption in edge-on discs is a problem we must avoid. We prune the original sample to leave only spiral galaxies having axis ratios >0.6, this ensures only relatively face-on discs remain, minimizing errors in the absolute magnitudes used (see Choi et al. 2006, for the choice of axis ratio cut). Also, we use the red band Tully–Fisher relations of Barton et al. (2001) to assign rotation velocities to observed galaxies. This relation shows a good fit to the data only in the range $-20 > M_R > -22.5$, so we must limit our galaxies to those falling in this range. The corresponding ranges we impose on inferred rotation velocities are $80 < V_R < 430$ in km s^{-1}, well within the range of applicability of the Tully–Fisher relation we are using. Still, the dispersion in this Tully–Fisher relation, plus that in the baryonic Tully–Fisher relation used in deriving equation (9), leaves us with a 25 per cent uncertainty in our individual estimates of λ for spirals.

After applying the two cuts described above, we are left with 0.366 of the original 21 184 spirals, 7753 disc systems, still large enough to yield significant statistical information on the distribution, and small enough to include only galaxies for which our estimates of λ are most accurate. Use of equation (9) for this sample yields a collection of 7753 values of λ for a complete volume-limited SDSS sample.

Having now a set of inferred, observational values of λ, we first explore the correlations of λ for spirals only, against the colour and colour-gradient information found by PC05 to be an accurate indicator of galactic type. Fig. 1, taken from PC05, shows some of the galaxies in our sample, with photos of galaxies representative of those
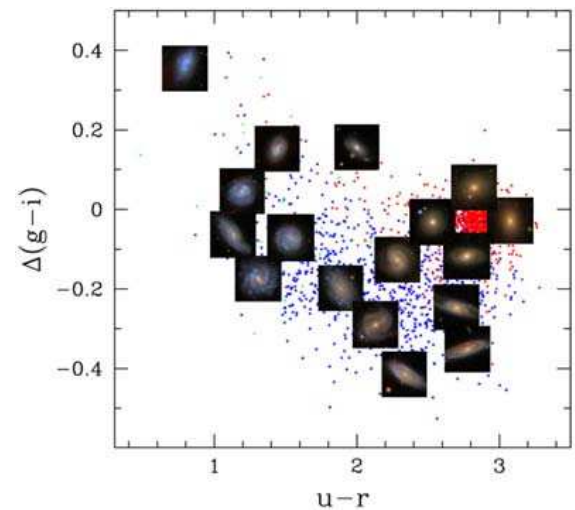

Figure 1. Some of the galaxies in our sample on a colour, colour-gradient plane, with photos of galaxies representative of those found in each region, as visually classified by PC05. Red dots (clear) are early-type galaxies and others are late types.
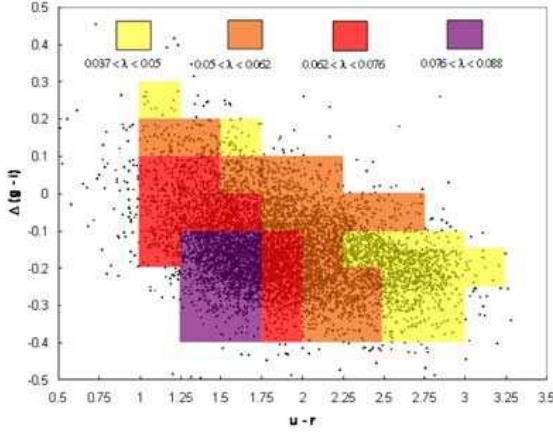
166   *X. Hernandez et al.*

Figure 2. Spiral galaxies in our sample on a colour, colour-gradient plane, the shading shows the average values of λ in each shaded region, using equation (9). Regions of high and low values of λ closely correspond to regions populated by late- and early-type spirals, respectively, as visually classified by PC05.

of those found in each region, as visually classified by PC05. Note the well-defined cluster of ellipticals centred on $\Delta(g - i) = -0.04$, $u - r = 2.82$. Fig. 2 shows all our spirals in a colour, colour-gradient plane, with the shading giving the average values of λ within each shaded square. We see that discs with high values of λ are found in the lower left-hand area, whilst discs having low values of λ populate the right-hand and upper regions. It is interesting that PC05 find precisely the same segregation pattern for late and early spirals, respectively, reinforcing the results of HC06 that the quantitative and objective λ parameter constructed in equation (9) is a good physical classification parameter for spirals, reproducing the broad trends of the classical subjective, qualitative Hubble sequence.
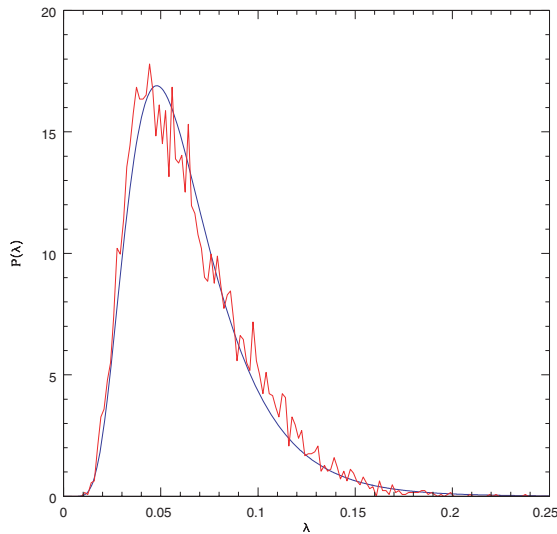
Next we use our collection of values of λ from our pruned sample of face-on spirals to construct a histogram, shown in Fig. 3 by the broken curve. The shape of this histogram suggests a lognormal distribution

$$P(\lambda_0, \sigma_\lambda; \lambda)\, d\lambda = \frac{1}{\sigma_\lambda \sqrt{2\pi}} \exp\left[-\frac{\ln^2(\lambda/\lambda_0)}{2\sigma_\lambda^2} \right] \frac{d\lambda}{\lambda}. \tag{14}$$

The moments of the above distribution are analytical, which allows one to express

$$M_1(\lambda_0, \sigma_\lambda) = \frac{\int_0^\infty P(\lambda)\lambda\, d\lambda}{\int_0^\infty P(\lambda)\, d\lambda} = \lambda_0 \exp\left(\sigma_\lambda^2/2\right), \tag{15}$$

$$M_2(\lambda_0, \sigma_\lambda) = \frac{\int_0^\infty P(\lambda)\lambda^2\, d\lambda}{\int_0^\infty P(\lambda)\, d\lambda} = \lambda_0^2 \exp\left(2\sigma_\lambda^2\right), \tag{16}$$

from which one solves

$$\lambda_0 = \frac{M_1^2}{M_2^{1/2}}, \sigma_\lambda = \left[\ln\left(\frac{M_2}{M_1^2} \right) \right]^{1/2}. \tag{17}$$

Equating the first- and second-order moments of our empirical distribution to M_1 and M_2, we find the best-fitting lognormal curve to our distribution for spiral galaxies. This is given by the smooth curve in Fig. 3, where the empirical histogram has been rescaled to a unit integral. The parameters of the best-fitting distribution are $\lambda_0 = 0.0585$ and $\sigma_\lambda = 0.446$. Both the form of this distribution and the particular values for the parameters we find are in good agreement with results from cosmological simulations (e.g. Shaw et al. 2006).

From Fig. 3, it is apparent that the lognormal functional form is a good description of our inferred data, a more formal confirmation is provided by a K–S test. We construct the cumulative distribution functions for both the lognormal $P(\lambda)$ and our data out to $\lambda = 0.2$, shown in Fig. 4 by the solid and dotted curves, respectively. These yield a maximum difference $D = 0.029$, and a significance given by

$$Q_{KS}(X) = 2 \sum_{j=1}^{\infty} (-1)^{j-1} \exp(-2j^2 X^2), \tag{18}$$

Figure 3. Distribution of values of λ for 7753 spirals using equation (9), binned into 150 intervals, broken curve. Best lognormal fit to the data, having parameters $\lambda_0 = 0.0585$ and $\sigma_\lambda = 0.446$, solid curve.
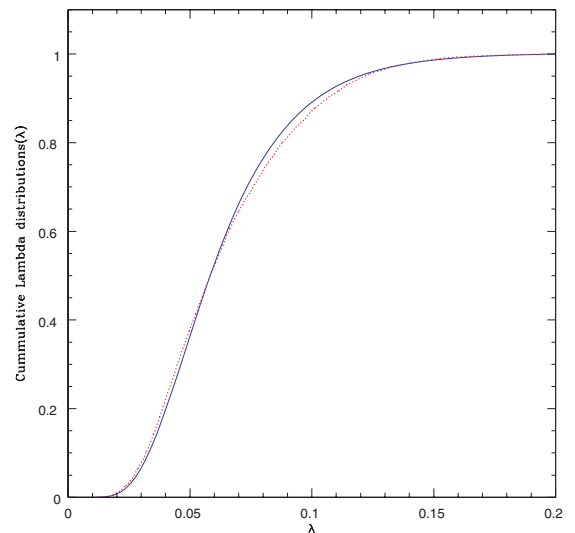

Figure 4. Cumulative distribution functions for both our spiral galaxies data and the best-fitting lognormal $P(\lambda)$, dotted and solid curves, respectively.
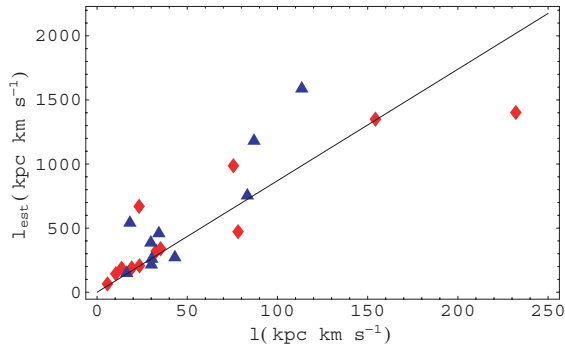
Figure 5. Specific angular momentum for elliptical galaxies from Pinkney et al. (2003) (triangles) and Halliday et al. (2001) (rhombi), determined directly from their measurements of rotation velocity and deprojected light profiles, x-axis. The y-axis shows values for the same quantity, but estimated through equation (19) using $C = 1$, the solid line gives the best-fitting linear relation. We then estimate C by forcing the best-fitting linear relation to coincide with the identity.

where $X = N^{1/2} D$, N is the total number of points in our sample, 7746, giving $X = 2.55$ and a significance level of $Q_{KS} = 0.000\,004$. We hence see that our inferred distribution of galactic λs is consistent with having come from the best-fitting lognormal $P(\lambda)$, to a very high degree. We note the important precedent of Syer, Mao & Mo (1999) who, using similar estimates for λ for spiral galaxies, using a sample from Lauberts (1982) find a distribution of values of λ well fitted by a lognormal function, with parameters $\lambda_0 = 0.05$ and $\sigma_\lambda = 0.36$. The small differences with our inference might come from their lack of a large volume-limited unbiased sample, their lack of an attempt at modelling λ for ellipticals, which further limited the scope of comparison which could then be made against cosmological N-body models, or their use of a disc formation model calibrated directly from cosmological N-body simulations.

From equation (8), we see that our inferred λs are proportional to the constants (F/A_{TF}), since the validity and constancy of the Tully–Fisher relation is well established, we can think of our inferred λs as $\lambda(25F)$, where F is the baryon fraction of a spiral system. We have shown that under the simplest assumption of a constant $F = 1/25$, a lognormal distribution results from the data, clearly, any other constant F will also yield a lognormal distribution, with the same σ_λ, and a mean of $25 F \lambda_0$. Also, note that most cosmological simulations yield distributions of λ being independent of mass (e.g. Bullock et al. 2001) which if true, ensures our inferences will not be skewed by the velocity cuts applied to the spirals.

A baryon fraction being a strong function of R_d or V_d, however, could easily result in a best-fitting $P(\lambda)$ no longer looking like a lognormal distribution. In the absence of any definitive handle on F or its possible variations, we limit ourselves to concluding that a constant F implies a lognormal $P(\lambda)$ for the spirals from the SDSS we studied, while varying $F(R_d, V_d)$ could doubtlessly imply something else.

3 λ DISTRIBUTIONS FOR THE COMPLETE SAMPLE

Before attempting an empirical total distribution of λs, we must derive an estimate for this parameter for an elliptical galaxy, we propose a model equivalent to the one used for spirals, including only

two components: a baryonic matter distribution with a Hernquist density profile and a dark matter halo having a singular, truncated isothermal profile.

In order to calculate the energy of the galaxy, we assume that the total potential is dominated by the energy of the virialized dark matter halo. In principle, we expect that haloes, where elliptical galaxies are found, are no different from those of disc galaxies (White & Rees 1978; Kashlinsky 1982). In the case of a disc galaxy, the halo density profile has the form $4\pi G\rho(r) = (V_c/r)^2$, with potential energy $-V_c^2 M_H$. The velocity V_c is the circular velocity of an element in centrifugal equilibrium with the halo. In an elliptical, nothing is actually moving at that velocity, which still can be used to characterize the halo. The dependence on velocity can be changed to one on mass using again a baryonic Tully–Fisher relation (Gurovich et al. 2004): $M_b = A_{TF} V_c^{3.5}$, thinking that the dynamics of a halo host of an elliptical galaxy are the same as those of disc galaxies. Finally, we define the baryonic mass fraction as $F = M_b/M_H$ to express the mass of the halo in terms of the baryonic mass. Validating the above assumptions, we note the interesting new results of Treu et al. (2006) and Koopmans et al. (2006) who find through dynamical studies of velocity dispersion in ellipticals, and direct inferences on the haloes of the studied ellipticals through lensing measurements, (i) the presence of extensive dark haloes and (ii) that these haloes have equivalent velocity dispersions equal to those of their galaxies, the dynamical equivalent of a flat rotation curve for ellipticals.

For the angular momentum, if we assume that the specific angular momenta of dark matter and baryons are equal, $l_b = l_H$, we can obtain the angular momentum of the entire configuration using only the directly observable component. It is important to remember that the baryonic component is susceptible of dissipating, while dark matter is not, this will affect the above assumption and our λ estimates, being the value obtained a lower limit. In order to obtain the angular momentum of the baryonic distribution, we need to know the rotation velocity, information not always available due to technical observational difficulties and the fact that in many elliptical galaxies, the rotational velocity is at best of the same order as that of the velocity dispersion (Pinkney et al. 2003; Sarzi et al. 2006). These force us to determine the angular momentum of the system using some other observable parameter. In many works (e.g. Binney 1978; Franx, Illingworth & Heckman 1989) it is shown that the ellipticity of a galaxy is related to its rotation velocity, more precisely to its angular momentum. By dimensional analysis, we expect the specific angular momentum of the galaxy to be proportional to $(GM_b a)^{1/2}$ and to the eccentricity e of the galaxy in the i-band, as shown by Gott & Thuan (1976) and in Marchant & Shapiro (1977). Introducing a proportionality constant C related to the details of the matter distribution, the specific angular momentum is given by

$$l_b = C e \sqrt{G M_b a}, \qquad (19)$$

with a being the de Vacouleurs radius of the galaxy. The constant C can be calibrated from cases where we know the actual angular momentum of the system. For a small sample of 22 closely studied elliptical galaxies, from Halliday et al. (2001) and Pinkney et al. (2003) we calculated the actual angular momentum, for a Hernquist profile and using the reported values of rotational velocity. Comparing with the angular momentum given by equation (19), we obtain $C = 0.114$, as shown in Fig. 5.

For the galactic mass, using again the assumption that the gravitational structure is virialized, we compute the dynamical mass at

168   *X. Hernandez et al.*

R_{50}, the half light radius, using the expression

$$M_{\rm dyn} = \frac{(1.65\sigma)^2 R_{50}}{G},\tag{20}$$

from Padmanabhan et al. (2004), where σ is the velocity dispersion. For elliptical galaxies, it is well known that the presence of dark matter in the inner part of the galaxy is negligible so the total baryonic mass will be simply $2M_{\rm dyn}$.

Now we have the tools to estimate the energy, the angular momentum and the mass of an elliptical galaxy. If we introduce this information into equation (1), we obtain

$$\lambda = \frac{0.051 e (a/{\rm kpc})^{2/7}}{(\sigma/{\rm km\ s^{-1}})^{3/7}},\tag{21}$$

where we used values for $A_{\rm TF}$ and F as calibrated in HC06. The above expression is the equivalent expression of equation (9) for elliptical galaxies, and has errors of 30 per cent, due to the dispersion in the observational relations used.

We must take into account that the values for eccentricity e and radius a, required must be the intrinsic parameters of the system, not the observed ones, as these will be systematically smaller due to projection effects. Also in many ellipticals, shape is the result not exclusively of rotational support, but also of dynamical pressure support (i.e. anisotropic velocity dispersion), with varying degrees of relative importance. Hence, unknown dissipational and projection effects make equation (21) a lower limit, whilst the participation of pressure support makes it an upper one. To what extent the above compensate each other is unclear, we will therefore assume equation (21) must be multiplied by a factor which remains a free parameter of our method, X_E.

Since ellipticals will generally have much lower values of λ than spirals, the relative mix of spirals and ellipticals will be an important factor in determining our final estimated distribution of galactic λs. We must hence leave this relative fraction equal to that of the original sample, before the velocity and projection cuts were applied to the spirals, we further remove randomly selected ellipticals to reduce the total number of galaxies to 0.366 of the original number, leaving only 3843 ellipticals. Our final sample is composed of a total of 11 597 galaxies, large enough to yield significant statistical information on the distribution.

Using equation (21) we estimate λ for the ellipticals in the sample, after which we can add the two distributions to obtain the total empirical $P(\lambda)$. As discussed previously, for ellipticals, a degree of uncertainty remains, in connection to the (varying) degree of pressure support, the degree of dissipation of angular momentum in the baryonic component, and projection effects, which to zeroth order we have incorporated as an unknown multiplicative factor X_E. For $X_E = 1$ the result of adding the distribution of λ parameters for spirals and ellipticals is a distinctly double peaked $P(\lambda)$, with the ellipticals coming in as a Gaussian distribution centred at $\lambda = 0.01$. In the interest of comparing with simulations, we will take as a working hypothesis that the full $P(\lambda)$ should also be a lognormal distribution. We then adjust X_E so as to obtain a lognormal total distribution, with the restriction that the values of λ for ellipticals should remain lower than those of spirals. The resulting histogram, requiring $X_E = 2.3$ is shown by the broken curve in Fig. 6, where the smooth solid curve gives a best-fitting lognormal curve to the full distribution, having parameters $\lambda_0 = 0.046$ and $\sigma_\lambda = 0.535$.

Given that we have used empirical scaling relations, which show a measure of dispersion, we now take the pessimistic view that such dispersions are intrinsic to the data (pessimistic in the sense that a measure of this dispersion is undoubtedly observational noise),

and hence, propagate as errors into our estimates of λ. We now estimate what is the best underlying lognormal distribution, assuming that the histograms we obtained are only a degraded version of an intrinsic lognormal distribution. We determine the best intrinsic lognormal function through a full maximum likelihood analysis of the data. This is done for purposes of comparison against predicted λ distributions, we fix the functional form of the distribution, and set out only to evaluate the best-fitting parameters λ_0 and σ_λ from equation (14).

We construct the likelihood function as the probability that an inferred set of n empirical values of λ, $\{\lambda_i(\lambda)\}^n$, might arise from a given model $(\lambda_0, \sigma_\lambda)$ as

$$\mathcal{L}(\lambda_0, \sigma_\lambda; \{\lambda_i(\lambda)\}^n) = \sum_{i=0}^{n} \ln \int_0^\infty P(\lambda_0, \sigma_\lambda; \lambda)\lambda_i(\lambda)\,{\rm d}\lambda,\tag{22}$$

where

$$\lambda_i(\lambda) = \frac{F_i}{\sigma_i \sqrt{2\pi}} \exp\left[-\frac{(\lambda - \lambda_{0i})^2}{2\sigma_i^2}\right],\tag{23}$$

λ_{0i} is the centre of a density distribution, the nominal inferred λ for the ith galaxy, σ_i is the assigned error and F_i is a normalization factor taking into account that no matter what the error, the domain of λ_i must always be the positive values of λ. Therefore, we normalize $\lambda_i(\lambda)$ as a truncated Gaussian having unit integral, giving $F_i = 2/[1 + {\rm erf}(\lambda_{0i}/\sqrt{2}\sigma_i)]$.

In the limit of the error in our inferred λ tending to zero, F_i tends to 1, and $\lambda_i(\lambda)$ tends to a Dirac delta function, reducing the integral in equation (22) to an evaluation of $P(\lambda)$ at the inferred value. The advantage of a full likelihood formulation is that parameter inference can be preformed in a way which naturally incorporates the errors in the data sample, without the need of binning the data, a process which intrinsically reduces the information content of the sample.

Equation (22) is then evaluated over a fine grid of values of $(\lambda_0, \sigma_\lambda)$, and the point where the maximum is found selected as the best-fitting model. For the 7753 spirals, the result is $(\lambda_0 = 0.0517, \sigma_\lambda = 0.362)$, with very small confidence intervals of ± 0.0003 and ± 0.004, respectively. Although our errors in individual λ estimates are of 25 per cent of λ, it is thanks to having a sample running into the thousands that we can retrieve details of the λ distribution with accuracy.

Finally, we repeat the evaluation of equation (22), but using this time the complete sample, of 11 597 spirals plus ellipticals. Here, λ for the ellipticals is taken as 2.3 times the estimate of equation (21). This factor cannot be much larger than what we are using, since then ellipticals would start overlapping significantly with spirals in their λ distributions, as mentioned previously, if this factor is much reduced, the total λ distribution becomes double peaked, with ellipticals appearing as a distinct population at very low λ, which would be hard to explain.

The results this time are $\lambda_0 = 0.0394$ and $\sigma_\lambda = 0.509$. A comparison of the maximum likelihood model and the collection of inferred λs is given in Fig. 6, which is analogous to Fig. 3, but includes the complete sample, binned into 150 discrete intervals. A direct fit of equation (14) to the full data gives $\lambda_0 = 0.046$, $\sigma_\lambda = 0.535$.

The formal errors in the method are again of the order of what was found for the spirals, but this time we are dominated by the unknown correction factor between our estimate and the actual λ for ellipticals. This uncertainty, although bounded, dominates our final error estimates and yields ± 0.005 in λ_0 and ± 0.05 in σ_λ. Another possible source of error in our estimates would be the existence of a large population of low surface brightness galaxies of high λ, which would lead to larger values of both λ_0 and σ_λ.
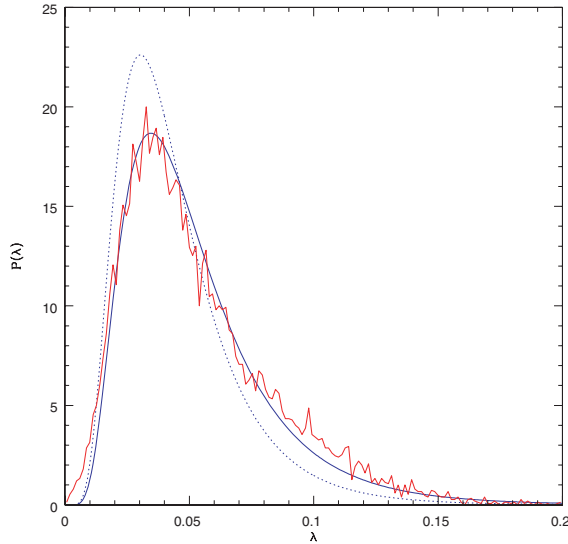
Figure 6. Distribution of values of λ for 11 597 spirals plus ellipticals using equations (9) and (21), binned into 150 intervals, broken curve. Best lognormal fit to the data, having parameters $\lambda_0 = 0.046$ and $\sigma_\lambda = 0.535$, smooth solid curve. Maximum likelihood underlying lognormal distribution, assuming a 30 per cent error in our inferred λs, with parameters $\lambda_0 = 0.0394$ and $\sigma_\lambda = 0.509$, dotted curve.

The above results qualitatively agree with generic predictions of structure formation models regarding the predicted values for λ_0 and σ_λ, e.g. Shaw et al. (2006) review recent results from the literature giving values in the range $0.03 < \lambda_0 < 0.05$ and $0.48 < \sigma_\lambda < 0.64$. The availability of empirical measurements of these parameters could serve as a further independent guideline for models of structure formation.

We stress that for the full sample, the lognormal nature of both the inferred and the underlying λ distributions is an assumption which we cannot confirm, taken only to permit a comparison with models. Under this assumption, the parameters of the distribution can be derived from the data. An inference of the actual functional form of the total distribution would require more solid constraints on the hypothesis introduced in the derivation of the λs for ellipticals. However, we do note that any similar scheme modelling ellipticals as residing in haloes equivalent to those of spirals, and having significantly lower angular momentum than spirals, will also yield a $P(\lambda)$ not very different from what is shown in Fig. 6.

4 CONCLUSIONS

We apply simple estimates of the λ spin parameter to a large volume-limited sample from the SDSS. The sample splits into ellipticals and spirals using colour, concentration and colour gradients.

We find that for spiral galaxies, the average value of the inferred λ correlates well with standard type, as determined by visual inspection. This highlights the potential of λ as an objective and quantitative classification tool for spiral galaxies.

For the spiral galaxies sample, we obtain a distribution which is statistically consistent with a lognormal distribution, as what is commonly found in cosmological *N*-body simulations, we find parameters $\lambda_0 = 0.0585$, $\sigma_\lambda = 0.446$.

Ellipticals have, as expected, average values of λ an order of magnitude lower than spirals. The details of their λ distribution are harder to quantify, but average values of around 0.005 are derived.

If the distribution of λ parameters for the full sample is fitted by lognormal distribution, of the type found to reproduce the corresponding distribution of modelled haloes arising in cosmological simulations, the parameters we find are $\lambda_0 = 0.0394 \pm 0.005$ and $\sigma_\lambda = 0.509 \pm 0.05$, derived this time from a sample of real galaxies.

REFERENCES

Barton E. J., Geller M. J., Bromley B. C., van Zee L., Kenyon S. J., 2001, AJ, 121, 625
Binney J., 1978, MNRAS, 183, 501
Binney J., Tremaine S., 1987, Galactic Dynamics. Princeton Univ. Press, Princeton, NJ
Bullock J. S., Dekel A., Kollatt T. S., Kravtsov A. V., Klypin A. A., Porciani C., Primack J. R., 2001, ApJ, 555, 240
Choi Y., Park C., Vogeley M. S., 2006, ApJ, in press (astro-ph/0611607)
Courteau S., 1996, ApJS, 103, 363
Courteau S., 1997, AJ, 114, 2402
Dalcanton J. J., Spergel D. N., Summers F. J., 1997, ApJ, 482, 659
Davis M., Efstathiou G., Frenk C. S., White S. D. M., 1985, ApJ, 292, 371
de Grijs R., 1998, MNRAS, 299, 595
Dopita M. A., Ryder S. D., 1994, ApJ, 430, 163
Fall S. M., Efstathiou G., 1980, MNRAS, 193, 189
Firmani C., Hernandez X., Gallagher J., 1996, A&A, 308, 403
Flores R., Primack J. R., Blumenthal G. R., Faber S. M., 1993, ApJ, 412, 443
Franx M., Illingworth G., Heckman T., 1989, 344, 613
Gardner J. P., 2001, ApJ, 557, 616
Gott J. R., Thuan T. X., 1976, ApJ, 204, 649
Gurovich S., McGaugh S. S., Freeman K. C., Jerjen H., Staveley-Smith L., De Blok W. J. G., 2004, Publ. Astron. Soc. Aust., 21, 412
Halliday C., Davies R. L., Kuntschner H., Birkinshaw M., Bender R., Saglia R. P., Baggley G., 2001, MNRAS, 326, 473
Hernandez X., Cervantes-Sodi B., 2006, MNRAS, 368, 351 (HC06)
Hernandez X., Gilmore G., 1998, MNRAS, 294, 595
Hernandez X., Avila-Reese V., Firmani C., 2001, MNRAS, 327, 329
Kashlinsky A., 1982, MNRAS, 200, 585
Koeppen J., Theis C., Hensler G., 1995, A&A, 296, 99
Koopmans L. V. E., Treu T., Bolton A. S., Burles S., Moustakas L. A., 2006, ApJ, 649, 599
Kregel M., van der Kruit P. C., de Grijs R., 2002, MNRAS, 334, 646
Kregel M., van der Kruit P. C., Freeman K. C., 2005, MNRAS, 358, 503
Lauberts A., 1982, The ESO/Uppsala Survey of the ESO(B) Atlas. European Southern Observatory, Munich
Marchant A. B., Shapiro S. L., 1977, ApJ, 215, 1
Mo H. J., Mao S., White S. D. M., 1998, MNRAS, 295, 319
Naab T., Ostriker J. P., 2006, MNRAS, 366, 899
Padmanabhan N. et al., 2004, New. Astron., 9, 329
Park C., Choi Y., 2005, ApJ, 635, L29 (PC05)
Pinkney J. et al., 2003, ApJ, 596, 903
Sarzi M. et al., 2006, MNRAS, 366, 1151
Shaw L. D., Weller J., Ostriker J. P., Bode P., 2006, ApJ, 646, 815

170 *X. Hernandez et al.*

Silk J., 2001, MNRAS, 324, 313

Syer D., Mao S., Mo H. J., 1999, MNRAS, 305, 357

Treu T., Koopmans L. V. E., Bolton A. S., Burles S., Moustakas L. A., 2006, ApJ, 640, 662

van der Kruit P. C., 1987, A&A, 173, 59

White S. D. M., Rees M. J., 1978, MNRAS, 183, 341

Wilkinson M. I., Evans N. W., 1999, MNRAS, 310, 645

Yoachim P., Dalcanton J. J., 2006, AJ, 131, 226

Zhang B., Wyse R. F G., 2000, MNRAS, 313, 310

This paper has been typeset from a TEX/LATEX file prepared by the author.

Capítulo 5

Dependencias de λ con la masa y el medio ambiente galácticos.

En el capítulo anterior estudiamos la distribución total de λ y obtuvimos que nuestros resultados, derivados de una muestra de galaxias observadas del SDSS, concuerdan con resultados teóricos previos. En este capítulo nos enfocaremos a estudiar estas distribuciones, pero en función de la masa total de las galaxias y de la densidad del medio ambiente en que se encuentran. En este caso, empleamos la misma muestra de galaxias además de una muestra de halos provenientes de una simulación cosmológica de n-cuerpos, con el fin de comparar los resultados de uno y otro, aplicando los mismos criterios.

La obtención de λ para la muestra observacional se llevó a cabo de la misma manera que en el capítulo precedente, mientras que para la muestra de halos simulados, se calculó a partir de la definición general, una vez identificados los halos y subhalos empleando un algoritmo basado en el método friend-of-friend (FOF).

Para caracterizar la densidad del medio ambiente, en vez de discriminar entre cúmulos, filamentos o vacíos, empleamos una medida continua que aplicamos tanto a la muestra observacional como a la muestra de halos simulados y que consiste en una medida de la densidad numérica local de galaxias a una escala dada. De esta manera, los resultados obtenidos analizando la muestra de halos simulados es directamente comparable con los resultados provenientes de la muestra de galaxias del SDSS.

Analizamos si existía alguna dependencia entre el valor promedio de λ y el valor de la densidad local del medio, tomando en cuenta desde galaxias de campo hasta grupos relajados, sin estudiar específicamente cúmulos densos. Encontramos que tanto para los halos simulados como para las galaxias observadas, el valor de λ no depende del valor de la densidad del medio ambiente, en concordancia con resultados teóricos previos.

En cambio, analizando la dependencia de λ con la masa total de la galaxia, encontramos que ésta era fuerte en el caso de la muestra de galaxias observadas, para las que sistemas muy masivos tienden a presentar valores bajos de λ, mientras que las galaxias poco masivas, en promedio, presentan λ grandes pero también una gran dispersión. En el caso de la muestra de halos simulados, no se encuentra este comportamiento, que muestra una dependencia nula entre la masa y el espín,

resultado que frecuentemente se reporta en los estudios más recientes de simulaciones cosmológicas, siendo un punto discrepante entre las predicciones teóricas y lo que se obtiene de las observaciones.

Trabajo publicado en:

- Cervantes-Sodi B., Hernández X., Park C., Kim J., 2008, MNRAS, 388, 863

Environment and mass dependencies of galactic λ spin parameter: cosmological simulations and observed galaxies compared

B. Cervantes-Sodi,[1]★ X. Hernandez,[1]★ Changbom Park[2] and Juhan Kim[2]

[1]*Instituto de Astronomía, Universidad Nacional Autónoma de México A. P. 70-264, México 04510 D.F., Mexico*
[2]*Korea Institute for Advanced Study, Dongdaemun-gu, Seoul 130-722, Korea*

ABSTRACT

We use a sample of galaxies from the Sloan Digital Sky Survey (SDSS) to search for correlations between the λ spin parameter and the environment and mass of galaxies. In order to calculate the total value of λ for each observed galaxy, we employed a simple model of the dynamical structure of the galaxies, which allows a rough estimate of the value of λ using only readily obtainable observables from the luminous galaxies. Use of a large volume-limited sample (upwards of 11 000) allows reliable inferences of mean values and dispersions of λ distributions. We find, in agreement with some *N*-body cosmological simulations, no significant dependence of λ on the environmental density of the galaxies. For the case of mass, our results show a marked correlation with λ, in the sense that low-mass galaxies present both higher mean values of λ and associated dispersions, than high-mass galaxies. These results provide interesting constrain on the mechanisms of galaxy formation and acquisition of angular momentum, a valuable test for cosmological models.

Key words: galaxies: formation – galaxies: fundamental parameters – galaxies: statistics – galaxies: structure – cosmology: observations.

1 INTRODUCTION

One of the most studied parameters in numerical simulations of formation and evolution of galaxies is the λ spin parameter, first introduced by Peebles in 1969, where it was used to test the gravitational instability picture as a theory for the origin of galaxies. Since then, there have been several studies using the λ parameter as an indispensable tool of analysis, or characterizing its distribution in cosmological *N*-body simulations. As the first numerical simulations were done, some estimates of mean values of λ were obtained (Peebles 1971; Efstathiou & Jones 1979; Blumenthal et al. 1984; Barnes & Efstathiou 1987), as well as probability distributions. In general, the distributions of this parameter are well fitted by a lognormal function, characterized by two parameters; λ_0, the most probable value, and σ_λ, which accounts for the spread of the distribution. In a recent work, Shaw et al. (2006) showed a compilation of results for estimates of these parameters, arising from numerical studies performed by several authors, lying in the ranges: $0.03 < \lambda_0 < 0.05$ and $0.48 < \sigma_\lambda < 0.66$. Besides numerical simulations, there have been several analytical attempts (Peebles 1969; Doroshkevich 1970; White 1984; Heavens & Peacock 1988) at predicting λ_0 and σ_λ with similar results. More recently, Syer, Mao

& Mo (1999) confirmed the form of the distribution for λ using observational data of 2500 objects, and some of us in a previous work (Hernandez et al. 2007), using the same sample of 11 597 galaxies from the Sloan Digital Sky Survey (SDSS) we treat here, obtained the distribution of this parameter, with results well fitted by a lognormal function with parameters $\lambda_0 = 0.04 \pm 0.005$ and $\sigma_\lambda = 0.51 \pm 0.05$, for the first time derived from a statistical sample of real galaxies. Using the same model, Puech et al. (2007) obtained a similar result using a sample of intermediate-redshift galaxies.

The origin of galactic angular momentum is commonly explained as a result of tidal torques of neighbouring protogalaxies on the forming galactic halo. As the protogalaxy breaks away from the general expansion of the Universe, and since in the general case, it is unlikely to be spherically symmetric, the forming galaxy is torqued up through coupling with the ambient tidal field. This picture appeared with Hoyle in 1949 and was developed at first order analytically where the growth of the angular momentum is proportional to time, and later explored using numerical *N*-body simulations where the complicated processes of gravitational interactions can be tracked (e.g. Sugerman, Summers & Kamionkowski 2000). Other explanations for the origin of the angular momentum have been proposed, like the model of Vitvitska et al. (2002), in which the haloes obtain their spin through the cumulative acquisition of angular momentum from satellite accretion, obtaining distributions well modelled by lognormal functions with parameters similar to the ones obtained with the tidal torque theory. Variations to the general

★E-mail: bcervant@astroscu.unam.mx (BC-S); xavier@astroscu.unam.mx (XH)

864   *B. Cervantes-Sodi et al.*

theory have been tested by e.g. Maller, Dekel & Somerville (2002), proposing mainly two scenarios; in the first, the halo spin is generated by the transfer of orbital angular momentum from satellites that merge with the main halo, and a second one where linear tidal-torque theory is applied to shells of infalling matter. The evolution for λ at different redshift is completely different for both scenarios, as well as the dependence with mass, where a trend in the tidal-torque scenario is clear, in the sense that more massive galaxies tend to present low λ values and low dispersions. The study by Barnes & Efstathiou (1987) revealed a weak trend towards decreasing λ_0 with increasing mass, confirmed in some *N*-body simulations (Cole & Lacey 1996; Bett et al. 2007) and not found in others (Maccio et al. 2007).

A direct measure of the real distribution of galactic λ distributions, as a function of environment density and mass, would therefore constrain and inform theories of angular momentum acquisition and galaxy formation. It is precisely this that we attempt, using a first-order estimate of galactic halo λ, to derive distributions of this parameter as functions of mass and environment density from a large SDSS sample, and compare against results from large cosmological *N*-body simulations.

The existence of a correlation between galaxy morphology and local density environment (Dressler 1980; Goto et al. 2003; Park et al. 2007) is a motivation to search for other correlations between local environment and internal properties of galaxies. Lemson & Kauffmann (1999), using an *N*-body simulation, found that the only quantity which varies as a function of environment was the mass distribution, and Maccio et al. (2007) confirmed an absence of correlation between λ and environment in cosmological simulations, although the opposite is sometimes claimed by other studies using similar techniques (e.g. Avila-Reese et al. 2005). Even the spin alignment of dark matter haloes in different environments, has been studied in some *N*-body simulations (Aragón-Calvo et al. 2007). In this work, we present a study using a sample of galaxies from the SDSS, in an attempt to give an observational counterpart to such studies performed using *N*-body simulations.

The paper is organized as follows. In Section 2, we present a review of the derivation of the λ parameter for inferred haloes of any galaxy, spiral or elliptical, developed in Hernandez & Cervantes-Sodi (2006) (hereafter Paper I) and Hernandez et al. (2007), hereafter Paper II. In Section 3 we introduce the sample used to perform the study, and there we present our general results, including a comparison against a recent high-resolution cosmological *N*-body simulation. Finally, in Section 4 we present a discussion of the results and the final conclusions.

2 ESTIMATION OF λ FROM OBSERVABLE PARAMETERS

The currently accepted picture for galaxy formation is the Lambda cold dark matter (ΛCDM) model where dark matter overdensities in the expanding Universe at high redshift, accrete baryonic material through their gravitational potential, and via gravitational evolution grow to become galaxies. Their principal integral characteristics, according to theoretical studies, are their mass and angular momentum. In this section we briefly summarize the hypothesis behind the estimates derived in Papers I and II, used to estimate λ for the haloes of observed galaxies, from observable parameters. A comparison of our estimate with results coming from numerical simulations is also included. The following are intended only as first-order estimates. The errors for individual galaxies are of the order of 30 per cent

(see below), it is only through the use of extensive samples that meaningful inferences on the distribution of λ can be derived.

2.1 Estimates of halo λ parameters from observed galactic properties

The angular momentum is commonly characterized by the dimensionless angular momentum parameter

$$\lambda = \frac{L \, |E|^{1/2}}{G \, M^{5/2}}, \tag{1}$$

where *E*, *M* and *L* are the total energy, mass and angular momentum of the configuration, respectively. In Paper I we derived a simple estimate of λ for disc galaxies in terms of observational parameters, and showed some clear correlations between this parameter and structural parameters, as the disc to bulge ratio, the scale height and the colour, after estimating λ for a sample of real galaxies. Here we recall briefly the main ingredients of the simple model. The model consider only two components, a disc for the baryonic component with an exponential surface mass density $\Sigma(r)$:

$$\Sigma(r) = \Sigma_0 e^{-r/R_d}, \tag{2}$$

where *r* is a radial coordinate and Σ_0 and R_d are two constants which are allowed to vary from galaxy to galaxy, and a dark matter halo having an isothermal density profile $\rho(r)$, responsible for establishing a rigorously flat rotation curve V_d throughout the entire galaxy:

$$\rho(r) = \frac{1}{4\pi G} \left(\frac{V_d}{r} \right)^2. \tag{3}$$

We assume that (1) the specific angular momentum of the disc and halo are equal, e.g. Fall & Efstathiou (1980), Mo, Mao & White (1998); (2) the total energy is dominated by that of the halo which is a virialized gravitational structure; (3) the disc mass is a constant fraction of the halo mass $F = M_d/M_H$. These assumptions allow us to express λ as

$$\lambda = \frac{2^{1/2} V_d^2 R_d}{G M_H}. \tag{4}$$

Finally, we introduce a disc Tully–Fisher (TF) relation: $M_d = A_{TF} V_d^{3.5}$, and taking the Milky Way as a representative example, we evaluate F and A_{TF} to obtain

$$\lambda = 21.8 \frac{R_d/\text{kpc}}{(V_d/\text{km s}^{-1})^{3/2}}. \tag{5}$$

In Paper II, we presented a derivation for an equivalent expression to equation (5) for elliptical galaxies, again using a model of two components: a baryonic matter distribution with a Hernquist density profile and a dark matter halo, in principle, showing no difference from that of disc galaxies (White & Rees 1978; Kashlinsky 1982). Following this hypothesis, the energy can be obtained from the density profile described by equation (3) assuming again a virialized structure, which allow us to calculate the mass at the half-light radius, R_{50}:

$$M_{dyn} = \frac{(1.65\sigma)^2 R_{50}}{G} \tag{6}$$

from Padmanabhan et al. (2004), where σ is the velocity dispersion. For the angular momentum, again we suppose that the specific angular momentum of dark matter and baryons are equal, and using dimensional analysis we expect that it will be proportional to the eccentricity of the system, *e*; and the factor $(GM_b a)^{1/2}$, where M_b is

the baryonic mass and *a* is the mayor axis. Introducing a numerical factor to account for the dissipation of the baryonic component, its dynamical pressure support and the projection effects, we finally obtain

$$\lambda = \frac{0.1173 e (a/\text{kpc})^{2/7}}{(\sigma/\text{km s}^{-1})^{3/7}}. \qquad (7)$$

With equations (5) and (7), we can obtain an estimate of λ for the halo of any galaxy using just the most basic information available.

2.2 Testing the model against detailed galactic simulations

To check our estimate of λ we made use of numerical simulations where this parameter acts as an input parameter, or its value can be estimated with high accuracy.

The model by Hernandez, Avila-Reese & Firmani (2001) includes a very wide range of physics, initial conditions are supplied by an statistical sampling of a cosmological primordial fluctuation spectrum, giving a mass aggregation history of gas and dark matter. No TF type of relation is assumed a priori, indeed, this codes attempt to recover such a relation as a final result of the physics included. A fixed value of λ is assumed for the infalling material which settles into a disc in centrifugal equilibrium and differential rotation, viscous friction results in radial flows of matter and angular momentum. The redistribution of mass affects the rotation curve in a self-consistent way, through a Poisson equation including the disc self gravity and a dark halo which responds to mass redistributions through an adiabatic contraction. The star formation is followed in detail, with an energy balance cycle.

A simple population synthesis code then traces the luminosities and colours of various stellar populations at all radii and times. The van den Bosch & Dalcanton (2000) models are qualitatively similar to the previous ones, but vary in numerical approaches, resolution, time-step issues and the level of approximation and inclusion of many different physical aspects of the complicated problem.

Kaufmann et al. (2007) explore the angular momentum transport, disc morphology and how radial profiles depend sensitively on force and mass resolution. They study systematically this effect with controlled *N*-body/smoothed hydrodynamics simulations of disc galaxy formation by cooling a rotating gaseous mass distribution inside equilibrium cuspy spherical and triaxial dark matter haloes employing up to 10^6 gas and dark matter particles. Their models are calibrated using the Milky Way and M33 models for the comparisons. Varied and detailed physical effects are introduced self-consistently in their simulations, from the end results of which we use resulting galactic properties to estimate halo λ using equation (5), and compare to their input values.

Avila-Reese et al. (2005) employed a Λ CDM *N*-body simulation to study the properties of galaxy-size dark matter haloes as a function of global environment, where λ was one of the studied properties of the halo, in particular its value in different environments such as clusters, voids or field. We then used reported values of the final resulting galactic properties, disc scale lengths and rotation curves to estimate the λ parameters through equation (5), and compare against the input values used in the simulations.

With the aim of studying the origin of the TF relation, Koda, Sofue & Wada (2000), used a *N*-body/smoothed particle hydrodynamic method, including cooling, star formation and stellar feedback of energy, mass and metals, to trace the evolution of the galaxies from $z = 25$ to 0 in a CDM cosmology. The resulting spiral galaxies, with exponential disc profiles and generically flat rotation curves, including disc self-gravity and which reproduce the slope and scatter
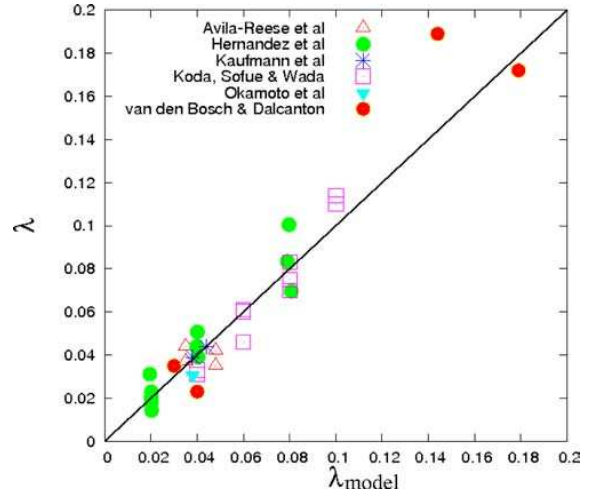

Figure 1. Comparison between the calculated λ value using equation (5) and the actual value, using simulated galaxies from different groups.

of the TF relation, all these as results of the evolved physics, not input suppositions, were reported.

The work of Okamoto et al. (2005), was performed using hydrodynamic simulations of galaxy formation in a Λ CDM universe with different models of star formation and feedback, to see their effect on the morphology of disc galaxies. Also giving as output present day galactic properties from which we estimated halo λ through equation (5), and compared against their input model value.

The comparison between the input λ values of the galaxies modelled by the different groups (λ_model), and our estimate using equation (5) is presented in Fig. 1, where the *x*-axis value correspond to the exact value coming from the detailed study of the system, and the *y*-axis value is our estimate using 'observable' parameters through equation (5). We can appreciate a very good agreement between the calculated value with our simple model, and the actual value of λ for simulated galaxies, regardless of the complexity of the models used. While all the above models include fairly detailed physics, it is remarkable that our simple dimensional estimate agrees so well, always better than 30 per cent, in most cases much better. As no systematics are apparent, we can now use equation (5) with a sample of real galaxies, to obtain statistical properties of the distributions of λ in the real universe.

3 COMPARISONS OF λ DISTRIBUTIONS FROM THE SDSS AND COSMOLOGICAL *N*-BODY SIMULATIONS

3.1 Observational sample

The sample of real galaxies employed for the study comes from the SDSS Data Release 5 (Adelman-McCarthy et al. 2007). It is a volume-limited sample having galaxies in the redshifts interval $0.025 < z < 0.055$ and absolute magnitudes $M_r - 5\log h \leq -18.5$. Since most of the studies concerning spin distributions from simulations presents their results at $z = 0$, we limited the sample to low redshifts. This sample contains 32 550 galaxies for which Choi, Park & Vogeley (2007) have determined the exponential disc scales, absolute magnitudes, velocity dispersions, de Vacouleurs radii and seeing corrected isophotal ellipticities for each galaxy, assuming a

866 *B. Cervantes-Sodi et al.*

ΛCDM universe with $\Omega_M = 0.27$, $\Omega_\Lambda = 0.73$ and $h = 0.71$. To obtain λ for each galaxy, we need to discriminate between elliptical and disc galaxies; in order to do that we used the prescription of Park & Choi (2005), in which early (ellipticals and lenticulars) and late (spirals and irregulars) types are segregated in a $u - r$ colour versus $g - i$ colour gradient space and in the concentration index space. In order to apply equation (5) to the disc galaxies of the sample, we need the rotation velocity, which is inferred from the absolute magnitude using a TF relation (Barton et al. 2001), then, to avoid the problem of internal absorption in edge-on galaxies, we employed only spiral galaxies having axis ratios >0.6 and inferred rotation velocities in the range of $80 < V_R < 430$, well within the range of applicability of the TF relation we are using. After applying these two cuts, and removing a randomly selected fraction of ellipticals, so as to maintain the original early- to late-type fraction, we are left with a total of 11 597 galaxies.

The measurement of R_d for our SDSS galaxies comes from the total distribution of light, without any decomposition of the light coming from the bulge or the disc, in this way, systems with prominent bulges, where an important fraction of mass is present in the bulge with low angular momentum, present short R_d values, which imply a low λ value assigned trough equation (5), accounting implicitly for the low angular momentum of the bulge fraction. We note that of the simulated galaxies in Fig. 1, Avila-Reese et al. (2005) and Koda et al. (2000) include prominent bulge components. It is reassuring of the implicit bulge accounting described above that no systematics are apparent in Fig. 1, regarding either the early-type simulated galaxies, or any other ones. For the elliptical galaxies we apply equation (7), as fully described in Paper II, using the corrected isophotal ellipticities to calculate the eccentricity.

3.2 Simulation and subhalo finding

To compare our observational sample with a numerical simulation, we have made a cosmological *N*-body simulation of a ΛCDM model in a cubic box with a side length of $614\ h^{-1}$ Mpc. The model parameters are $h = 0.7$, $\Omega_m = 0.27$, $\Omega_b = 0.046$ and $\Omega_\Lambda = 0.73$, given by the *Wilkinson Microwave Anisotropy Probe* 1-yr data (Spergel et al. 2003). The simulation gravitationally evolved 1024^3 CDM particles from redshift $z = 48$ to 0 taking 1880 global time-steps. The linear density fluctuations of matter at the present epoch is normalized by $\sigma_8 = 0.9$, the RMS density fluctuation at the $8\ h^{-1}$ Mpc top-hat smoothing scale. The mass of each simulation particle is $M_p = 1.4 \times 10^{10}\ h^{-1}\ M_\odot$ and the force resolution is about $60\ h^{-1}$ kpc.

To identify subhaloes in the simulation, we first extracted the dark matter particles located in virialized regions by applying the standard friend-of-friend (FOF) method with a linking length equal to one-fifth of the mean particle separation. This length is a characteristic scale for the identification of virialized structures. To each FOF particle group, we applied the PSB method (Kim & Park 2006; Kim, Park & Choi 2008) to find subhaloes. The method identifies subhaloes that are gravitationally self-bound in terms of the total energy and stable against the external tidal force. The resulting subhalo population is complete down to $M_h = 4.3 \times 10^{11}\ h^{-1}\ M_\odot$. This has been found from a comparison of the subhalo mass function with that of the base mass functions of subhaloes obtained from other higher resolution simulations (Kim & Park, in preparation). The minimum halo mass amounts to a collective mass of 30 particles and corresponds to an early-type galaxy with $M_r = -19$ in the subhalo–galaxy correspondence model, which assumes that each subhalo contains one and only one optical galaxy (Kim et al. 2008).

Henceforth, the term halo, when applied to our simulations, will refer to subhalo, as defined above.

For comparisons with our observational results we randomly selected 100 000 haloes from the simulation, for which the spin parameter λ was calculated numerically. The normalized local density parameter is obtained following the same method as used for our SDSS sample (see Section 3.4 for more details, see also Park et al. 2007; Kim et al. 2008).

3.3 Integral properties of the λ distributions

In Fig. 2, we present the distribution of the spin parameter for the SDSS and the simulated samples; the broken curves show histograms after dividing the data into 150 bins, and the dotted curves
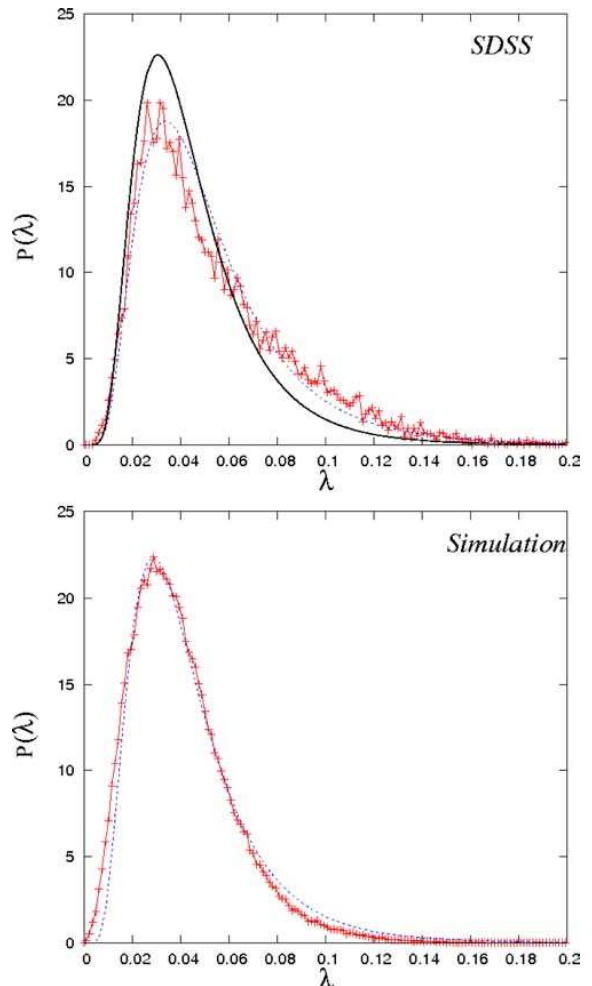

Figure 2. Distribution of λ values, broken curve corresponding to the data binned into 150 intervals and dotted curve best lognormal fit to the data. Top: Data from the SDSS sample using 11 597 galaxies, with parameters $\lambda_0 = 0.046$ and $\sigma_\lambda = 0.535$, solid curve being the maximum likelihood underlying distribution, assuming a 30 error in our inferred λ values, with parameters $\lambda_0 = 0.0394$ and $\sigma_\lambda = 0.509$. Bottom: Data from the *N*-body simulation using 100 000 simulated dark matter haloes, with parameters $\lambda_0 = 0.038$ and $\sigma_\lambda = 0.525$.

give the best direct fit to a lognormal distribution of the form

$$P(\lambda_0, \sigma_\lambda; \lambda)\,d\lambda = \frac{1}{\sigma_\lambda \sqrt{2\pi}}\exp\left[-\frac{\ln^2(\lambda/\lambda_0)}{2\sigma_\lambda^2}\right]\frac{d\lambda}{\lambda}. \tag{8}$$

We can appreciate that the distributions are well fitted by this function, where the corresponding values from the SDSS and the simulation are: $\lambda_0 = 0.046$, $\sigma_\lambda = 0.535$ and $\lambda_0 = 0.038$, $\sigma_\lambda = 0.525$, both results in agreement with previous predictions from *N*-body simulations (from a recent compilation for λ_0 and σ_λ values, see Shaw et al. 2006).

The empirical scaling relations used for our estimation of λ show a measure of dispersion. In the case that these dispersions were intrinsic to the data, they would propagate as errors in our λ estimates. In order to estimate what is the best underlying distribution, assuming that the distribution of the data is a degraded version of the intrinsic lognormal distribution, in Paper II we employed a full maximum likelihood analysis, which gave us a best fit with parameters $\lambda_0 = 0.0394$ and $\sigma_\lambda = 0.509$, showed in Fig. 2, top panel, as a solid line. The maximum likelihood fit and the direct fit over the data from the sample are extreme cases, one assuming that the dispersions in the empirical scalings used are fully intrinsic to the data, and the other that they are strictly measurement errors, the actual λ distribution should lie between these two cases, in very good agreement with the distribution from the simulation, we can hence see that the integral distribution of galactic halo λ spin parameters in real galaxies is consistent with what current structure formation theories predict.

That both the λ distributions inferred from the SDSS sample, and those coming from all published cosmological simulations are well fitted by lognormal distributions, is interesting. We note that lognormal distributions often arise as a consequence of the central limit theorem. Whenever the particular outcome of a variable is the sum of a large number of independent distributions, we are guaranteed that the final distribution will be a Gaussian. If the particular outcome of a variable is the product of a large number of independent distributions, it follows that the logarithm of the variable will be normally distributed. What the many independent distributions might in this case be, we can only speculate, the repeated merger events leading to the formation of a galaxy, or perhaps the tidal fields due to surrounding density fields as they sequentially detach from the overall expansion of the universe and virialize.

3.4 Correlations between λ and environment density

To study if there is any correlation between spin and the environment, we use an estimation of the local background density defined directly from the observations that is continuous and able to characterize the full range of galaxy environments. It measures the local number density of galaxies at a given smoothing scale.

Being a continuous measure, it does not make any difference on field, voids, filaments or clusters but their estimation can be done based on the present density measure. The measurement of the environmental density was done by Park et al. (2007), where they adopt a Spline kernel with adaptive smoothing scale to include a fixed number of galaxies within the centrally weighted kernel. The details of the method using the spline kernel are summarized in Park et al. (2007). The local density at a given location for each galaxy is measured by

$$\rho(\boldsymbol{x})/\langle\rho\rangle = \sum_{i=1}^{20} W_i(|\boldsymbol{x}_i - \boldsymbol{x}|)/\langle\rho\rangle, \tag{9}$$

using the spline kernel weight $W(r)$ for the background density estimation as in Park, Gott & Choi (2008). The mean mass density of the sample is obtained by

$$\langle\rho\rangle = \sum_{\text{all}} 1/V, \tag{10}$$

where the summation is over all galaxies in the sample contained in the total volume *V*.

With this measure for the local density of the environment, we are able to search for any correlation among environment and spin. In several studies, the samples of simulated galaxies are divided according to their location in field, voids, filaments or clusters, by cuts in the overdensity of the environment or simply by cuts of the normalized local density, and then mean values of λ for each subsample are obtained or λ_0 values from fits of lognormal functions to the distributions at each cut. We divided our sample into six cuts according to the normalized environmental density, and for each cut we obtained the mean λ value and its dispersion. The result is presented in the upper left-hand panel of Fig. 3, where the value of total inferred λ versus $\rho/\langle\rho\rangle$ for each galaxy is plotted and we show the mean λ value for each cut as a function of the normalized density, the solid error bars corresponds to the dispersion and the broken error bars to the standard error in the calculation of the mean value, this convention will be kept in the following figures. As can be seen, there is no clear trend, taking into account the dispersion in each bin.

As discussed in Paper II, our λ estimation for early-type galaxies is not as accurate as the estimation for disc galaxies due to the uncertainties in the way dissipation, pressure support and projection effects are taken into account to obtain equation (7); with this in mind, we also checked if being more rigorous in the estimation of λ, we could find any trend with the environment. Using only the 7753 disc galaxies, and dividing the sample again in six bins, we obtain the result presented in the upper right-hand panel of Fig. 3, again showing little trend if any, between λ and the normalized local density of the environment.

Using the full sample of haloes from our *N*-body simulation, divided into six bins and calculating the mean λ value and dispersion for each bin, we obtain the result shown in Fig. 3, bottom left-hand panel. The small change in the mean value and large dispersion are consistent with there being no correlation between the two properties, in agreement with what was obtained using the SDSS sample. To compare the results arising from the numerical simulation with our sample of disc galaxies, where we are more confident of the λ estimation, we can take as a first-order criterion for haloes harbouring 'late-type galaxies' only the haloes with $\lambda > \lambda_0$, where λ_0 comes from the fit of the whole sample to a lognormal function, in this case, $\lambda_0 = 0.0354$. The behaviour of the spin for the high spin haloes of the *N*-body simulation, as a function of density, is shown in Fig. 3 bottom right-hand panel, with the same qualitative result as obtained using the whole sample.

Recent works studying the variation of λ in different environments, sometimes find a weak dependence for high-mass galaxies, in the sense that higher spin galaxies are more strongly clustered than lower spin galaxies (Bett et al. 2007; Hahn et al. 2007). We inspect if keeping only the high-mass galaxies, we can find such a significant correlation. For both samples, the SDSS and the simulation, we took into account disc galaxies with total halo masses $M > 1 \times 10^{13}\,M_\odot$, and simulates haloes in the same mass range. To obtain the mass of the SDSS galactic haloes we used a mass–luminosity relation which relates the baryonic mass of the galaxy with its absolute magnitude (e.g. Kassin, de Jong & Weiner 2006),
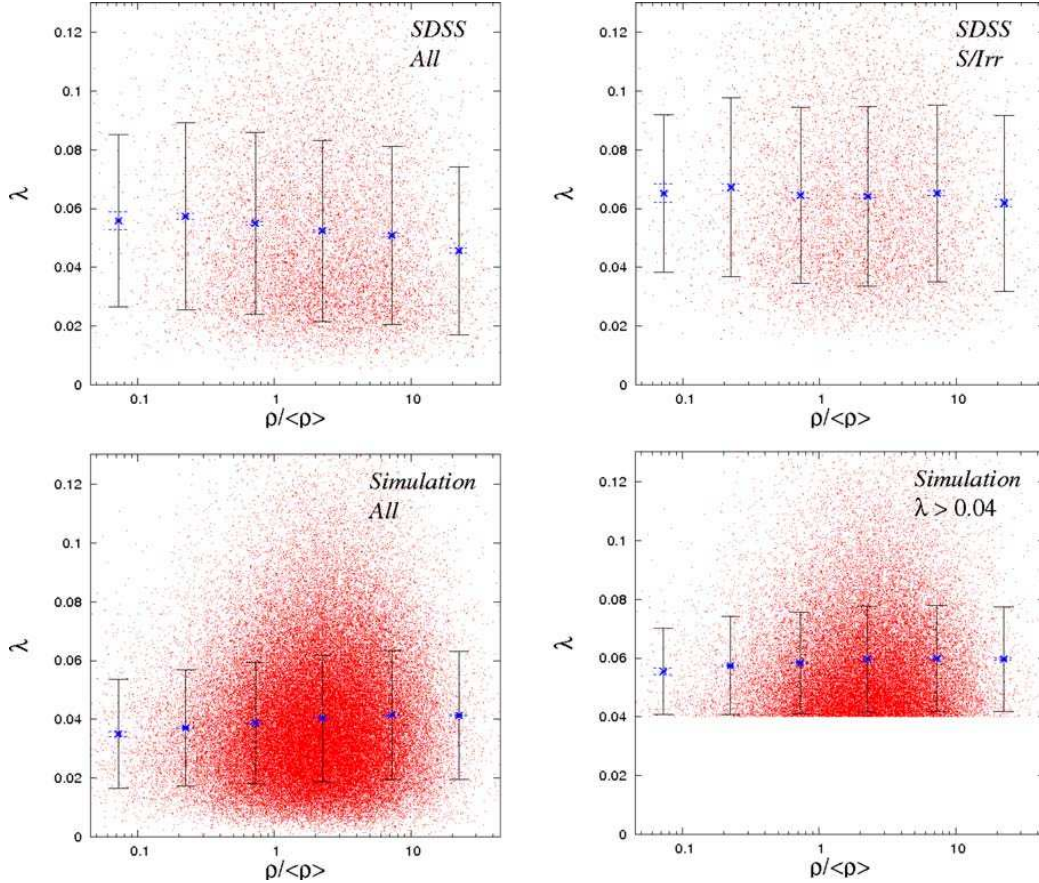
Figure 3. Relations between spin and environmental density, showing the mean λ value for each bin as a function of the normalized density, the solid error bars corresponds to the dispersion and the broken error bars to the standard error in the calculation of the mean value. Top panels correspond to the SDSS sample: on the left-hand side the entire sample using the 11 597 galaxies and on the right-hand side using only the 7754 disc galaxies. Bottom panels correspond to the simulated dark matter haloes: on the left-hand side the whole 100 000 sample, on the right-hand side 52 950 haloes with λ > 0.04

and we hold the same baryonic to dark matter fraction introduced in Section 2. The behaviour found is presented in Fig. 4, top panel corresponding to the SDSS sample and bottom panel corresponding to the *N*-body simulation, where we can see that the trend, almost imperceptible in Fig. 3 is now a little more clear but still not significant, taking into account the large dispersion in each bin. In the case of the SDSS sample, we find the same behaviour as in Fig. 3.

To summarize the results of this subsection, we can conclude that we could not find any clear correlation between the λ spin parameter and the environment where the galaxies are located, as pointed out by several theoretical studies for dark matter haloes in simulations (Lemson & Kauffmann 1999; Bett et al. 2007; Maccio et al. 2007). Neither at low nor at high masses, not for real galaxies or simulated haloes, do we find any significant trend in the parameters describing the distribution of λ with environment density. Up to this point, current cosmological modelling appears fully consistent with real galaxies.

3.5 Correlations between λ and halo mass

After having found no correlation between λ and the local environment, we now search for a correlation with internal properties of the galaxies. In many analytic and numerical studies, λ has been

established as an important, if not the most important, parameter determining the galactic type (Fall & Efstathiou 1980; Flores et al. 1993; Firmani, Hernandez & Gallagher 1996; Silk 2001). In that sense, we expect it to correlate with the most important structural parameters such as thickness of the disc, bulge-to-disc ratio, colours, metallicity among others. van den Bosch (1998) emphasizes the important role of this parameter in explaining the origin of the Hubble sequence, and shows correlations of λ with the bulge-to-disc ratio, in the sense that systems with high λ presents systematically lower bulge-to-disc ratios. Kregel et al. (2005) explain the role of λ in the stellar velocity dispersion and predict extended thin disc in galaxies immersed in high spin angular momentum dark matter haloes. Trends with star formation efficiencies, gas fractions, metallicities, abundance gradients and colours have also been predicted in several studies (e.g. Dalcanton et al. 1997; Boissier et al. 2001; Churches, Nelson & Edmunds 2001). In Paper I and in Cervantes-Sodi & Hernandez (2008), we showed this type of scaling but using samples of real galaxies, confirming the general results of theoretical studies.

But still, more important than all these properties is the mass of the galaxy. The results arising from early works are rich and varied, some of them pointing in the sense that no correlation is found between λ and mass (e.g. Warren et al. 1992; Lemson &
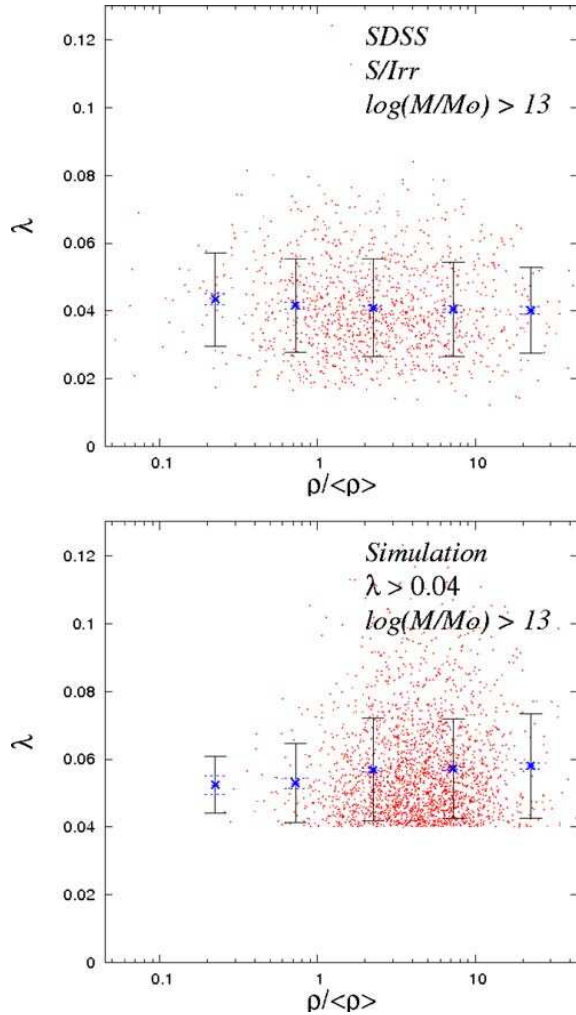
Figure 4. Relation between spin and the environmental density for massive disc galaxies. Top: 1238 disc galaxies form SDSS sample. Bottom: 3536 haloes with high λ from the *N*-body simulation, with halo masses in the same range as the SDSS galaxies shown above.

using the corresponding equation, and using the TF relation presented in the preceding subsection, we obtained the upper left-hand panel of Fig. 5, plotting λ as a function of *mass*. In this case, the trend is very clear, low-mass galaxies present typically higher λ values and larger dispersion, exactly what the association of λ and Hubble type mentioned previously would have suggested. We note that precisely such a trend is reported in the theoretical study of Maller et al. (2002) for the case of a tidal-torque scenario for the acquisition of angular momentum, as opposed to the scenario where angular momentum grows through the merger of satellites. We take our results as evidence of a mechanism of acquisition of angular momentum for galaxies, where it is the ambient tidal field what torques up a halo, with little participation of repeated mergers.

The lower left-hand panel in Fig. 5 shows halo λ as a function of *mass* for the simulation, although a certain trend is present in the same sense as in the SDSS sample, its magnitude is small and the dispersion large.

Our estimates of λ are more precise for disc galaxies, in both parameters, the spin and the mass. Taking only these galaxies, the corresponding figures for the SDSS sample and the above average λ simulated haloes are presented in Fig. 5, right-hand panels. In the case of the SDSS sample, the trend found using the whole sample, disc galaxies plus ellipticals, appears even stronger. The response in the case of the simulation is similar, the trend is kept but the dispersion decreases for larger galaxies, as in the SDSS sample but at a much lower level.

4 DISCUSSION

We have presented our results in the study of a large sample of galaxies taken from the SDSS and compared to the situation found in recent cosmological *N*-body simulations. We looked for correlations of the total galactic λ spin parameter distribution with both halo mass and local environmental density. With the local environment density we find no correlation, as reported in several theoretical studies and reproduced here using a cosmological *N*-body simulation. The large dispersion and little trend seen when dividing the samples into bins with different normalized environment density, are consistent with no correlation at all for a λ–⟨ρ⟩ relation, for both; inferred haloes of observed galaxies and modelled haloes.

The case of the λ–mass relation is quite different. Analysing our SDSS sample, we notice that the mean value of λ tends to decrease as the mass increases. But not only the mean value, also the dispersion of λ tends to decrease as the value of the mass increases. The effect is stronger using only the disc galaxies, where our estimate is more precise. Large galaxies are seen to form a more coherent low-λ sample with small dispersion, while small galaxies show mean values of λ of about a factor of 3 larger than what is found for our most massive galaxies. The dispersion about mean values shows the same trend, with small galaxies in our SDSS sample having a much larger dispersion than the large galaxies. Analysing the *N*-body simulation we found a very weak trend in the same sense using the high spin galaxies, which would correspond to disc galaxies.

Burkert (2003), found a correlation between the spin parameter and the baryon fraction of the form $\lambda \propto F^{2/3}$. In our simple model used to calculate λ from observable parameters, the dependence is even stronger; $\lambda \propto F$, this could be invoked to explain the relation found between mass and λ, strong star formation can drive galactic winds which clear a fraction of the baryonic material, preferentially in small systems. This would lead to a lower effective baryon
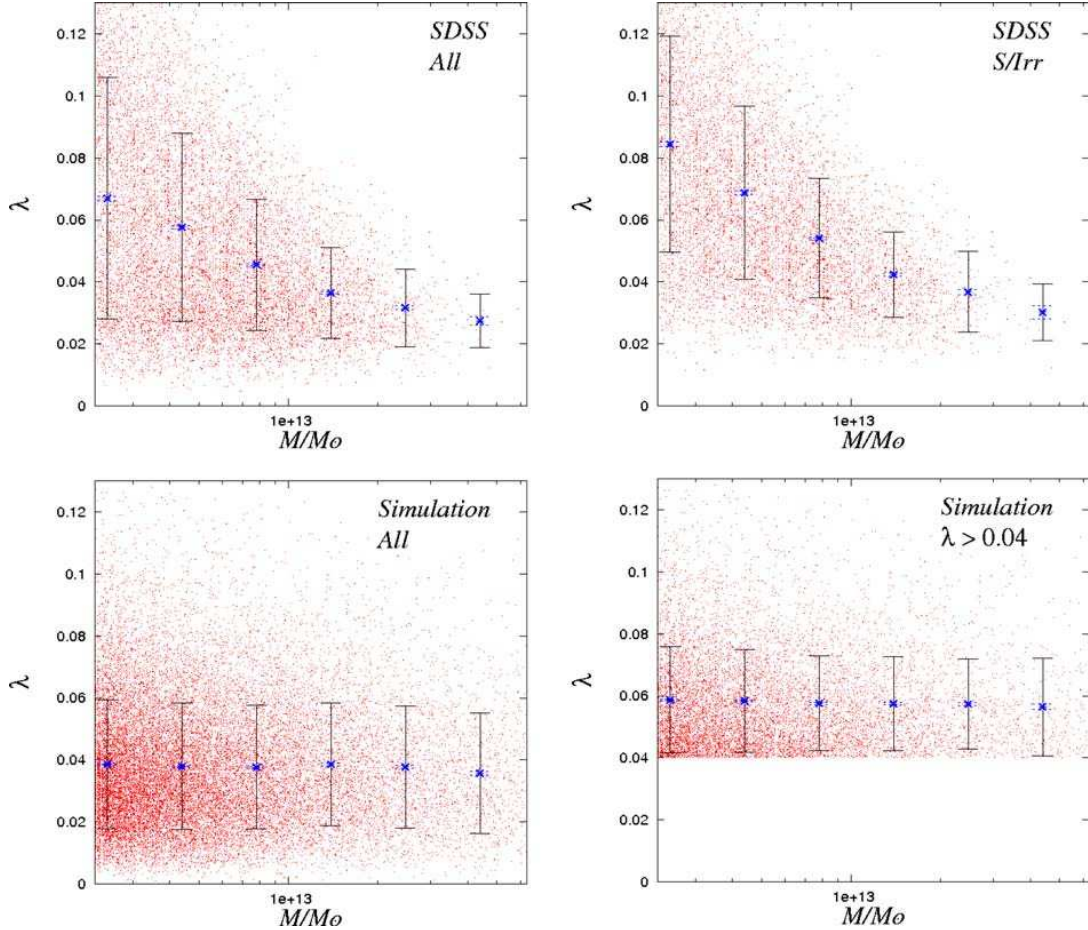
Kauffmann 1999; Shaw et al. 2006; Maccio et al. 2007) and others showing from weakly to marked trends between these two parameters, again, always for cosmological simulations (e.g. Cole & Lacey 1996; Jang-Codell & Hernquist 2001 – although the low resolution of this particular study might make this results questionable, Bett et al. 2007). We showed in Papers I and II a strong correlation between halo λ as estimated through equation (5), and visually assigned morphological type, in the expected sense, with later type galaxies corresponding to high values of inferred λ. Given the tight correlation that exists between Hubble type and mass, where high-mass systems tend to be of earlier types, it is natural to expect a trend to appear when cutting the sample of λ as a function of mass. We expect high-mass galaxies to be found preferentially amongst the low-λ haloes.

We investigate whether our SDSS sample presented this correlation or not. Once total λ values were obtained for all the galaxies

870   *B. Cervantes-Sodi et al.*

Figure 5. Relations between spin and mass. Top panels correspond to the SDSS sample: on the left-hand side the entire sample using the 11 597 galaxies and on the right-hand side using only the 7754 disc galaxies. Bottom panels correspond to the simulated dark matter haloes: on the left-hand side the whole 100 000 galaxies, on the right-hand side 52 950 galaxies with λ > 0.04.

fraction F in smaller systems, and hence, the assumption of a constant baryon fraction would lead us to overestimate λ in small systems. However, as has been shown recently by several authors studying the accretion and expulsion of baryons in cosmological scenarios (e.g. Crain et al. 2007; Brooks et al. 2007), the galactic baryon fraction is almost constant in the range of masses we are dealing with in this work. A fractional variation in F of over a factor of 3, over the 1.5 orders of magnitude in galactic mass we are dealing with here, is inconsistent with the physics of galaxy formation. We excluded galaxies of smaller masses, partly to guarantee completeness of the sample, and partly to stay well above the limit where galactic winds can be expected the change the baryon fraction differentially.

If the baryonic component is susceptible to angular momentum dissipation or baryonic to dark halo angular momentum transfer, and this effect is sharper in more massive systems, the trend observed with the mass could be due to a subestimation of the halo spin. Again, we can discard this hypothesis based on the study of Kaufmann et al. (2007), in which the loss of angular momentum of disc particles on a smoothed particle hydrodynamic simulation is traced. They found that almost half of the initial angular momen-

tum is lost via different mechanisms in low-resolution cosmological simulations, but when a high-resolution simulation is used only 10-20 per cent of the original angular momenta is lost, not enough to explain the strong correlation presented here between mass and λ. Further, no trend with mass is seen.

van den Bosch et al. (2002), using a numerical simulation of structure formation in a ΛCDM cosmology, concluded that the detailed angular momentum distributions of the gas and dark matter components in individual haloes are remarkably similar, and the differences between them present no significant dependence on the halo virial mass, result that supports the model used to calculate λ. A similar conclusion was obtained by Zavala, Okamoto & Frenk (2008). Tracing the evolution of the specific angular momenta of the dark matter and baryonic components on a cosmologically forming disc galaxy, they show that the baryonic component tracks the specific angular momentum of the halo, and their actual values are very similar throughout the entire history of the galaxy. The lack of a strong trend with mass in the effect of baryonic angular momentum transfer or dissipation found in detailed hydrodynamical simulations, shows that the correlation we find in mean values of λ which decrease with increasing galactic halo mass, is real. In addition, the

relation between R_d, V_d and λ of equation (5) is practically the same as what is found in the results of the high-resolution simulation of Okamoto et al. (2005), as seen in Fig. 1.

To summarize, we find a good accordance between the integral distributions of λ inferred from the large SDSS sample we studied, and results from current cosmological simulations, both in terms of the functional form of the distributions, and the parameters describing these distributions. The same is the case when comparing the samples as a function of environment density, with no clear trend apparent. However, when looking at the samples as a function of mass, no clear trend is seen in the simulated haloes, but in the sample of real galaxies we find a strong tendency for both mean values and dispersions in λ to decrease with increasing galactic mass; Tonini et al. (2006) reached similar conclusions through a more indirect study of galactic populations, and in order to explain the inferred baryonic scaling relations for a sample of around 80 isolated disc galaxies, using models of galactic evolution, Avila-Reese et al. (in preparation) required an anticorrelation between the mass, and both, the spin and the baryon fraction. This provides constrains on the form of acquisition of the angular momenta in galactic systems and important clues to discriminate cosmological models, given the dependency of this relations on the cosmology assumed, e.g. Eke, Efstathiou & Wright (2000). Comparing with existing studies of galaxy formation, we see that the trend we find cannot be ascribed to astrophysical effects associated with baryonic loss or dissipation. It must rather be understood as evidence in favour of an angular momentum acquisition mechanism where ambient tidal fields torque up galactic haloes as a whole at high redshift, rather than the progressive spin up caused by a repeated and prolonged satellite accretion process. To first order, the trend for a lower mean value of λ at larger halo masses can be understood by thinking of a constant ambient tidal field, which then results in higher λ for smaller systems.

REFERENCES

Adelman-McCarthy J. K. et al., 2007, ApJS, 172, 634
Aragón-Calvo M. A., van de Weygaert R., Jones B. J. T., van der Hulst J. M., 2007, ApJ, 655, L5
Avila-Reese V., Colin P., Gottlöber S., Firmani C., Maulbetsch C., 2005, ApJ, 634, 51
Barnes J., Efstathiou G., 1987, ApJ, 319, 575
Barton E. J., Geller M. J., Bromley B. C., van Zee L., Kenyon S. J., 2001, ApJ, 121, 625
Bett P., Eke V., Frenk C. S., Jenkins A., Helly J., Navarro J., 2007, MNRAS, 376, 215
Blumenthal G. R., Faber S. M., Primack J. R., Rees M. J., 1984, Nat, 311, 517
Boissier S., Boselli A., Prantzos N., Gavazzi G., 2001, MNRAS, 321, 733
Brooks A. M., Governato F., Booth C. M., Willman B., Gardner J. P., Wadsley J., Stinson G., Quinn T., 2007, ApJ, 655, L17
Burkert A., 2003, A&SS, 284, 697
Cervantes-Sodi B., Hernandez X., 2008, New Astron., preprint (arXiv:0802.3689)
Choi Y., Park C., Vogeley M. S., 2007, ApJ, 658, 884
Churches D. K., Nelson A. H., Edmunds M. G., 2001, MNRAS, 327, 610
Cole S., Lacey C., 1996, MNRAS, 281, 716
Crain R. A., Eke V. R., Frenk C. S., Jenkiins A., McCarthy I. G., Navarro J. F., Pearce F. R., 2007, MNRAS, 377, 41
Dalcanton J. J., Spergel D. N., Summers F. J., 1997, ApJ, 482, 659
Doroshkevich A. G., 1970, Astrophysics, 6, 320
Dressler A., 1980, ApJ, 236, 351
Efstathiou G., Jones B. J. T., 1979, MNRAS, 186, 133
Eke V., Efstathiou G., Wright L., 2000, MNRAS, 315, L18
Fall S. M., Efstathiou G., 1980, MNRAS, 193, 189
Firmani C., Hernandez X., Gallagher J., 1996, A&A, 308, 403
Flores R., Primack J. R., Blumenthal G. R., Faber S. M., 1993, ApJ, 412, 433
Giovanelli R., Haynes M. P., da Costa L. N., Freudling W., Salzer J. J., Weger G., 1997, ApJ, 477, L1
Goto T., Yamauchi C., Fujita Y., Okamura S., Sekiguchi M., Smail I., Bernardi M., Gomez P. L., 2003, MNRAS, 346, 601
Hahn O., Porciani C., Carollo C. M., Dekel A., 2007, MNRAS, 375, 489
Heavens A., Peacock J., 1988, MNRAS, 232, 339
Hernandez X., Cervantes-Sodi B., 2006, MNRAS, 368, 351 (Paper I)
Hernandez X., Avila-Reese V., Firmani C., 2001, MNRAS, 327, 329
Hernandez X., Park C., Cervantes-Sodi B., Choi Y., 2007, MNRAS, 375, 163 (Paper II)
Hoyle F., 1949, MNRAS, 109, 365
Jang-Codell H., Hernquist L., 2001, ApJ, 548, 68
Kashlinsky A., 1982, MNRAS, 200, 585
Kassin S. S., de Jong R. S., Weiner B. J., 2006, ApJ, 643, 804
Kaufmann T., Mayer L., Wadsley J., Stadel J., Moore B., 2007, MNRAS, 375, 53
Kim J., Park C., 2006, ApJ, 639, 600
Kim J., Park C., Choi Y., 2008, ApJ, preprint (arXiv:0801.3169)
Koda J., Sofue Y., Wada K., 2000, ApJ, 532, 214
Kregel M., van der Kruit P. C., Freeman K. C., 2005, MNRAS, 358, 503
Lemson G., Kauffmann G., 1999, MNRAS, 302, 111
Maccio A. V., Dutton A. A., van den Bosch F. C., Morre B., Potter D., Stadel J., 2007, MNRAS, 378, 55
Maller A. H., Dekel A., Somerville R., 2002, MNRAS, 329, 423
Mo H. J., Mao S., White S. D. M., 1998, MNRAS, 295, 319

872   *B. Cervantes-Sodi et al.*

Okamoto T., Eke V. R., Frenk C. S., Jenkins A., 2005, MNRAS, 363, 1299
Padmanabhan N. et al., 2004, New Astron., 9, 329
Park C., Choi Y., 2005, ApJ, 635, L29
Park C., Choi Y., Vogeley M. S., Gott J. R., Blanton M. R., 2007, ApJ, 658, 898
Park C., Gott J. R., Choi Y.-Y., 2008, ApJ, 674, 784
Peebles P. J. E., 1969, ApJ, 155, 393
Peebles P. J. E., 1971, A&A, 11, 377
Puech M., Hammer F., Lehnert M. D., Flores H., 2007, A&A, 466, 83
Shaw L. D., Weller J., Ostriker J. P., Bode P., 2006, ApJ, 646, 815
Silk J., 2001, MNRAS, 324, 313
Spergel D. N. et al., 2003, ApJS, 148, 175
Sugerman B., Summers F. J., Kamionkowski M., 2000, MNRAS, 311, 762
Syer D., Mao S., Mo H. J., 1999, MNRAS, 305, 357

Tonini C., Lapi A., Shankar F., Salucci P., 2006, ApJ, 638, L13
Tully R. B., Fisher J. R., 1977, A&A, 64, 661
van den Bosch F. C., 1998, ApJ, 507, 601
van den Bosch F. C., Dalcanton J. J., 2000, ApJ, 534, 146
van den Bosch F. C., Abel T., Croft R. A. C., Hernquist L., White S. D. M., 2002, ApJ, 576, 21
Vivitska M., Klypin A. A., Kravtsov A. V., Wechsler R. H., Primack J. R., Bullock J. S., 2002, ApJ, 581, 799
Warren M. S., Quinn P. J., Salmon J. K., Zurek W. H., 1992, ApJ, 399, 405
White S. D. M., 1984, ApJ, 286, 38
White S. D. M., Rees M. J., 1978, MNRAS, 183, 341
Zavala J., Okamoto T., Frenk C. S., 2008, MNRAS, 387, 364

This paper has been typeset from a TEX/LATEX file prepared by the author.

Capítulo 6

Conclusiones.

En este trabajo presentamos una forma sencilla de estimar el valor del parámetro de momento angular adimensional λ, a partir de un modelo simple que tiene la ventaja de requerir el mínimo de información accesible para su estimación.

A pesar de la simplicidad de nuestro modelo, haciendo uso de simulaciones provenientes de 6 diferentes grupos de investigación, mostramos que el error típico que cometemos por todas las simplificaciones, como es el uso de un perfil de densidad isotermo para el halo, un disco de materia bariónica no autogravitante y la perfecta conservación del momento angular total; es relativamente pequeño.

Las simulaciones que empleamos para probar nuestro modelo difieren entre si en su enfoque y los objetivos que persiguen, algunas de los cuales usan métodos semianalíticos con códigos de síntesis de poblaciones estelares y autogravedad, mientras que otras hacen uso de simulaciones de n-cuerpos incluyendo hidrodinámica con enfriamiento y retroalimentación de energía por procesos de formación estelar. En la mayoría de los casos, los perfiles de densidad que se obtienen en estos trabajos no son isotermos y algunos de estos modelos, como el de Okamoto et al. (2005), no imponen una conservación detallada del momento angular. En todos estos trabajos, el valor preciso de λ para las galaxias simuladas es conocido, al igual que es posible estimar su valor mediante la ecuación que nosotros dedujimos para galaxias de disco reales, dado que entre los datos de salida, estas simulaciones proporcionan valores del radio de escala del disco bariónico así como valores de la velocidad de rotación. A pesar de la variedad de métodos empleados en las diferentes simulaciones, el valor real de λ y nuestra estimación guardan una relación, casi de uno a uno, tal como mostramos en la figura 1 del capítulo 4. El motivo por el cual una aproximación a primer orden funciona tan bien, es porque estamos estimado el valor de un parámetro global que depende a su vez de parámetros globales; el momento angular total, la masa y la energía del sistema. Por ello, aunque nuestro modelo es incapaz de describir detalles en la estructura de las galaxias, da cuenta con suficiente precisión de las cantidades a medir, sin importar que el perfil real de la galaxia en cuestión no sea isotermo, que su momento angular no se haya conservado a la perfección o que el sistema no se encuentre completamente virializado, en tanto que la curva de rotación sea relativamente plana, el brillo superficial del disco sea exponencial y la dinámica esté dominada por la componente de materia obscura.

Mediante un análisis general establecimos las relaciones que esperábamos ob-

servar entre diferentes parámetros estructurales de las galaxias y el parámetro de espín λ. Para mostrar cómo tres de estos parámetros, cruciales en la asignación del tipo morfológico de Hubble para galaxias de disco, correlacionan con λ, compilamos una muestra de galaxias a partir del Atlas for Structural Studies of Spiral Galaxies (ASSSG) presentada por Courteau (1996, 1997) y una muestra proveniente de de Grijs (1998) basada en el Surface Photometry Cataloge del catálogo de galaxias ESO-Uppsala (Lauberts & Valentijn 1989) y el subsecuente análisis de Kregel et al. (2002). Como resultado obtuvimos que:

- El color de las galaxias tardías, cuantificado por el término $B - R$, correlaciona marcadamente con λ, siendo las galaxias más azules aquellas con un valor de λ más alto, es decir, se observa una disminución del valor de $B - R$ al aumentar λ, tendencia subyacente en la secuencia de Hubble.

- El espesor del disco, cuantificado por el cociente h/R_d, decrece al aumentar λ, comportamiento que también se observa en función del tipo de Hubble.

- El cociente bulbo-disco disminuye para galaxias con valores altos de λ, de la misma manera que ocurre al ir de tipos tempranos a tardíos.

Aunado a estas correlaciones encontradas con parámetros determinantes del tipo de Hubble, también obtuvimos una marcada tendencia entre la velocidad de rotación del disco y el tipo de Hubble que es reproducida al emplear el parámetro λ; tipos morfológicos tempranos, con valores típicos de λ bajos, tienden a presentar velocidades de rotación mayores que galaxias tardías con valores promedio de λ mayores.

También analizamos la dependencia de la metalicidad y el contenido de gas como función del espín, empleando una muestra observacional proveniente de los estudios de Pulyugin, Vílchez & Contini (2004), Garnett (2002) y Zaritsky, Kennicutt & Huchra (1994), con los que obtuvimos que:

- Al ser el índice de eficiencia de formación estelar inversamente proporcional a λ, aquellos sistemas con valores bajos de espín son más eficientes para transformar su gas en estrellas y, por lo tanto, presentan menores fracciones de masa de gas que aquellos con valores altos de λ.

- Tal como estudios teóricos previos lo predecían, sistemas con bajo valor de λ, eficientes en los procesos de formación estelar, presentan típicamente metalicidades más altas que sistemas con valores altos de λ.

- En sistemas de baja masa, los gradientes de abundancias son más pronunciados para galaxias con valores bajos de λ.

El incremento en el valor medio de λ al pasar de un tipo morfológico temprano a uno tardío, junto con los resultados anteriores, refuerzan la idea de emplear λ como un parámetro de clasificación galáctica cuantitativo y objetivo, además de proveer una nueva herramienta de comparación entre los resultados de diferentes modelos de formación galáctica y muestras de galaxias reales.

Es importante considerar que, en todas estas relaciones, existe una dispersión importante debida a la dispersión intrínseca en los valores de la masa de los sistemas, dado que las características físicas no dependen exclusivamente del espín galáctico, sino también de su masa y otros factores tales como son las interacciones con otros sistemas y las colisiones.

El objetivo de la primera parte de la tesis, no era el buscar algún parámetro que sustituyera a los sistemas actuales de clasificación de galaxias por mostrar una correlación más estrecha con parámetros estructurales de las galaxias, sino obtener una estimación, a primer orden, del valor del espín galáctico, una herramienta teórica indispensable en el estudio de formación y evolución galácticas, y con esta estimación comprobar las relaciones causales esperadas entre λ y algunas propiedades físicas, que tanto estudios analíticos como semianalíticos, proponen. Existen algunos trabajos como los de Syer, Shude & Mao (1999) que de forma indirecta comprueban la influencia del espín en la estructura observada de las galaxias, pero nuestros resultados son los primeros que, a partir de inferencias directas sobre galaxias particulares, mostramos el importante papel que juega este parámetro en la estructura de las galaxias.

El acceso a grandes bases de datos de galaxias, en particular las provenientes del SDSS (Adelman-McCarthy et al. 2007 y Choi, Park & Vogley 2007) nos permitieron obtener por primera vez, la distribución de λ a partir de una muestra de galaxias reales. Empleando únicamente galaxias de disco, para las cuales nuestra estimación de λ es más confiable, obtuvimos una distribución que se encuentra bien descrita por una función log-normal, tal como las provenientes de simulaciones numéricas de n-cuerpos para la descripción de la distribución de probabilidad de este parámetro. La función log-normal que describe la distribución de nuestra muestra de galaxias de disco está definida por los parámetros; $\lambda_0 = 0.0585$ y $\sigma_\lambda = 0.446$. Empleando la muestra completa de galaxias, tanto espirales como elípticas, e imponiendo una distribución unimodal para la muestra completa, los parámetros que ajustan esta distribución con una función log-normal son: $\lambda_0 = 0.0394$ ± 0.005 y $\sigma_\lambda = 0.509$ ± 0.05, cuyos valores son compatibles con los obtenidos a partir de simulaciones, como se muestra en la figura 4, en donde los diferentes puntos provienen de simulaciones de diferentes grupos de investigación, uno de ellos (triángulo azul), el de la simulación presentada aquí, con valores $\lambda_0 = 0.038$ y $\sigma_\lambda = 0.525$, y la cruz negra con barras de error muestra nuestro intervalo de confianza obtenido a partir de la muestra de galaxias observadas del SDSS.

La gran semejanza, tanto cualitativa como cuantitativa de nuestro resultado
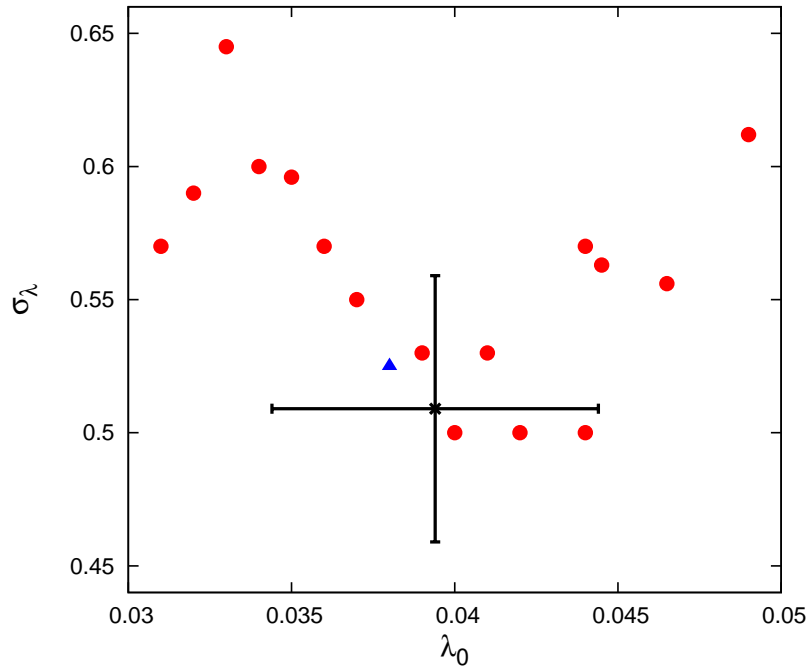
Figura 6.1: Compilación de valores para λ_0 y σ_λ provenientes de diferentes grupos de investigación usando simulaciones numéricas, proveniente de Shaw et al. (2006). Se muestran los valores obtenidos empleando la simulación cosmológica presentada en este trabajo (triángulo azul), y el resultado proveniente de la muestra del SDSS (cruz negra con barras de error).

con los resultados teóricos provenientes de simulaciones, nos impulsó a reproducir otros estudios realizados que emplean únicamente simulaciones de n-cuerpos, pero en esta ocasión usando muestras observacionales de galaxias.

La mayoría de los estudios teóricos basados en simulaciones numéricas, muestran una carencia de dependencia entre el valor de λ y la densidad del medio ambiente en que se encuentran las galaxias (Lemson & Kauffmann 1999, Maccio et al. 2007), aún cuando hay algunos que reportan haber encontrado alguna tendencia ligera, como es el caso de Avila-Reese et al. (2005) en el sentido que los sistemas en medios ambientes muy densos típicamente presentan valores bajos de λ. En nuestro estudio, empleando la muestra de halos simulados, no observamos ninguna dependencia entre el valor de λ y la densidad del medio ambiente, un resultado consistente con el observado con la muestra de galaxias proveniente del SDSS, en donde solamente una ligera dependencia es visible en regiones de alta densidad, donde el valor de λ tiende a decrecer, resultado que puede ser atribuido

a la dependencia del tipo morfológico con el medio ambiente, que establece una sobreabundancia de tipos galácticos tempranos en regiones densas, cuyos halos presentan λ's pequeñas, pero que deja de presentarse al analizar la submuestra de galaxias de disco, en donde nuestra estimación de λ es más precisa. En cualquier caso, ya sea analizando los halos de materia obscura de nuestra simulación, o la muestra de galaxias del SDSS, nuestros resultados se encuentran en acuerdo con la mayoría de los estudios previos, situación que no se repite al analizar la dependencia con la masa.

En cuanto a la dependencia de λ con la masa total, nuestros resultados, analizando la muestra del SDSS, difieren visiblemente de resultados previos. Tanto la mayoría de los estudios teóricos previos como nuestra muestra de halos simulados, no muestran ninguna dependencia de λ con la masa total de los sistemas, pero el análisis de la muestra del SDSS presenta un comportamiento muy claro; al incrementarse la masa de las galaxias, el valor medio de λ inferido tiende a decrecer, al igual que la dispersión en torno al valor medio; de manera que los sistemas poco masivos conforman una población con valores típicos de λ elevados y dispersiones grandes alrededor de este valor medio, mientras que los sistemas masivos se presentan como una población coherente con valores típicos de λ bajos.

Recientemente Berta et al. (2008) confirmaron estos resultados. Para su estudio emplearon una muestra de galaxias espirales proveniente del SDSS con cerca de 50,000 galaxias, alrededor de cinco veces más grande que nuestra muestra de galaxias, y calcularon λ con el método que nosotros propusimos empleándolo básicamente en la forma en que describimos en este trabajo, así como sustituyendo el uso de la relación Tully-Fisher por la implementación de un algoritmo que permite calcular la masa total de estrellas y gas en la galaxia en cuestión, de manera que su estimación de la masa bariónica es más precisa que la nuestra. Ya sea empleando el método más sencillo o el de mayor sofisticación, sus resultados se encuentran en total concordancia con los nuestros, tanto en lo referente a la dependencia de λ con la masa total de los sistemas como con la relación entre la tasa de formación estelar y el espín galáctico. Podemos encontrar otro indicio de esta dependencia de λ con la masa en los estudios de Avila-Reese et al. (2008) que requieren precisamente este comportamiento para explicar las relaciones de escala bariónicas que encuentran en una muestra de 80 galaxias aisladas. Es importante hacer notar que la escala de masas que se presenta en el capítulo 5 y en Cervantes-Sodi et al. (2008) resulta un poco extrema para la muestra de galaxias involucradas; en realidad una estimación más conservadora estaría en acuerdo con el rango de masas que presentan Berta et al.(2008), con masas entre 1×10^{10} y 1×10^{12}, pero el comportamiento observado se mantiene, tal como lo corrobora el mismo estudio de Berta et al.

Los resultados aquí presentados proporcionan restricciones a la forma en que las galaxias adquieren su momento angular y así, valiosas pistas para discriminar

entre distintos modelos cosmológicos, dada la dependencia de las relaciones presentadas con la cosmología supuesta, tal como señalan Eke, Efstathiou & Wright (2000). Comparando con estudios de formación galáctica, concluimos que las tendencias que descubrimos difícilmente pueden ser atribuidas a efectos astrofísicos como disipación de momento angular o pérdida de bariones, en cambio, deben ser entendidas como evidencia en favor a un mecanismo específico de adquisición de momento angular, aún cuando es importante tener en cuenta todas las hipótesis planteadas para, en función de ellas, interpretar los resultados. En particular, es difícil aceptar la suposición de una perfecta conservación del momento angular total, tanto de la componente bariónica como de la componente de materia oscura, dado el impacto que tienen perturbaciones tales como la presencia de barras y brazos espirales en la distribución del momento angular, sin mencionar las interacciones con otras galaxias o incluso las colisiones que llevan a la reconfiguración de los sistemas, pero la comunidad no ha alcanzado aún un consenso sobre éste asunto, con una gran variedad de resultados que van desde una conservación casi perfecta de la relación $j_d/m_d = 1$, a desviaciones importantes debidas a disipación y transferencia de momento angular entre las diferentes componentes, cuyas tendencias difícilmente podrían explicar, en su conjunto, los resultados aquí mostrados.

A primer orden, la tendencia a valores bajos de λ en halos masivos puede ser explicada pensando en un campo de torcas de marea constante, el cual resulta en valores altos de λ para aquellos sistemas más vulnerables como las galaxias poco masivas.

Capítulo 7

Trabajo a futuro.

En el modelo de adquisición de momento angular por torcas de marea, se espera que pares de galaxias relativamente aisladas, que se hayan formado inmersas en el mismo campo de marea, adquieran aproximadamente la misma cantidad de momento angular, por lo que el producto λM para las galaxias de un mismo par debería ser muy semejante. Existen algunos indicios de que esta relación puede no ser muy estrecha, tal sería el caso de la alta fracción de pares de galaxias con morfología mixta, es decir, aquellos conformados por una galaxia elíptica y otra espiral, en donde típicamente la galaxia elíptica posee un espín mucho menor al de la espiral. Uno de nuestros objetivos próximos es el estudio de pares de galaxias determinando el valor de su momento angular, tanto su magnitud mediante el parámetro de espín λ, como su dirección determinada por su ángulo de posición.

Para dicho estudio utilizaremos una muestra de pares de galaxias proveniente del estudio de Park, Gott & Choi (2008), en donde los pares deben cumplir las siguientes tres características: (a) la galaxia vecina no puede ser más tenue que la galaxia blanco por más de 0.5 mag, de manera de que sean de tamaño semejante, (b) se considera galaxia vecina a aquella que tenga la distancia proyectada en el cielo más pequeña y (c) deben presentar una diferencia en la velocidad radial menor a 1000 km/s. A partir de esta muestra limitada por volumen, con un rango en el corrimiento al rojo de $0{,}001 < z < 0{,}5$, podemos construir una muestra de pares de galaxias en la que podamos determinar λ y así probar si el momento angular adquirido por los miembros de un mismo par es el mismo. Determinando la distancia de separación entre la galaxia blanco y su vecina más próxima, podemos también investigar si aquellas galaxias en interacción, cuyas distancias de separación sean cercanas a sus radios viriales, muestran alguna reacción a la interacción en el valor de su espín.

Finalmente, también estamos interesados en estudiar con mayor profundidad la dependencia de la tasa de formación estelar en el valor de λ, así como su influencia en la actividad nuclear y, en particular, si la población de galaxias que presenta actividad nuclear conforman un grupo con valores de espín bajos, tal como lo predice la teoría (Loeb & Eisenstein 1995, Haehnelt, Natarajan & Rees 1998), de forma que el bajo momento angular del gas que funciona como combustible en estos sistemas, le permita precipitarse al agujero negro central, con lo que también la masa del mismo agujero negro sería función de λ. Para dicho estudio estamos buscando hacer uso de las muestras provenientes del SDSS

de Lee et al. (2007) y Choi, Woo & Park (2009) en donde la actividad de las galaxias es determinada por cocientes de líneas (Kewley et al 2001 y Kauffmann et al. 2003), lo que permite clasificarlas como galaxias con formación estelar activa o núcleos activos de galaxias (AGN) que a su vez pueden ser divididos en LINERs o Seyferts.

Capítulo 8

Bibliografía.

Abraham R. G., Valdes F., Yee H. K. C., van den Bergh, S., 1994, ApJ, 432, 75

Abraham R. G., Tanvir N. R., Santiago B. X., Ellis R. S., Glazebrook K., van den Bergh S., 1996, MNRAS, 279, L47

Adams A., Woolley A., 1994, VA, 38, 273

Adelman-McCarthy, J. K., et al. 2007, ApJS, 172, 634

Aragón-Calvo M. A., van de Weygaert R., Jones B. J. T., van der Hulst J. M., 2007, ApJ, 655, L5

Avila-Reese V., Colin P., Gottlöber S., Firmani C., Maulbetsch C., 2005, ApJ, 634,51

Barnes J., Efstathiou G.,1987, ApJ, 319, 575

Barton, E. J., Geller M. J., Bromley B. C., van Zee L., Kenyon S. J., 2001, AJ, 121, 625

Bell E. F., 2002, ApJ, 581, 1013

Berta Z., Jimenez R., Heavens A. F., Panter B., 2008, MNRAS, 391, 197

Bett P., Eke V., Frenk C. S., Jenkins A., Helly J., Navarro J., 2007, MNRAS, 376, 215

Binney, J., 1978, MNRAS, 183, 501

Binney J., Tremaine S., 1987, Galactic Dynamics (Princeton: Princeton Univ. Press)

Blumenthal G. R., Faber S. M., Primack J. R., Rees M. J.,1984, Nat, 311, 517

Boissier S., Boselli A., Prantzos N., Gavazzi G., 2001, MNRAS, 321, 733

Boissier S., Prantzos N., 2000, MNRAS, 312, 398

Brooks A. M., Governato F., Booth C. M., William B., Gardner J. P., Wadsley J., Sinson G., Quinn T., 2007, ApJ, 655, L17

Brosche P., 1973, A&A, 23, 259

Bullock, J. S., et al., 2001, ApJ, 555, 240

Burkert A., 2003, A&SS, 284, 697

Catelan P., Theuns T., 1996, MNRAS, 282, 455

Cervantes-Sodi B., Hernández X., Park C., Kim J., 2008, MNRAS, 388, 863

Cervantes-Sodi B., Hernández X., 2008, RevMexA&A, 45, 75

Choi Y., Park C., Vogeley M. S., 2007, ApJ, 658, 884

Choi Y., Woo J., Park C., 2009, ApJ, enviado.

Churches D. K., Nelson A. H., Edmunds M. G., 2001, MNRAS, 327, 610

Cole S., Lacey C., 1996, MNRAS, 281, 716

Connolly A. J., et al. 1995, AJ, 110, 1071

Conselice C., 2003, ApJS, 147, 1

Courteau S., 1996, ApJS, 103, 363

Courteau S., 1997, AJ, 114, 2402

Crain R. A., Eke V. R., Frenk C. S., Jenkiins A., McCarthy I. G., Navarro J. F., Pearce F. R., 2007, MNRAS, 377, 41

Dalcanton J. J., Spergel D. N., Summers F. J., 1997, ApJ, 482, 659

Davis, M., Efstathiou, G., Frenk, C. S., White, S. D. M., 1985, ApJ, 292, 371

de Blok W. J. G., van der Hulst, J., M., 1998, A&A, 335, 421

de Grijs R., 1998, MNRAS, 299, 595

de Vaucouleurs G., de Vaucouleurs A., Corwin H. G., 1976, Second Reference Catalogue of Bright Galaxies (Austin: Univ Texas Press), 1977.

Dopita M. A., Ryder S. D., 1994, ApJ, 430, 163

Doroshkevich A. G., 1970, Ap, 6, 320

Dressler A., 1980, ApJ, 236, 351

Dutton A. A., van den Bosch F. C., 2008, MNRAS submitted, arXiv:0810.4963

Efstathiou G., Jones B. J. T., 1979, MNRAS, 186, 133

Eisenstein D. J., Loeb A., 1995, ApJ, 443, 11

Eke V., Efstathiou G., Wright L., 2000, MNRAS, 315, L18

Elmegreen D. M., Elmegreen B. G., 1984, ApJS, 54, 127

Ellis S. C., Driver S. P., Allen P. D., Liske J., Bland-Hawthorn J., De Propris R., 2005, MNRAS, 363, 1257

Faber S. M., Jackson R. E., 1976, ApJ, 204, 668

Fall S. M., Efstathiou G., 1980, MNRAS, 193, 189

Ferguson A. M. N., Clarke C. J., 2001, MNRAS, 325, 781

Firmani C., Hernández X., Gallagher J., 1996, A&A, 308, 403

Flores R., Primack J. R., Blumenthal G. R., Faber S. M., 1993, ApJ, 412, 433

Franx M., Illingworth G., Heckman T., 1989, 344, 613

Frenk C. S., White S. M. D., Efstathiou G., Davis M., 1985, Nat, 317, 595

Frenk C. S., White S. M. D., Davis M., Efstathiou G., 1988, ApJ, 327, 507

Gardner, J. P., 2001, ApJ, 557, 616

Garnett D. R., Shields G. A., 1987, ApJ, 317, 82

Garnett D. R., 1998, RevMexAC, 7, 58

Garnett D. R., 2002, ApJ, 581, 1019

Giovanelli R., Haynes M. P., da Costa L. N., Freudling W., Salzer J. J., Weger G., 1997, ApJ, 477, L1

Goto T., Yamauchi C., Fujita Y., Okamura S., Sekiguchi M., Smail I., Bernardi M., Gomex P. L., 2003, MNRAS, 346, 601

Gott J. R., Thuan T. X., 1976, ApJ, 204, 649

Gottlöber S., Yepes G., 2007, ApJ, 664, 117

Graham A. W., 2001, AJ, 121, 820

Graham A. W., Merritt D., Moore B., Diemand J., TerzicB́., 2006, ApJ, 132, 2701

Grosbol P., Patsis P. A., Pomoei E., 2004, A&A, 423, 849

Guimarães A. C. C., Sodré L., 2009, astro/ph 0904.4381

Gurovich S., et al., 2004, PASA, 21, 412

Haehnelt M. G., Natarajan P., Rees M. J., 1998, MNRAS, 300, 817.

Hahn O., Porciani C., Carollo C. M., Dekel A., 2007, MNRAS, 375, 489

Halliday, C., et al., 2001, MNRAS, 326, 473

Haynes M. P., Giovanelli R., 1984, AJ, 89, 758

Heavens A., Peacock J., 1988, MNRAS, 232, 339

Heller C. H., Shlosman I., Athanassoula, E., 2007, ApJ, 671, 226

Henry R. B. C., Worthey G., 1999, PASP, 111, 919

Hernández X., Avila-Reese, V., Firmani, C., 2001, MNRAS, 327, 329

Hernández X., Cervantes-Sodi B., 2006, MNRAS, 368, 351

Hernández X., Gilmore G., 1998, MNRAS, 294, 595

Hernández X., Park C., Cervantes-Sodi B., Choi Y., 2007, MNRAS, 375, 163

Hoyle F., 1949, MNRAS, 109, 365

Hubble E. P., 1926, ApJ, 64, 321

Hubble E. P., 1936, Realm of the Nebulae. Yale Univ. Press, New Heaven

Hunter D. A., Hoffman L., 1999, ApJ, 117, 2789

Jang-Codell H., Hernquist L., 2001, ApJ, 548, 68

Jimenez, R., Padoan, P., Matteucci, F., Heavens, A. F., 1998, MNRAS, 299, 123

Kashlinsky A., 1982, MNRAS, 200, 585

Kassin S. S., de Jong R. S., Weiner B. J., 2006, ApJ, 643, 804

Kaufmann T., Mayer L., Wadsley J., Stadel J., Moore B., 2007, MNRAS, 375, 53

Kelly B. C., McKay T. A., 2004, AJ, 127, 625

Kennicutt R. C., Oey M. S., Zaritsky D., Huchra J. P., 1993, RevMexAA, 27, 21

Kennicutt R. C., 1998, ApJ, 498, 541

Kim J., Park C., 2006, ApJ, 639, 600

Kim J., Park C., Choi Y., 2008, ApJ, preprint (arXiv:0801.3169)

Klypin A., Zhao H. Somerville R. S., 2002, ApJ, 573, 597

Koda J., Sofue Y.,Wada K., 2000, ApJ, 532, 214

Koeppen J., Theis C., Hensler G., 1995, A&A, 296, 99

Koopmans L. V. E., Treu T., Bolton A. S., Burles S., Moustakas L. A., 2006, astro-ph/0601628, ApJ in press

Kormendy J., 1979, ApJ, 227, 714

Kregel M., van der Kruit P. C., de Grijs R., 2002, MNRAS, 334, 646

Kregel M., van der Kruit P. C., Freeman K. C., 2005, MNRAS, 358, 503

Kuchinski L. E., et al., 2000, ApJS, 131, 441

Labbe I., et a.l, 2003, ApJ, 591, L95

Lahav O., et al., 1995, Science, 267, 859

Lauberts A., 1982, The ESO/Uppsala Survey of the ESO(B) Atlas, European Southern Observatory

Lee J. H., Lee M. G., Kim T., Hwang H. S., Park C., Choi Y. Y., 2007, ApJ, 663, L69

Lemson G., Kauffmann G., 1999, MNRAS, 302, 111

Longair, M. S.,2008, Galaxy formation, (Springer)

Lotz L. M., Primack J., Madau P., 2004, AJ, 128, 163

Ma J., 2002, A&A, 388, 389

Maccio A. V., Dutton A. A., van den Bosch F. C., Morre B., Potter D., Stadel J., 2007, MNRAS, 378, 55

Maller A. H., Dekel A., Somerville R., 2002, MNRAS, 329, 423

Marchant A. B., Shapiro S. L., 1977, ApJ, 215, 1

Melbourne J., Salzer J. J., 2002, AJ, 123, 2302

Milne W. H., McCrea E. A., 1934, Q. J. Math., 5, 64 & 73

Mo H. J., Mao S., White S. D. M., 1998, MNRAS, 295, 319

Naab T., Ostriker J. P., 2006, MNRAS, 366, 899

Navarro J. F., Frenk C. S., White S. D. M., 1997, ApJ, 490, 493

Navarro J. F., Steinmetz M., 2000, ApJ, 538, 477

Naim A., et al., 1995, MNRAS, 274, 1107

Okamoto t., Eke V. R., Frenk C. S., Jenkins A., 2005, MNRAS, 363, 1299

Oey M. S., Kennicutt R. C., 1993, ApJ, 411, 137

Padmanabhan T., 1995, Structure formation in the universe, (Cambridge University Press)

Padmanabhan T., 2002, Theoretical astrophysics Volume III: Galaxies and Cosmology, (Cambridge University Press)

Padmanabhan N., et al., 2004, New Astron., 9, 329

Pahre M. A., Ashby M. L. N., Fazio G. G., Willner S. P., 2004, ApJS, 154, 235

Park C., Choi Y., 2005, ApJ, 635, L29

Park C., Choi Y., Vogeley M. S., Gott J. R., Blanton M. R., 2007, ApJ, 658, 898

Park C., Gott J. R., Choi, Y.-Y., 2008, ApJ, 674, 784

Peebles P. J. E., 1969, ApJ, 155, 393

Peebles P. J. E., 1971, A&A, 11, 377

Pilyugin L. S., 2001, A&A, 374, 412

Pilyugin L. S., 2003, A&A, 399, 1003

Pilyugin L. S., Vílchez J. M., Contini T., 2004, A&A, 425, 849

Pinkney J., et al., 2003, ApJ, 596, 903

Pizagno et al., 2007, AJ, 134, 945

Prantzos N., Boissier S., 2000, MNRAS, 313, 338

Puech M., Hammer F., Lehnert M. D., Flores H., 2007, A&A, 466, 83

Roberts M. S., Haynes M. P., 1994, ARA&A, 32, 115

Sandage A., 1961, The Hubble Atlas of Galaxies. Carnegie Institution of Washington, Washington D. C.

Sandage A., Freeman K. C., Stokes N. R., 1970, ApJ, 160, 831

Saio H., Yoshii Y., 1990, ApJ, 363, 40

Sarzi M., et al., 2006, MNRAS, 366, 1151

Schade D., Lilly S. J., Cramton D., Hammer F., LeFevre O., Tresse L., 1995, ApJ, 451, L1

Sedov L. I., 1993, Similarity and Dimensional Methods in Mechanics, 10th ed. CRC Press Boca Raton FL

Shaw L. D., Weller J., Ostriker J. P., Bode, P., 2006, ApJ, 646, 815

Silk J., 2001, MNRAS, 324, 313

Somverville R. S., Primack J. R., 1999, MNRAS, 310, 1087

Somerville R. S., Primack J. R., Faber S. M., 2001, MNRAS, 320, 504

Spergel, D. N., et al. 2003, ApJS, 148, 175

Steinmets M., Navarro J. F., 1999, ApJ, 513, 555

Struck-Marcell C., 1991, ApJ, 368, 348

Sugerman B., Summers F. J., Kamionkowski, M., 2000, MNRAS, 311, 762

Swaters R. A., Madore B. F., van den Bosch F. C., Balcells M., 2003, Apj, 583, 732

Syer D., Mao S., Mo H. J., 1999, MNRAS, 305, 357

Takamiya M., 1999, ApJS, 122, 109

Tonini C., Lapi A., Shankar F., Salucci P., 2006, ApJ, 638, L13

Toomre A., 1964, ApJ, 139, 1217

Treu T., Koopmans L. V. E., Bolton A. S., Burles S., Moustakas L. A., 2006, ApJ, 640, 662

Tully R. B., Fisher J. R., 1977, A&A, 64, 661

Tutukov A. V., 2006, ARep, 50, 526

van den Bosch F. C., 1998, ApJ, 507, 601

van den Bosch F. C., Dalcanton J. J., 2000, ApJ, 534, 146

van den Bosch F. C., Abel T., Croft R. A. C., Hernquist L., White S. D. M., 2002, ApJ, 576, 21

van der Kruit, P. C., 1987, A&A, 173, 59

Vila-Costas M. B., Edmunds M. G., 1992, MNRAS, 259, 121

Vitvitska M., Klypin A. A., Kravtsov A. V., Wechsler R. H., Primack J. R., Bullock J. S., 2002, ApJ, 581, 799

Warren M. S., Quinn P. J., Salmon J. K., Zurek W. H., 1992, ApJ, 399, 405

Wilkinson M. I., Evans N. W., 1999, MNRAS, 310, 645

White S. D. M., 1984, ApJ, 286, 38

White S. D. M.,1993, en: Schaeffer R., et al., Les Houches Session LX Cosmology and Large Scale Structure, Elsevier, p. 349.

White S. D. M., Frenk C. S., 1991, ApJ, 379, 52

White S. D. M., Rees M. J., 1978, MNRAS, 183, 341

Wong T., Blitz L., 2002, ApJ, 569, 157

Yoachim P., Dalcanton J. J., 2006, AJ, 131, 226

Zaritsky D., Kennicutt R. C., Huchra J. P., 1994, ApJ, 420, 87

Zavala J., Okamoto T., Frenk C. S., 2008, MNRAS, 387, 364

Zhang B., Wyse R. F G., 2000, MNRAS, 313, 310